AEC Category: HEALTH AND SAFETY

CEX-62.2

CIVIL EFFECTS STUDY

NUCLEAR BOMB EFFECTS COMPUTER (Including Slide-rule Design and Curve Fits for Weapons Effects)

E. Royce Fletcher, Ray W. Albright,
Robert F. D. Perret, Mary E. Franklin,
I. Gerald Bowen, and Clayton S. White

Issuance Date: February 15, 1963

CIVIL EFFECTS TEST OPERATIONS
U.S. ATOMIC ENERGY COMMISSION

NOTICE

This report is published in the interest of providing information which may prove of value to the reader in his study of effects data derived principally from nuclear weapons tests and from experiments designed to duplicate various characteristics of nuclear weapons.

This document is based on information available at the time of preparation which may have subsequently been expanded and re-evaluated. Also, in preparing this report for publication, some classified material may have been removed. Users are cautioned to avoid interpretations and conclusions based on unknown or incomplete data.

The *Nuclear Bomb Effects Computer* can be purchased from the Superintendent of Documents, U. S. Government Printing Office, Washington 25, D. C., for ~~$1.00~~.

PRINTED IN USA
Price $1.00. Available from the Office of Technical Services, Department of Commerce, Washington 25, D. C.

USAEC Division of Technical Information Extension, Oak Ridge, Tennessee

NUCLEAR BOMB EFFECTS COMPUTER (Including Slide-rule Design and Curve Fits for Weapons Effects)

E. Royce Fletcher, Ray W. Albright, Robert F. D. Perret,
Mary E. Franklin, I. Gerald Bowen, and Clayton S. White

Approved by: L. J. DEAL
Acting Chief
Civil Effects Branch

Lovelace Foundation for Medical Education and Research
Albuquerque, New Mexico
April 1962

ABSTRACT

Based on data from the 1962 edition of *The Effects of Nuclear Weapons*, a circular slide rule was designed to evaluate 28 different effects of nuclear weapons. Of these 28 different effects, 13 relate to blast, 5 to thermal radiation, 1 to initial nuclear radiation, 2 to early fallout, 6 to crater dimensions, and 1 to fireball dimensions. Most of the parameters are presented as functions of range and yield (1 kt to 20 Mt). Simple techniques are described which make it possible to estimate most of the effects parameters for yields greater than 20 Mt or smaller than 1 kt.

The report presents (1) curve fits of weapons-effects data, (2) design analysis for the slide rule, and (3) instructions for use of the rule along with some of the implications of the data in regard to biological and structural damage. The machine techniques are mentioned which were used to prepare the original graphs necessary for the production of the slide rule.

FOREWORD AND ACKNOWLEDGMENTS

The Lovelace Foundation for Medical Education and Research became involved in the development of special-purpose slide rules in 1959 because of the need for an easy and convenient method of evaluating the *free-field* effects of nuclear weapons. (Free-field is used here to denote weapons effects occurring near the surface of the earth in the absence of structures or of unusual terrain features, such as hills, dales, and forests.) The first to recognize and give expression to this need was R. L. Corsbie, then Director, Civil Effects Test Operations, Division of Biology and Medicine, United States Atomic Energy Commission (USAEC). A circular slide rule was developed in 1959 and produced in 1960 (based on the 1957 edition of *The Effects of Nuclear Weapons*) which was similar to the one reported here except that it was smaller and permitted evaluation of fewer effects parameters. Soon after the production of this rule, plans were made by the Defense Atomic Support Agency (DASA) and the USAEC to revise and update *The Effects of Nuclear Weapons*. Concurrently, plans were made to update the slide rule; thus the present computer was designed and produced to conform with the revised data appearing in the effects manual. The new slide rule was designed to include pertinent material that had not appeared on the previous one.

The interest and encouragement of Samuel Glasstone, editor of *The Effects of Nuclear Weapons,* is gratefully acknowledged. Through his cooperation and the concurrence of DASA, it was possible to obtain the needed effects data as they became available, many months before the revised manual was published.

The authors wish to thank Chester W. Lytle and other personnel of the Lytle Corporation for their assistance in constructing prototype slide rules and for their advice relative to manufacturing problems.

The finished drawings from which the slide rule was produced were prepared by Robert A. Smith of the Department of Medical Illustration, Lovelace Foundation. From the same group, Mrs. Joyce Blaine prepared the illustrative material and George Bevil handled the photographic work for this report.

Kevin A. Doherty and Orville R. Pratt of the Physics Department assisted in the numerical treatment (both machine and manual) of effects data.

The manuscript was typed by Mrs. Maureen K. Gilmore, Mrs. Ruth P. Lloyd, and Mrs. Isabell D. Benton.

CONTENTS

CONTENTS (Continued)

ILLUSTRATIONS

CHAPTER 2 NUMERICAL EVALUATION OF WEAPONS-EFFECTS DATA

ILLUSTRATIONS (Continued)

TABLES

TABLES (Continued)

LIST OF SYMBOLS

Symbol	Definition
AB	air burst: a burst for which the fireball does not touch the ground
CSB	contact surface burst—a burst directly on the surface or at a burst height not more than 5 $W^{0.3}$ ft above, or below, the surface
c_0	ambient speed of sound
d	distance from Ground Zero or range, miles
d_s	slant distance from point of burst or slant range, miles
D	depth of crater, ft
$(E_{ly})\%$	standard error of estimate of log y in percentage of y, % (Subscripts S and R refer to dry soil and rock, respectively)
H	height of burst, ft
H_m	minimum height of burst for negligible fallout, ft
I	total initial nuclear radiation (neutron plus gamma), rem
kt	kiloton, energy of nuclear explosion which is equivalent to 1000 tons of TNT
Mt	megaton, energy of nuclear explosion which is equivalent to 1,000,000 tons of TNT
OBH	optimum burst height: height of burst to maximize value of given parameter at the range of interest or to maximize range at which a given value of the parameter occurs
P	ambient pressure, psi
p_m	maximum or shock overpressure, psi
P_0	14.7 psi
p_r	maximum reflected overpressure, psi
q_m	maximum dynamic pressure, psi
Q	thermal radiation, cal/cm^2
Q%	percentage of total thermal radiation delivered at time t for a given yield, %
Q_{1st}	thermal radiation producing first-degree burns (bare white skin), cal/cm^2
Q_{2nd}	thermal radiation producing second-degree burns (bare white skin), cal/cm^2
R	early fallout dose rate, any consistent units
R_0	early fallout dose rate measured at time t_0, any consistent units
R_A	apparent radius of crater, miles (Subscripts S and R refer to dry soil and rocks, respectively)
R_{ab}	maximum fireball radius for air burst, miles
R_{sb}	maximum fireball radius for surface burst, miles
$\overline{R}$	maximum fireball radius, average for surface and air bursts, miles
R_L	radius of crater lip, miles (Subscripts S and R refer to dry soil and rock, respectively)
ρ/ρ_0	ratio of ambient air density to air density at sea-level
SB	surface burst: a burst at the surface of the ground or at a height above the surface (1) less than the radius of the fireball at maximum luminosity (second thermal maximum) or (2) less than minimum height of burst for negligible fallout ($H < 180\ W^{0.4}$ ft)

Symbol	Definition
t	time after detonation, units as specified
t_0	time after detonation at which early fallout dose rate (R_0) is measured, units as specified
t_a	
t_p	duration of the positive overpressure, sec
t_u	duration of the positive winds, sec
T_0	ambient temperature, degrees Rankine (degrees Farenheit plus 459.69)
u_m	maximum wind velocity, mph
$v_{10\ ft}$	velocity of object after 10-ft displacement, ft/sec (Additional subscript, m, is for 165-lb man and g is for 0.1- to 10-g window-glass fragments, $\frac{1}{8}$ in. thick)
W'	scaling factor for computation of initial gamma radiation, units same as W
W	yield or total effective energy released in a nuclear explosion, kt unless otherwise specified

Chapter 1

INTRODUCTION

1.1 GENERAL

The primary purpose of this report is to describe the analytical procedures involved in the design of a circular slide rule and to discuss its usage and limitations in the evaluation of the effects of nuclear weapons.* The information on the computer, taken from the 1962 edition† of *The Effects of Nuclear Weapons*,[1] shows the major free-field environmental variations associated with nuclear detonations which represent a potential hazard to man. Tabular material that relates particular values of the effects parameters to various levels of biologic response and structural damage is also presented on the computer (discussed in Chap. 4) to help establish the significance of the effects parameters.

Although a number of factors, such as burst conditions, weather, terrain, and weapon design, introduce uncertainties in the assessment of weapons effects, the data presented offer the best available approximations for purposes of orientation and protective planning. The ease with which quick reference information can be obtained is closely related to the simplicity of presentation. This simplicity of presentation greatly aids those new to the weapons-effects field as well as experienced personnel from technical to professional levels.

Some readers may be interested in only one or two of the topics covered in this report. For this reason each of the three major sections summarized and discussed in this chapter was written as an entity with little dependence on the others.

1.2 NUMERICAL EVALUATION OF WEAPONS-EFFECTS DATA

It was expedient to express many of the parameters of nuclear-weapons effects as polynomials, whose coefficients were determined by the least squares method, to facilitate computation of the slide-rule scales. The data used for input were obtained from curves and from semiempirical equations published in Ref. 1. Chapter 2 contains all the effects equations used in the preparation of the slide rule as well as equations describing blast effects for heights of burst which were not included on the circular computer. Most of the material presented in equation form is also represented graphically.

---

*Although it is not the purpose of this report to discuss the production of the circular slide rule, some material is presented in the Appendix relative to the preparation of the machine drawings from which the slide rule was produced.

†A similar, but smaller, circular slide rule based on the 1957 edition of *The Effects of Nuclear Weapons*[2] was designed in 1959 by the Lovelace Foundation for the Division of Biology and Medicine, USAEC. The development of this computer was not documented.

1.3 DESIGN OF THE CIRCULAR SLIDE RULE

A cursory search of scientific literature for design criteria of special-purpose slide rules revealed some interesting information. It was found, among other things, that special-purpose slide rules have been described in journals appropriate to their use and that they can be found in a wide variety of periodicals, e.g., *Journal of Forestry,*[3] *Transactions of the American Geophysical Union,*[4] *Mechanical World,*[5] and *The Engineer.*[6] With two exceptions (Refs. 3 and 5), these reports were concerned primarily with the information to be presented rather than with establishing general principles of slide-rule design. The general treatments found were for many-variable problems where the variables could be expressed in separate terms. It was tacitly assumed that separate slide rules would be constructed for each equation to be solved.

The analytical problems encountered in the design of the Nuclear Bomb Effects Computer were somewhat different from those which would be encountered in the design of single-problem many-variable computers. It was desired to place many problems on a single slide rule.* However, with one exception, the equations to be represented involved only two or three variables. Also, in many cases it was possible to express different problems using one or two scales in common. Only one three-variable problem (initial nuclear radiation) was encountered where it was not possible to express functions of each variable in separate terms. This problem was placed on the slide rule in a unique fashion (see Sec. 3.2.2).

A semigeneral treatment of slide-rule-design problems is used in Chap. 3; i.e., general derivations were made first and then applications to the specific problems at hand were made. No attempt was made to present general analyses of slide-rule problems of types other than those encountered in the present work.

1.4 COMPUTER (SLIDE-RULE) EVALUATION OF WEAPONS-EFFECTS DATA

A detailed description of the use of the slide rule is presented in Chap. 4. This includes enumeration and discussion of the assumptions made in the computation of weapons-effects parameters. A total of 28 different problems can be solved: 13 parameters relate to blast, 5 to thermal radiation, 1 to initial nuclear radiation, 2 to early fallout, 6 to crater dimensions, and 1 to fireball dimensions.

The tabular material placed on the slide rule to help establish the significance of blast, thermal, and ionizing-radiation effects is briefly discussed in Chap. 4, and appropriate reference material is noted.

Although the slide rule can be used directly only for yields between 1 kt and 20 Mt, simple extrapolation techniques are described which make it possible to estimate effects parameters for yields greater than 20 Mt or smaller than 1 kt.

REFERENCES

1. S. Glasstone (Ed.), *The Effects of Nuclear Weapons*, rev. ed., Superintendent of Documents, U. S. Government Printing Office, Washington, D. C., 1962.
2. S. Glasstone (Ed.), *The Effects of Nuclear Weapons*, Superintendent of Documents, U. S. Government Printing Office, Washington, D. C., 1957.
3. J. H. Buell, Circular Slide Rules for Solving Linear Equations, *J. Forestry, 40:* 26-32 (January 1942).
4. Margaret F. Culbertson, An Oceanographic Slide Rule for Computing Temperature, Depth, and Salinity, *Trans. Am. Geophys. Union, 36:* 473-480 (June 1955).

*Table 4.1 lists 28 different problems that can be evaluated on the slide rule described in this report.

5. R. K. Allan, *Mech. World Eng. Record,* The Elements of Scales, Special Slide Rules, and Disc Calculators, *138* (3462): 6-12 (January 1958); Scales for Disc Calculators and Calculators for Practical Formulae, *138* (3463): 67-71 (February 1958); and Scales for Disc Calculators and Calculators for Practical Formulae, *138* (3464): 124-129 (March 1958).
6. A. W. Swan, Retracing the Steps in the Design of a Special Rule, *Engineer, 211:* 691-692 (April 1961).

Chapter 2

NUMERICAL EVALUATION OF WEAPONS-EFFECTS DATA

2.1 GENERAL

The weapons-effects information used to prepare the slide rule was obtained from the 1962 edition of *The Effects of Nuclear Weapons*,[1] where, with a few exceptions, the data for various effects parameters are presented in graphical form. It was necessary to determine mathematical relations for each of the parameters by curve fitting to facilitate computation of the several scales for the slide rule. This procedure also smoothed the data, thus eliminating any irregularities or discontinuities which might have been present in the original graphical presentation.

The results of the numerical analysis of weapons-effects data in equation and graphical form are presented in this chapter. The same information will also be given for those effects parameters used on the slide rule for which curve fitting was unnecessary.

Each variable was used in its scaled form, where possible, to simplify the task of curve fitting. In only one of the three-variable problems does weapon yield appear as a separate and distinct variable, viz., that for initial ionizing radiation. All the other effects problems involving three variables could be described in terms of two variables; e.g., maximum overpressure (p_m) as a function of range (d) and weapon yield (W) is specified by the relation between p_m (14.7/P) and d $(1/W)^{1/3}$ $(P/14.7)^{1/3}$, where P is the ambient or barometric pressure in pounds per square inch and W is expressed in kilotons. Although P is included as a parameter, all numerical evaluations on the slide rule and in this report were made for an ambient pressure of 14.7 psi. Similarly, the ambient temperature, T_0, and the velocity of sound, c_0, were assigned the standard sea-level values of 519° Rankine and 1117 ft/sec, respectively.

All curve fits were made using the least-squares method employing (with several exceptions*) the following equation form:

$$\log y = \sum_{i=0}^{i=1,2,\text{ or } 3} a_i (\log x)^i \qquad (2.1)$$

where x and y are the independent and dependent variables, respectively, and the a_i's are the regression coefficients. Transformation of the variables to the logarithmic form was desirable for two reasons. First, it made the relations more linear, thus making possible a better polynomial fit with only a few terms. Second, it allowed an easy and convenient separation of the quantities within a scaled parameter; e.g., log $(d/W^{1/3})$ can be written as log $d-(1/3)$ log W.

For convenience in computing the slide-rule scales it was usually necessary to consider scaled range (e.g., $d/W^{1/3}$) as the dependent variable (y) and the effects parameter as the independent variable (x) (see Eq. 2.1). Since the reverse arrangement is more satisfactory for other purposes, the curve fits were made by both methods. Also, curve fits of blast data are reported for heights of bursts which were not placed on the slide rule because of space limi-

*See Eqs. 2.112, 2.113, 2.115, and 2.116.

tations. Thus the information presented in this chapter can be used to augment that which can be read from the slide rule.

The accuracy with which the fitted curves represent the input data (from about 5 to 20 points, depending on the nature of the charts in Ref. 1) is indicated by the standard error of estimate of log y in percentage of y, $(E_{1y})\%$. If, for example, $(E_{1y})\%$ is 1 per cent, then it can be said that about 68 per cent of the input points have values of y within ±1 per cent of the values specified by the regression equation.

The goodness-of-fit criterion previously discussed has the weakness that it does not indicate the uniformity with which the regression equation specifies the input data. It is possible, for instance, for the fit to be very good everywhere except for the higher values of y; this nonuniformity could result in a relatively low $(E_{1y})\%$. For this reason a visual comparison was made between the plotted regression equations and the plotted input points. Where the fit was not uniformly good over the entire curve, the data were fitted with two equations, one for the lower, and another for the higher, values of y.

The reliability of weapons-effects data is difficult, if not impossible, to define precisely. Although the data presented here have stated limitations (e.g., visibility, ambient pressure, and temperature), other factors cannot be assessed, such as atmospheric inversion layers and cloudiness which are known to affect the blast wave and thermal radiation, respectively. Discussions of these various effects can be found in *The Effects of Nuclear Weapons*.[1] It can be said, however, that, in comparison with uncertainties and inaccuracies inherent in weapons-effects data, those inaccuracies which may result from the curve-fitting procedure are quite insignificant.

2.2 BLAST-WAVE PARAMETERS

Blast-wave information placed on the slide rule and presented in this section defines for surface burst and optimum burst heights (see list of symbols for definition) the relations between maximum values of incident overpressure, dynamic pressure, or wind and range and yield and between duration or arrival time of the blast wave and maximum overpressure and yield or range and yield. Criteria for maximum overpressure, maximum dynamic pressure, and duration of positive overpressure are also presented in this section for seven heights of burst, even though they do not appear on the slide rule.

Table 2.1 contains the material defining blast-wave parameters for a surface burst. The polynomial used in the curve fitting, specified in the previous section in Eq. 2.1, is stated at the top of the table. The variables are listed under y and x in their scaled forms (see Chap. 3 of Ref. 1). The region of applicability for each equation is stated under "Limits of x" in the units specified in a footnote to the table. The columns "a," "b," "c," and "d" list the regression coefficients. The last column contains the goodness-of-fit criterion, $(E_{1y})\%$, which was discussed in Sec. 2.1. Note that each blast parameter appears in the first equation as the dependent variable and in the next equation as the independent one. The equations used in the preparation of the slide rule are noted in the table by ‡. The equations in the table marked with † are plotted in Fig. 2.1.

The evaluations of maximum wind velocity (u_m) were not obtained directly from Ref. 1; they were derived from values of maximum dynamic pressure (q_m) and maximum overpressure (p_m) by use of the following equations, which were obtained from Ref. 1,

$$u_m = \sqrt{\frac{2q_m}{\rho_m}} \tag{2.2}$$

where

$$\rho_m = \rho_0 \frac{7 + (6p_m/P_0)}{7 + (p_m/P_0)} \tag{2.3}$$

(Text continues on page 32.)

TABLE 2.1—EQUATIONS* FCR BLAST-WAVE PARAMETERS, SURFACE BURST: $H(1/W)^{1/3}(P/14.7)^{1/3} = 0$ FT

$\log y = a + b \log x + c (\log x)^2 + d (\log x)^3$

Eq.	y	x	Limits of x	a	b	c	d	$(E_{1y})\%$
2.4†	$p_m(14.7/P)$	$d(1/W)^{1/3}(P/14.7)^{1/3}$	0.0472 to 4.82	−0.1877932	−1.3986162	+0.3255743	−0.0267036	2.8
2.5‡	$d(1/W)^{1/3}(P/14.7)^{1/3}$	$p_m(14.7/P)$	0.1 to 200	−0.1307982	−0.6836211	+0.1091296	−0.0167348	1.6
2.6†	$q_m(14.7/P)$	$d(1/W)^{1/3}(P/14.7)^{1/3}$	0.0615 to 4.73	−1.9790344	−2.7267144	+0.5250615	−0.1160756	12.1
2.7‡	$d(1/W)^{1/3}(P/14.7)^{1/3}$	$q_m(14.7/P)$	0.000242 to 200	−0.6383041	−0.2831997	+0.0180404	−0.0010955	2.9
2.8†	$t_p(1/W)^{1/3}(P/14.7)^{1/3}(T_0/519)^{1/2}$	$d(1/W)^{1/3}(P/14.7)^{1/3}$	0.0677 to 0.740	−0.1739890	+0.5265382	−0.0772505	+0.0654855	0.8
2.9	$d(1/W)^{1/3}(P/14.7)^{1/3}$	$t_p(1/W)^{1/3}(P/14.7)^{1/3}(T_0/519)^{1/2}$	0.1 to 0.57	+0.3634010	+2.2244315	+0.8734061	+0.1814097	0.9
2.10	$t_p(1/W)^{1/3}(P/14.7)^{1/3}(T_0/519)^{1/2}$	$p_m(14.7/P)$	2.50 to 90	−0.2450537	−0.3809152			2.3
2.11‡	$p_m(14.7/P)$	$t_p(1/W)^{1/3}(P/14.7)^{1/3}(T_0/519)^{1/2}$	0.1 to 0.4	−0.6402582	−2.6204817			5.9
2.12†	$t_a(1/W)^{1/3}(P/14.7)^{1/3}(T_0/519)^{1/2}$	$d(1/W)^{1/3}(P/14.7)^{1/3}$	0.0570 to 1.10	+0.6078753	+1.1039021	−0.2836934	+0.1006855	1.5
2.13	$d(1/W)^{1/3}(P/14.7)^{1/3}$	$t_a(1/W)^{1/3}(P/14.7)^{1/3}(T_0/519)^{1/2}$	0.04 to 4.5	−0.4812621	+0.6936740	+0.1439396	+0.0275385	0.8
2.14	$t_a(1/W)^{1/3}(P/14.7)^{1/3}(T_0/519)^{1/2}$	$p_m(14.7/P)$	0.576 to 129.2	+0.4597434	−0.7913534	−0.0419376	−0.0003161	1.6
2.15‡	$p_m(14.7/P)$	$t_a(1/W)^{1/3}(P/14.7)^{1/3}(T_0/519)^{1/2}$	0.04 to 4.5	+0.5641315	−1.1923301	−0.0725151	−0.0069143	1.7
2.16†	$u_m(1117/c_0)$	$d(1/W)^{1/3}(P/14.7)^{1/3}$	0.0598 to 4.73	+1.3827823	−1.3518147	+0.1841482	+0.0361427	6.0
2.17‡	$d(1/W)^{1/3}(P/14.7)^{1/3}$	$u_m(1117/c_0)$	3.68 to 1760	+1.2135450	−1.0270209	+0.1260382	−0.0124891	3.9

* Definitions:

c_0, ft/sec (ambient velocity of sound)

$d(1/W)^{1/3}(P/14.7)^{1/3}$, miles (range)

$(E_{1y})\%$, % (standard error of estimate of log y in percentage of y)

$H(1/W)^{1/3}(P/14.7)^{1/3}$, ft (burst height)

P, psi (ambient pressure)

$p_m(14.7/P)$, psi (maximum overpressure)

$q_m(14.7/P)$, psi (maximum dynamic pressure)

T_0, degrees Rankine (ambient temperature)

$t_a(1/W)^{1/3}(P/14.7)^{1/3}(T_0/519)^{1/2}$, sec (time after detonation at which blast wave arrives)

$t_p(1/W)^{1/3}(P/14.7)^{1/3}(T_0/519)^{1/2}$, sec (duration of positive overpressure)

$u_m(1117/c_0)$, mph (maximum wind velocity)

W, kt (weapon yield)

† Plotted in Fig. 2.1 (with W = 1 kt, P = 14.7 psi, T_0 = 519° Rankine, c_0 = 1117 ft/sec)

‡ Used to determine circular-computer values.

TABLE 2.2—EQUATIONS* FOR BLAST-WAVE PARAMETERS, BURST HEIGHT: $H(1/W)^{1/3}(P/14.7)^{1/3} = 100$ FT

$\log y = a + b \log x + c (\log x)^2 + d (\log x)^3$

Eq.	y	x	Limits of x	a	b	c	d	$(E_{1y})\%$
2.18†	$p_m(14.7/P)$	$d(1/W)^{1/3}(P/14.7)^{1/3}$	0.0478 to 0.797	−0.1404953	−1.3987412	+0.3060928	−0.0257474	2.8
2.19	$d(1/W)^{1/3}(P/14.7)^{1/3}$	$p_m(14.7/P)$	1 to 200	−0.0985896	−0.6788230	+0.0846268	−0.0089153	1.3
2.20†	$q_m(14.7/P)$	$d(1/W)^{1/3}(P/14.7)^{1/3}$	0.0745 to 0.792	−1.9745441	−3.6856865	−1.7303483	−1.6155376	10.4
2.21	$d(1/W)^{1/3}(P/14.7)^{1/3}$	$q_m(14.7/P)$	0.0241 to 200	−0.6092885	−0.2895225	+0.0217332	+0.0031729	2.3
2.22†	$t_p(1/W)^{1/3}(P/14.7)^{1/3}(T_0/519)^{1/2}$	$d(1/W)^{1/3}(P/14.7)^{1/3}$	0.0685 to 0.790	−0.1786622	+0.6559447	+0.2062754	+0.2135306	1.2
2.23	$d(1/W)^{1/3}(P/14.7)^{1/3}$	$t_p(1/W)^{1/3}(P/14.7)^{1/3}(T_0/519)^{1/2}$	0.1 to 0.57	+0.3200273	+1.6949498	−0.2200029	−0.4337651	1.2

* See footnote to Table 2.1.

† Plotted in Fig. 2.2 (with W = 1 kt, P = 14.7 psi, T_0 = 519° Rankine).

TABLE 2.3 — EQUATIONS* FOR BLAST-WAVE PARAMETERS, BURST HEIGHT: $H(1/W)^{1/3}(P/14.7)^{1/3}$ = 200 FT

$\log y = a + b \log x + c (\log x)^2 + d (\log x)^3$

Eq.	y	x	Limits of x	a	b	c	d	$(E_{ly})\%$
2.24†	$p_m(14.7/P)$	$d(1/W)^{1/3}(P/14.7)^{1/3}$	0.0490 to 0.877	−0.0797506	−1.3959217	+0.2044584	−0.0898945	5.8
2.25	$d(1/W)^{1/3}(P/14.7)^{1/3}$	$p_m(14.7/P)$	1 to 200	−0.0564384	−0.7063068	+0.0838300	−0.0057337	2.7
2.26†	$q_m(14.7/P)$	$d(1/W)^{1/3}(P/14.7)^{1/3}$	0.0887 to 0.872	−1.8239388	−3.5829705	−2.2762727	−2.4710880	11.0
2.27	$d(1/W)^{1/3}(P/14.7)^{1/3}$	$q_m(14.7/P)$	0.0241 to 200	−0.5852208	−0.2805063	+0.0320775	+0.0013454	2.3
2.28†	$t_p(1/W)^{1/3}(P/14.7)^{1/3}(T_0/519)^{1/2}$	$d(1/W)^{1/3}(P/14.7)^{1/3}$	0.0759 to 0.878	−0.2072098	+0.6290804	+0.2717107	+0.3389482	1.2
2.29	$d(1/W)^{1/3}(P/14.7)^{1/3}$	$t_p(1/W)^{1/3}(P/14.7)^{1/3}(T_0/519)^{1/2}$	0.0898 to 0.57	+0.4510387	+2.2103485	+0.5317823	−0.1436087	1.2

* See footnote to Table 2.1.
† Plotted in Fig. 2.3 (with W = 1 kt, P = 14.7 psi, T_0 = 519° Rankine).

TABLE 2.4 — EQUATIONS* FOR BLAST-WAVE PARAMETERS, BURST HEIGHT: $H(1/W)^{1/3}(P/14.7)^{1/3}$ = 300 FT

$\log y = a + b \log x + c (\log x)^2 + d (\log x)^3$

Eq.	y	x	Limits of x	a	b	c	d	$(E_{ly})\%$
2.30†	$p_m(14.7/P)$	$d(1/W)^{1/3}(P/14.7)^{1/3}$	0.0714 to 0.930	−0.0578733	−1.7217232	−0.6158905	−0.5932959	5.9
2.31	$d(1/W)^{1/3}(P/14.7)^{1/3}$	$p_m(14.7/P)$	1 to 100	−0.0324052	−0.6430061	−0.0307184	+0.0375190	2.9
2.32†	$q_m(14.7/P)$	$d(1/W)^{1/3}(P/14.7)^{1/3}$	0.0901 to 0.933	−1.7219695	−3.4656308	−2.1033142	−2.3664168	9.7
2.33	$d(1/W)^{1/3}(P/14.7)^{1/3}$	$q_m(14.7/P)$	0.0241 to 200	−0.5634748	−0.2883645	+0.0311643	+0.0019967	2.3
2.34†	$t_p(1/W)^{1/3}(P/14.7)^{1/3}(T_0/519)^{1/2}$	$d(1/W)^{1/3}(P/14.7)^{1/3}$	0.0758 to 0.920	−0.2184009	+0.7221117	+0.5685217	+0.5805367	1.0
2.35	$d(1/W)^{1/3}(P/14.7)^{1/3}$	$t_p(1/W)^{1/3}(P/14.7)^{1/3}(T_0/519)^{1/2}$	0.0742 to 0.57	+0.5004257	+2.3087016	+0.6342833	−0.1293869	2.2

* See footnote to Table 2.1.
† Plotted in Fig. 2.4 (with W = 1 kt, P = 14.7 psi, T_0 = 519° Rankine).

TABLE 2.5 — EQUATIONS* FOR BLAST-WAVE PARAMETERS, BURST HEIGHT: $H(1/W)^{1/3}(P/14.7)^{1/3}$ = 400 FT

$\log y = a + b \log x + c (\log x)^2 + d (\log x)^3$

Eq.	y	x	Limits of x	a	b	c	d	$(E_{ly})\%$
2.36†	$p_m(14.7/P)$	$d(1/W)^{1/3}(P/14.7)^{1/3}$	0.0945 to 0.981	−0.0118234	−1.4592956	+0.1531863	−0.0521166	5.7
2.37	$d(1/W)^{1/3}(P/14.7)^{1/3}$	$p_m(14.7/P)$	1 to 50	−0.0083104	−0.6809590	+0.0443969	+0.0032291	3.1
2.38†	$q_m(14.7/P)$	$d(1/W)^{1/3}(P/14.7)^{1/3}$	0.104 to 0.976	−1.62521265	−3.3053984	−1.0236306	−0.9211364	4.3
2.39	$d(1/W)^{1/3}(P/14.7)^{1/3}$	$q_m(14.7/P)$	0.0241 to 30	−0.5459328	−0.3310994	+0.0133009	+0.0081654	1.2
2.40†	$t_p(1/W)^{1/3}(P/14.7)^{1/3}(T_0/519)^{1/2}$	$d(1/W)^{1/3}(P/14.7)^{1/3}$	0.0760 to 0.976	−0.2376787	+0.6059041	+0.1844921	+0.2508134	0.6
2.41	$d(1/W)^{1/3}(P/14.7)^{1/3}$	$t_p(1/W)^{1/3}(P/14.7)^{1/3}(T_0/519)^{1/2}$	0.092 to 0.57	+0.4643346	+1.9705520	+0.1038057	−0.3149834	1.0

* See footnote to Table 2.1.
† Plotted in Fig. 2.5 (with W = 1 kt, P = 14.7 psi, T_0 = 519° Rankine).

TABLE 2.6 — EQUATIONS* FOR BLAST-WAVE PARAMETERS, BURST HEIGHT: $H(1/W)^{1/3}(P/14.7)^{1/3}$ = 500 FT

$\log y = a + b \log x + c (\log x)^2 + d (\log x)^3$

Eq.	y	x	Limits of x	a	b	c	d	$(E_{1y})\%$
2.42†	$p_m(14.7/P)$	$d(1/W)^{1/3}(P/14.7)^{1/3}$	0.0959 to 1.03	+0.0212905	−1.2940302	+0.7501414	+0.3959222	6.6
2.43	$d(1/W)^{1/3}(P/14.7)^{1/3}$	$p_m(14.7/P)$	1 to 50	+0.0158545	−0.7504681	+0.1812493	−0.0573264	3.8
2.44†	$q_m(14.7/P)$	$d(1/W)^{1/3}(P/14.7)^{1/3}$	0.101 to 1.02	−1.5839066	−3.2497198	−0.8126391	−0.6391557	4.1
2.45	$d(1/W)^{1/3}(P/14.7)^{1/3}$	$q_m(14.7/P)$	0.0241 to 30	−0.5278705	−0.3409243	+0.0063541	+0.0070650	1.3
2.46†	$t_p(1/W)^{1/3}(P/14.7)^{1/3}(T_0/519)^{1/2}$	$d(1/W)^{1/3}(P/14.7)^{1/3}$	0.0758 to 1.04	−0.2514291	+0.5300260	−0.1210572	−0.0470312	1.0
2.47	$d(1/W)^{1/3}(P/14.7)^{1/3}$	$t_p(1/W)^{1/3}(P/14.7)^{1/3}(T_0/519)^{1/2}$	0.117 to 0.57	+0.5134322	+2.2431859	+0.8977344	+0.4007463	1.7

* See footnote to Table 2.1.

† Plotted in Fig. 2.6 (with W = 1 kt, P = 14.7 psi, T_0 = 519° Rankine).

TABLE 2.7 — EQUATIONS* FOR BLAST-WAVE PARAMETERS, BURST HEIGHT: $H(1/W)^{1/3}(P/14.7)^{1/3}$ = 600 FT

$\log y = a + b \log x + c (\log x)^2 + d (\log x)^3$

Eq.	y	x	Limits of x	a	b	c	d	$(E_{1y})\%$
2.48†	$p_m(14.7/P)$	$d(1/W)^{1/3}(P/14.7)^{1/3}$	0.128 to 1.10	+0.0432924	−1.0646446	+1.8298279	+1.3675448	7.7
2.49	$d(1/W)^{1/3}(P/14.7)^{1/3}$	$p_m(14.7/P)$	1 to 30	+0.0382755	−0.8763984	−0.4701227	−0.2046373	4.7
2.50†	$q_m(14.7/P)$	$d(1/W)^{1/3}(P/14.7)^{1/3}$	0.129 to 1.07	−1.5278955	−3.1879356	−0.4386330	−0.2751808	7.8
2.51	$d(1/W)^{1/3}(P/14.7)^{1/3}$	$q_m(14.7/P)$	0.0241 to 15	−0.5034153	−0.3368230	−0.0008120	+0.0026188	2.6
2.52†	$t_p(1/W)^{1/3}(P/14.7)^{1/3}(T_0/519)^{1/2}$	$d(1/W)^{1/3}(P/14.7)^{1/3}$	0.097 to 1.08	−0.2592632	+0.4814931	−0.4276645	−0.4020925	2.3
2.53	$d(1/W)^{1/3}(P/14.7)^{1/3}$	$t_p(1/W)^{1/3}(P/14.7)^{1/3}(T_0/519)^{1/2}$	0.170 to 0.57	+0.8798280	+4.9519163	+7.4283841	+5.3385521	3.8

* See footnote to Table 2.1.

† Plotted in Fig. 2.7 (with W = 1 kt, P = 14.7 psi, T_0 = 519° Rankine).

TABLE 2.8 — EQUATIONS* FOR BLAST-WAVE PARAMETERS, BURST HEIGHT: $H(1/W)^{1/3}(P/14.7)^{1/3}$ = 700 FT

$\log y = a + b \log x + c (\log x)^2 + d (\log x)^3$

Eq.	y	x	Limits of x	a	b	c	d	$(E_{1y})\%$
2.54†	$p_m(14.7/P)$	$d(1/W)^{1/3}(P/14.7)^{1/3}$	0.170 to 1.12	+0.0607198	−1.2947325	+1.3555552	+1.2238203	7.3
2.55	$d(1/W)^{1/3}(P/14.7)^{1/3}$	$p_m(14.7/P)$	1 to 20	+0.0468997	−0.7764501	+0.3312436	−0.1647522	4.7
2.56†	$q_m(14.7/P)$	$d(1/W)^{1/3}(P/14.7)^{1/3}$	0.160 to 1.10	−1.4842554	−3.2581558	−0.3032786	+0.0442789	11.3
2.57	$d(1/W)^{1/3}(P/14.7)^{1/3}$	$q_m(14.7/P)$	0.0241 to 8	−0.4786226	−0.3374592	−0.0151122	−0.0032678	3.9
2.58†	$t_p(1/W)^{1/3}(P/14.7)^{1/3}(T_0/519)^{1/3}$	$d(1/W)^{1/3}(P/14.7)^{1/3}$	0.152 to 1.12	−0.2662145	+0.4705849	−0.6812750	−0.7654669	1.3
2.59	$d(1/W)^{1/3}(P/14.7)^{1/3}$	$t_p(1/W)^{1/3}(P/14.7)^{1/3}(T_0/519)^{1/2}$	0.205 to 0.57	+1.3040684	+8.2999053	+16.0372656	+12.2125284	3.7

* See footnote to Table 2.1.

† Plotted in Fig. 2.8 (with W = 1 kt, P = 14.7 psi, T_0 = 519° Rankine).

TABLE 2.9 — EQUATIONS* FOR BLAST-WAVE PARAMETERS, OPTIMUM HEIGHT OF BURST†

$$\log y = a + b \log x + c (\log x)^2 + d (\log x)^3$$

Eq.	y	x	Limits of x	a	b	c	d	$(E_{1y})\%$
2.60‡	$p_m(14.7/P)$	$d(1/W)^{1/3}(P/14.7)^{1/3}$	0.0508 to 1.35	+0.1829156	−1.4114030	−0.0373825	−0.1635453	6.1
2.61§	$d(1/W)^{1/3}(P/14.7)^{1/3}$	$p_m(14.7/P)$	1 to 200	+0.1292768	−0.7227471	+0.0147366	+0.0135239	3.5
2.62‡	$q_m(14.7/P)$	$d(1/W)^{1/3}(P/14.7)^{1/3}$	0.154 to 1.37	+1.2488468	−2.7368746			6.3
2.63§	$d(1/W)^{1/3}(P/14.7)^{1/3}$	$q_m(14.7/P)$	0.0241 to 9.408	−0.4563356	−0.3650091			2.3
2.64‡	$q_m(14.7/P)$	$d(1/W)^{1/3}(P/14.7)^{1/3}$	0.0932 to 0.154	−3.8996912	−6.0108828			11.2
2.65§	$d(1/W)^{1/3}(P/14.7)^{1/3}$	$q_m(14.7/P)$	9.408 to 200	−0.6511707	−0.1648319			1.8
2.66‡	$t_p(1/W)^{1/3}(P/14.7)^{1/3}(T_0/519)^{1/2}$	$d(1/W)^{1/3}(P/14.7)^{1/3}$	0.0514 to 1.29	−0.3434670	+0.3708961	+0.0841782	+0.2382956	0.9
2.67	$d(1/W)^{1/3}(P/14.7)^{1/3}$	$t_p(1/W)^{1/3}(P/14.7)^{1/3}(T_0/519)^{1/2}$	0.064 to 0.5	+1.3237634	+4.9326611	+3.3766350	+0.9019516	0.1
2.68	$t_p(1/W)^{1/3}(P/14.7)^{1/3}(T_0/519)^{1/2}$	$p_m(14.7/P)$	1 to 200	−0.2969664	−0.2449086	−0.0065515	−0.0252191	2.4
2.69§	$p_m(14.7/P)$	$t_p(1/W)^{1/3}(P/14.7)^{1/3}(T_0/519)^{1/2}$	0.064 to 0.510	−1.5786513	−6.3356208	−3.7796571	−0.9943531	6.4
2.70‡	$t_a(1/W)^{1/3}(P/14.7)^{1/3}(T_0/519)^{1/2}$	$d(1/W)^{1/3}(P/14.7)^{1/3}$	0.0379 to 0.954	+0.6351033	+1.0691963	−0.1700728	+0.0059191	0.9
2.71	$d(1/W)^{1/3}(P/14.7)^{1/3}$	$t_a(1/W)^{1/3}(P/14.7)^{1/3}(T_0/519)^{1/2}$	0.057 to 4.10	−0.5458990	+0.7945565	+0.0919073	+0.0148927	0.7
2.72	$t_a(1/W)^{1/3}(P/14.7)^{1/3}(T_0/519)^{1/2}$	$p_m(14.7/P)$	1.65 to 382.9	+0.7782040	−0.7599115	−0.0649698	+0.0217023	0.7
2.73§	$p_m(14.7/P)$	$t_a(1/W)^{1/3}(P/14.7)^{1/3}(T_0/519)^{1/2}$	0.057 to 4.10	+0.9697326	−1.2090078	−0.0041401	−0.0598191	0.9
2.74‡	$u_m(1117/c_0)$	$d(1/W)^{1/3}(P/14.7)^{1/3}$	0.2568 to 1.4	+1.7110032	−1.2000278	+0.8182584	+1.0652528	2.1
2.75§	$d(1/W)^{1/3}(P/14.7)^{1/3}$	$u_m(1117/c_0)$	35.97 to 295.6	+4.4720967	−5.4493230	+2.2883925	−0.3681920	1.8
2.76‡	$u_m(1117/c_0)$	$d(1/W)^{1/3}(P/14.7)^{1/3}$	0.0762 to 0.2568	+3.8320701	+5.6357427	+6.6091754	+1.5690375	4.9
2.77§	$d(1/W)^{1/3}(P/14.7)^{1/3}$	$u_m(1117/c_0)$	295.6 to 3.981	+16.6081687	−15.9021473	+4.8732066	−0.5066940	2.4
2.78	$H(1/W)^{1/3}(P/14.7)^{1/3}$ ¶	$p_m(14.7/P)$	1 to 200	+3.2015016	−0.3263444			5.1
2.79‡	$H(1/W)^{1/3}(P/14.7)^{1/3}$ ¶	$d(1/W)^{1/3}(P/14.7)^{1/3}$	0.0512 to 1.35	+3.1356018	+0.3833517	−0.1159125		5.7

* See footnote to Table 2.1.

† Height of burst to maximize parameter of interest (see List of Symbols).

‡ Plotted in Fig. 2.9 (with W = 1 kt, P = 14.7 psi, T_0 = 519° Rankine, c_0 = 1117 ft/sec).

§ Used to determine circular-computer values.

¶ This is height of burst to maximize overpressure.

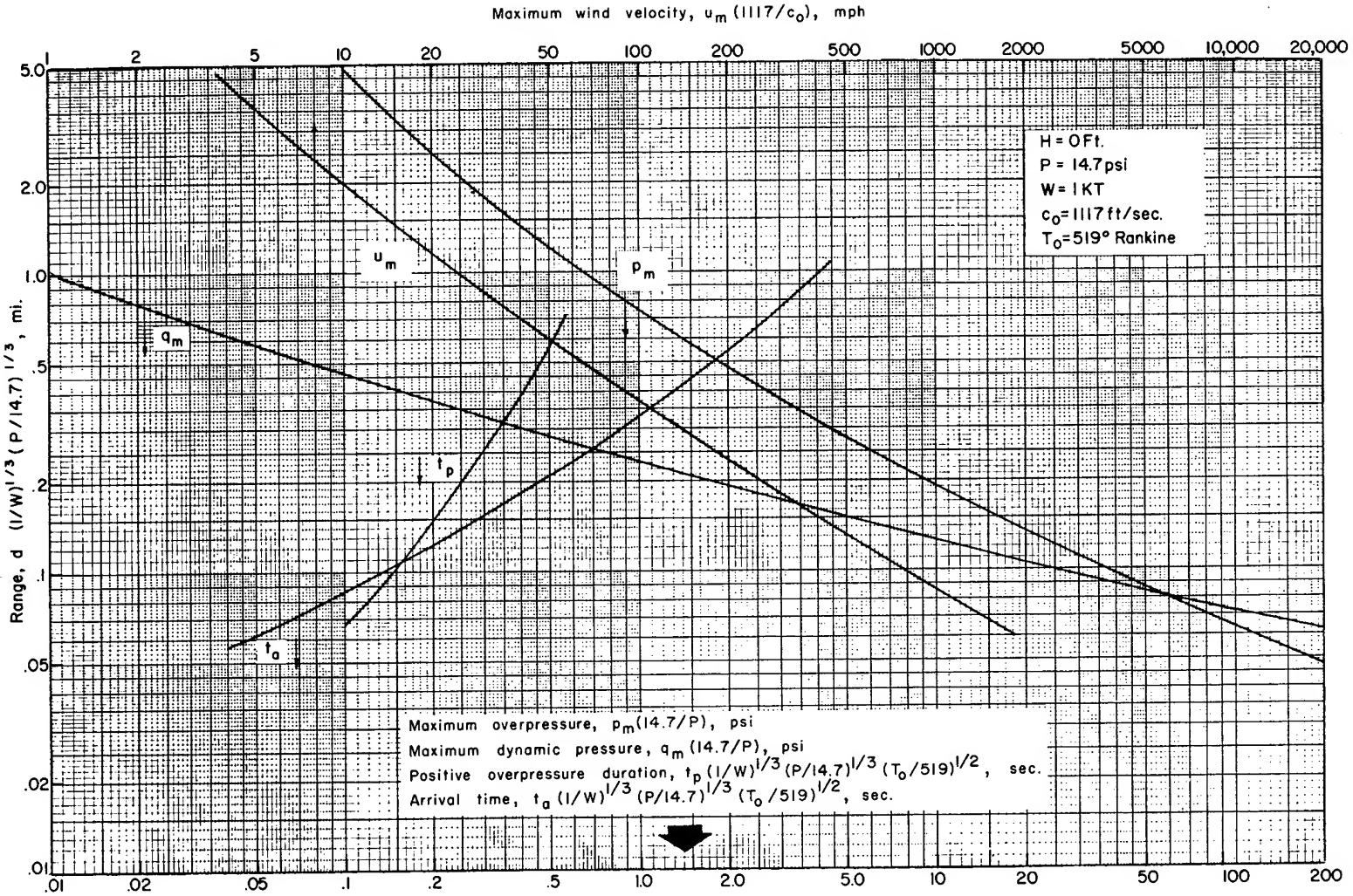

Fig. 2.1—Scaled blast parameters for surface bursts as a function of scaled range. These are plots of Eqs. 2.4, 2.6, 2.8, 2.12, and 2.16 given in Table 2.1. The four effects parameters listed at the bottom of the chart and the one at the top are read on the lower and upper scales, respectively.

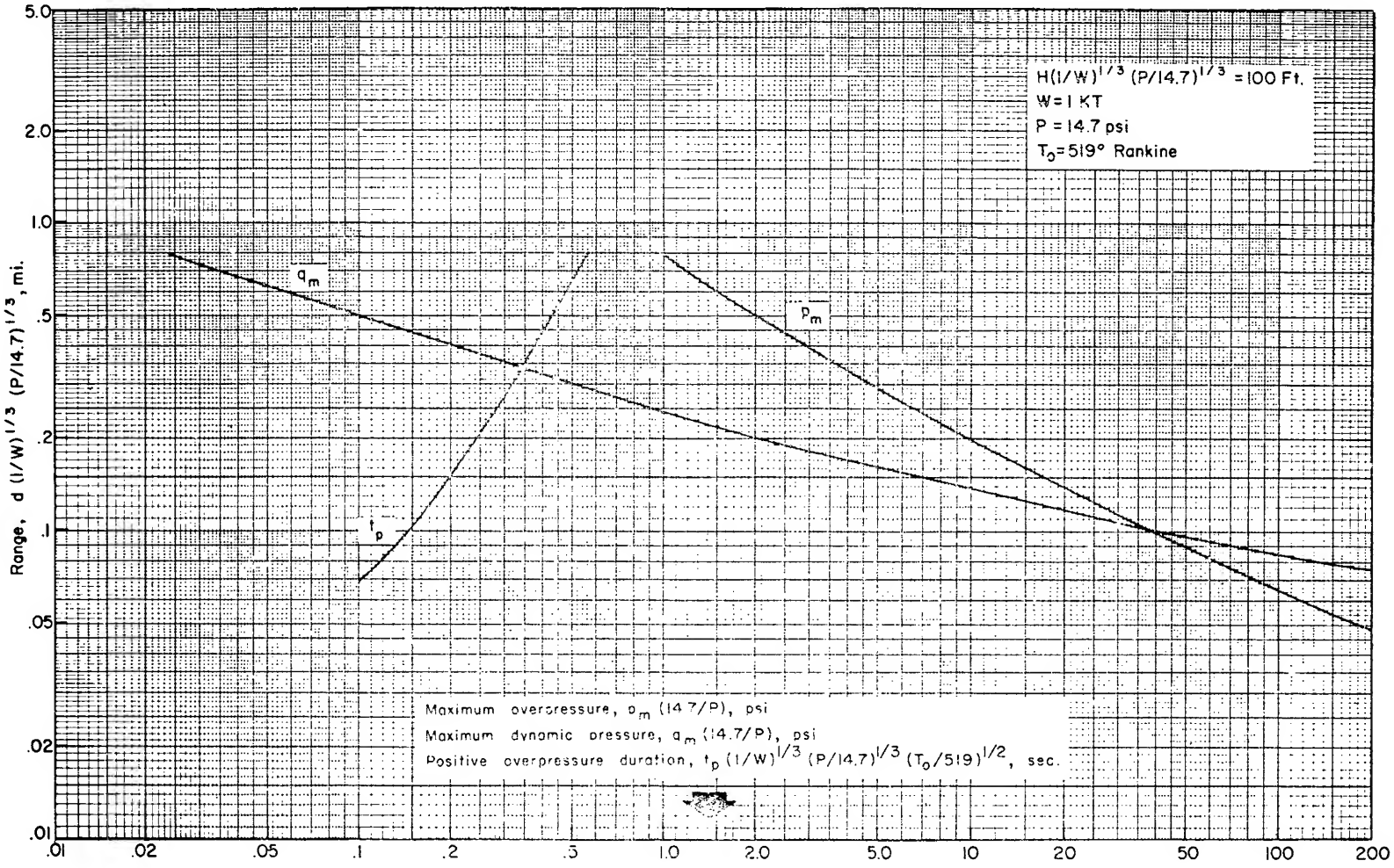

Fig. 2.2—Scaled blast parameters for a scaled height of burst of 100 ft as a function of scaled range. These are plots of Eqs. 2.18, 2.20, and 2.22 given in Table 2.2.

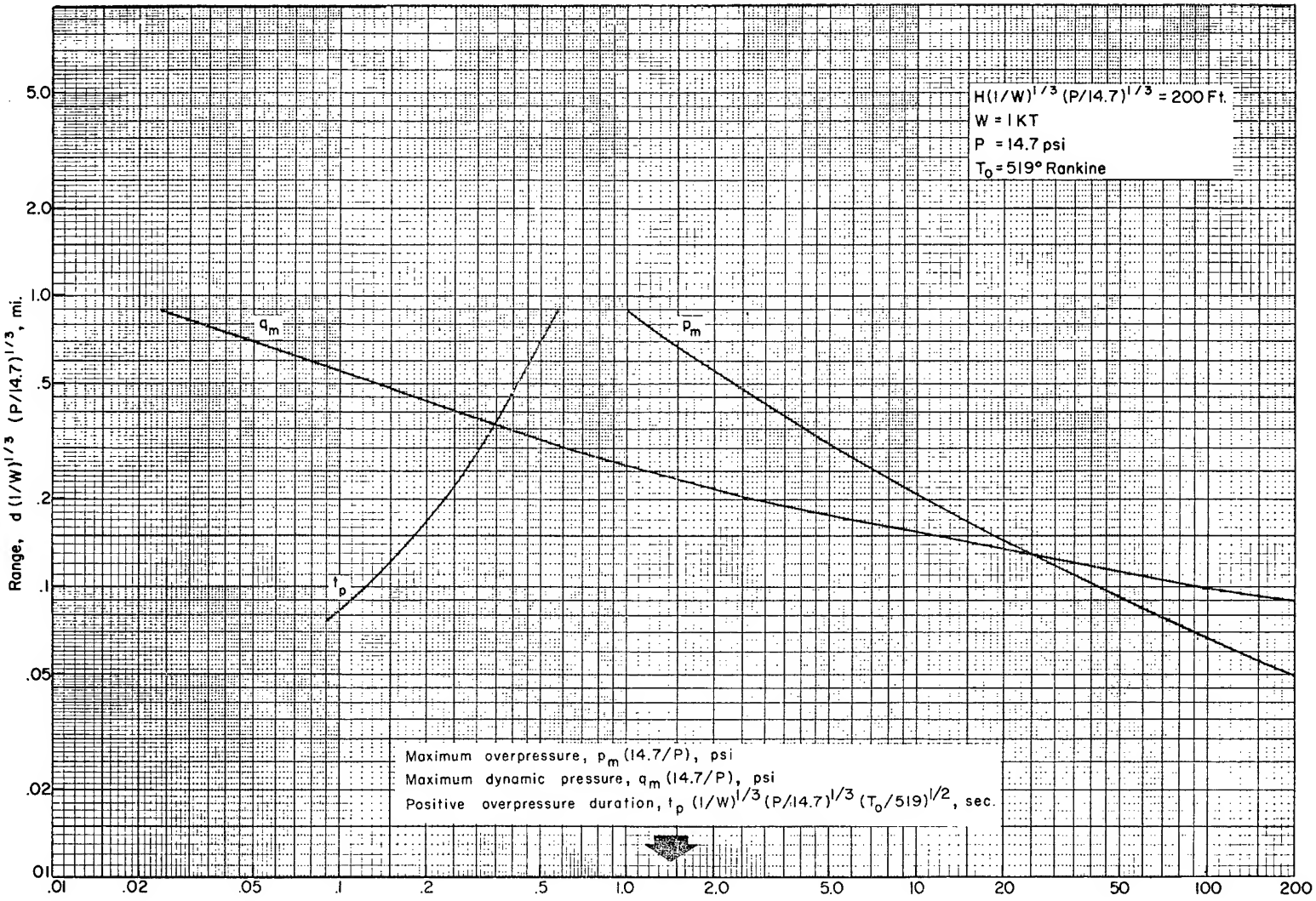

Fig. 2.3—Scaled blast parameters for a scaled height of burst of 200 ft as a function of scaled range. These are plots of Eqs. 2.24, 2.26, and 2.28 given in Table 2.3.

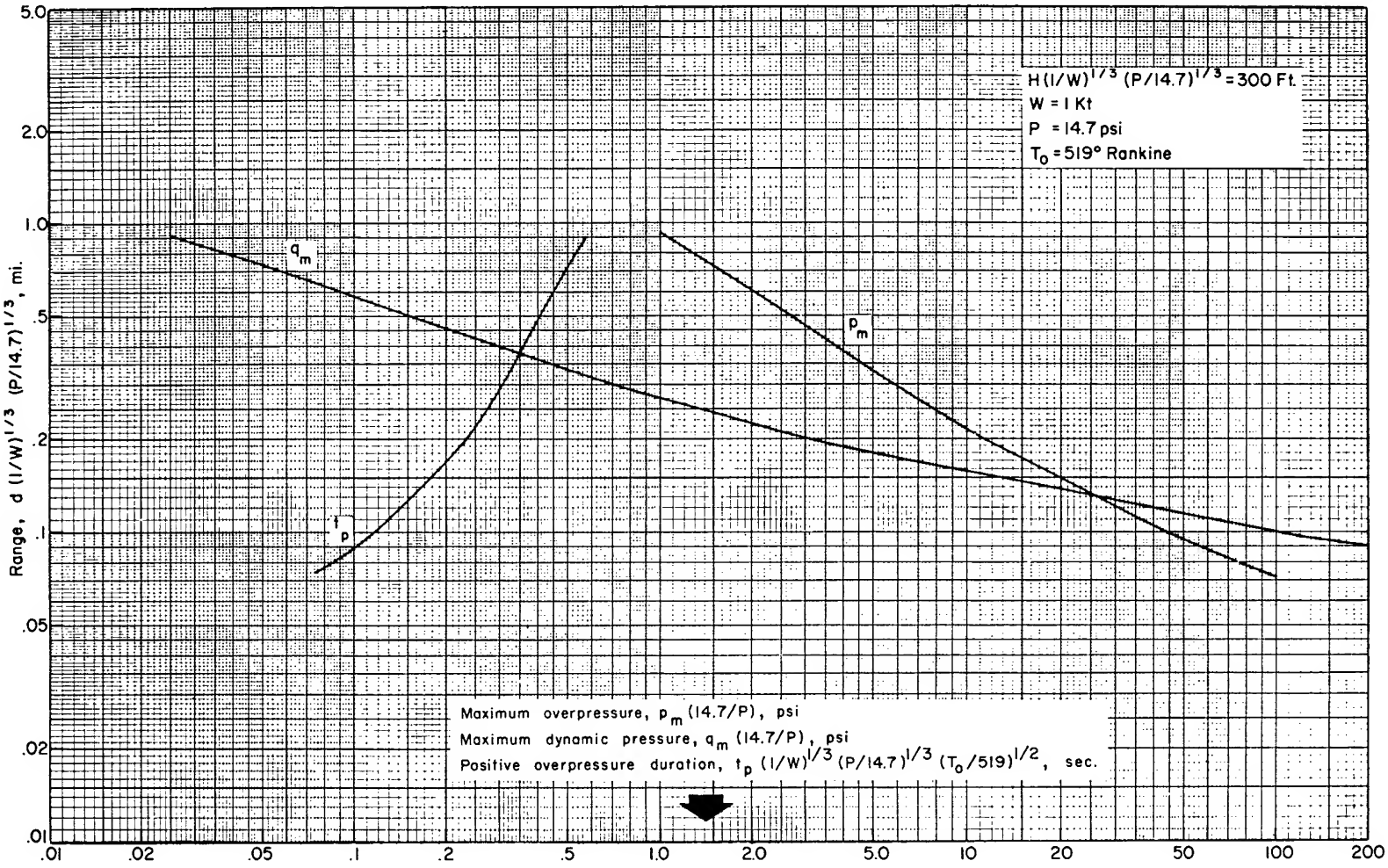

Fig. 2.4—Scaled blast parameters for a scaled height of burst of 300 ft as a function of scaled range. These are plots of Eqs. 2.30, 2.32, and 2.34 given in Table 2.4.

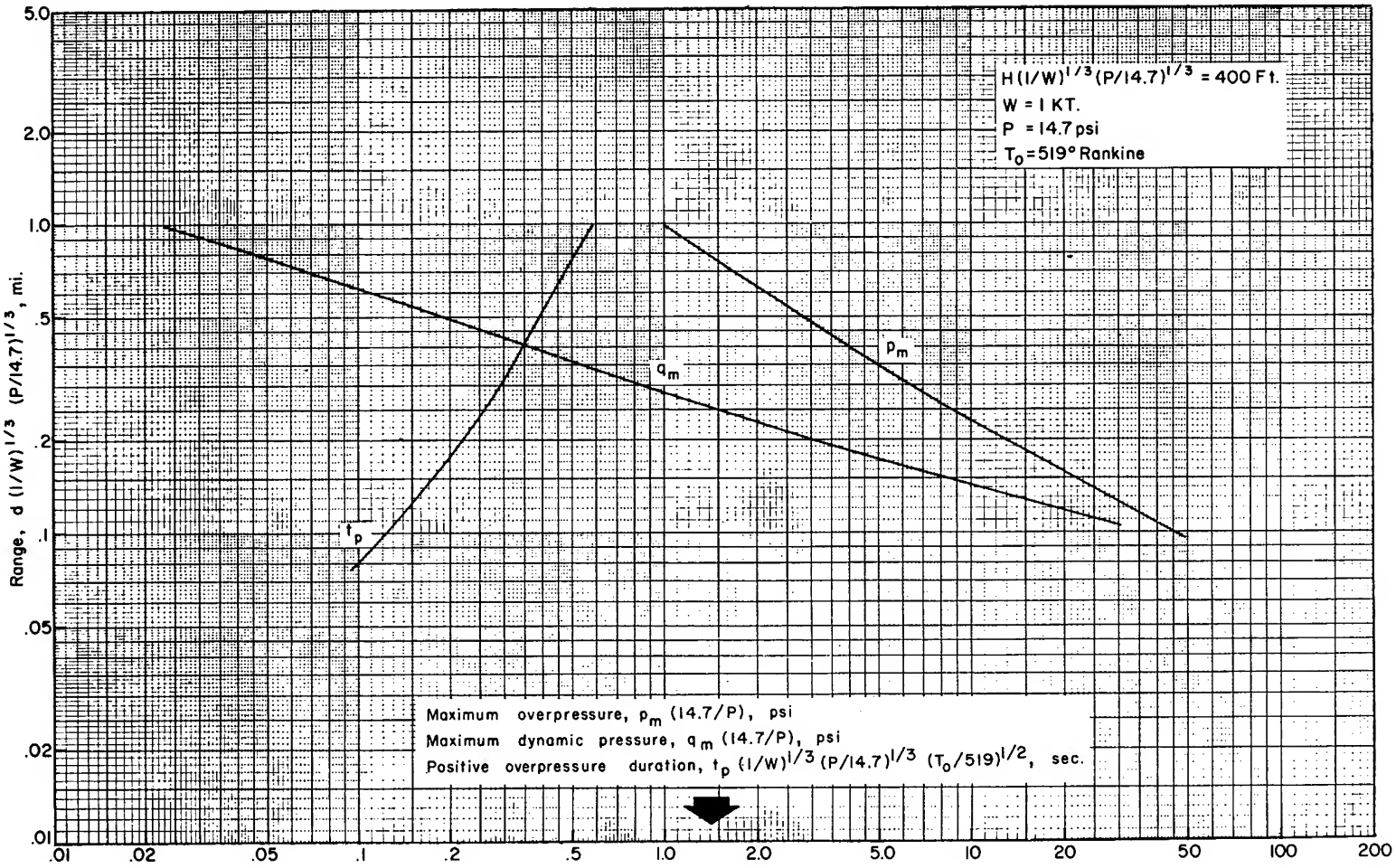

Fig. 2.5—Scaled blast parameters for a scaled height of burst of 400 ft as a function of scaled range. These are plots of Eqs. 2.36, 2.38, and 2.40 given in Table 2.5.

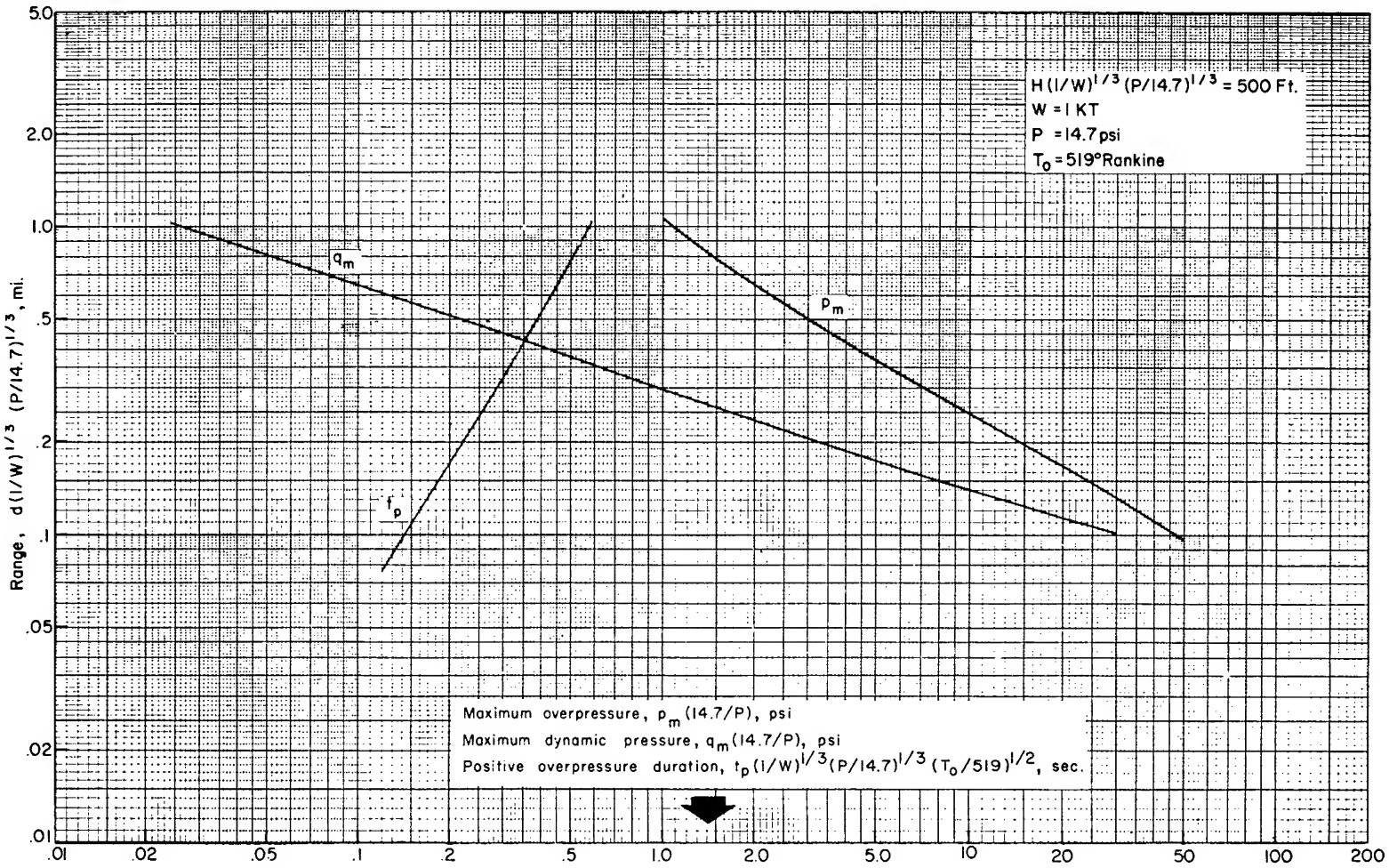

Fig. 2.6—Scaled blast parameters for a scaled height of burst of 500 ft as a function of scaled range. These are plots of Eqs. 2.42, 2.44, and 2.46 given in Table 2.6.

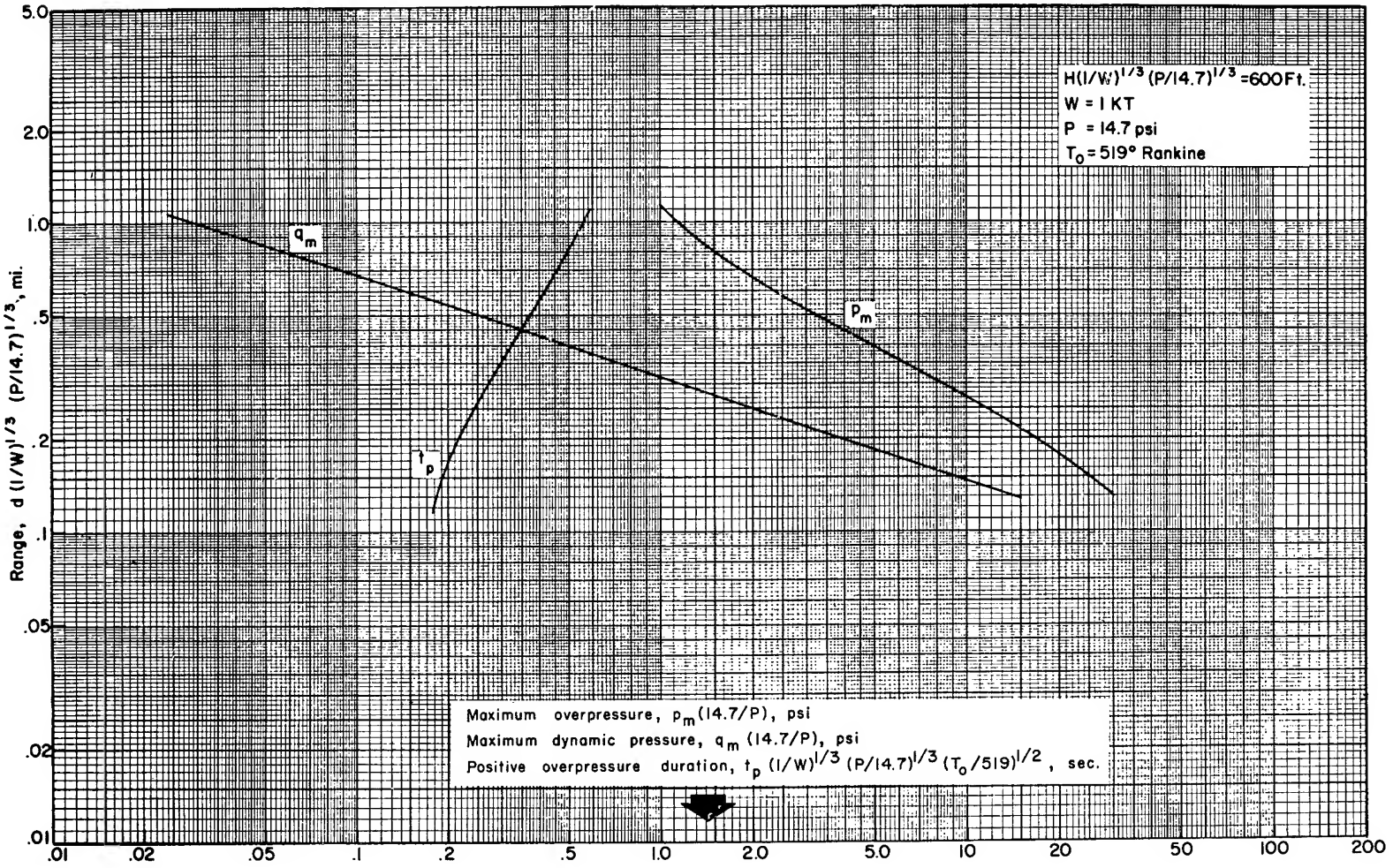

Fig. 2.7—Scaled blast parameters for a scaled height of burst of 600 ft as a function of scaled range. These are plots of Eqs. 2.48, 2.50, and 2.52 given in Table 2.7.

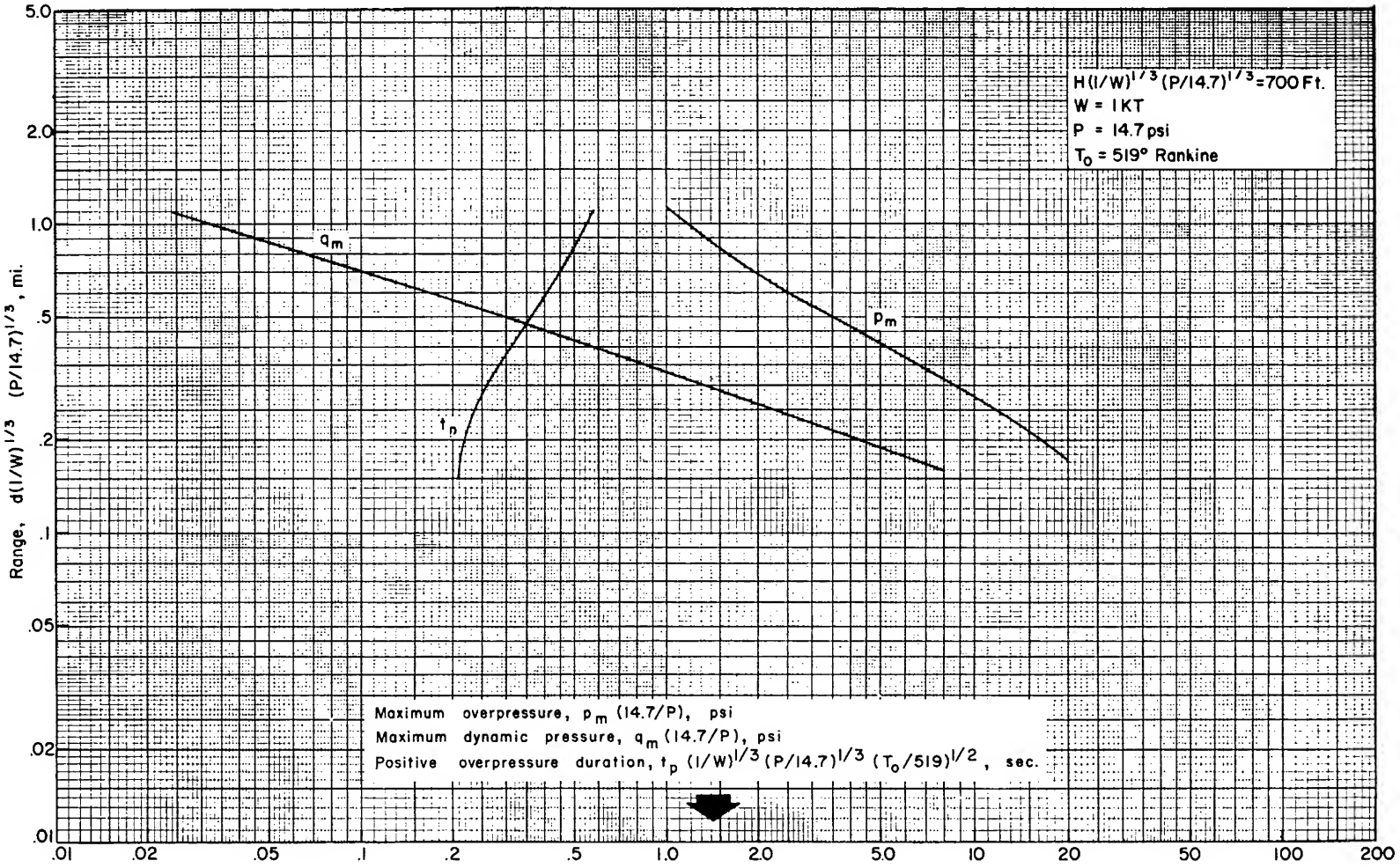

Fig. 2.8—Scaled blast parameters for a scaled height of burst of 700 ft as a function of scaled range. These are plots of Eqs. 2.54, 2.56, and 2.58 given in Table 2.8.

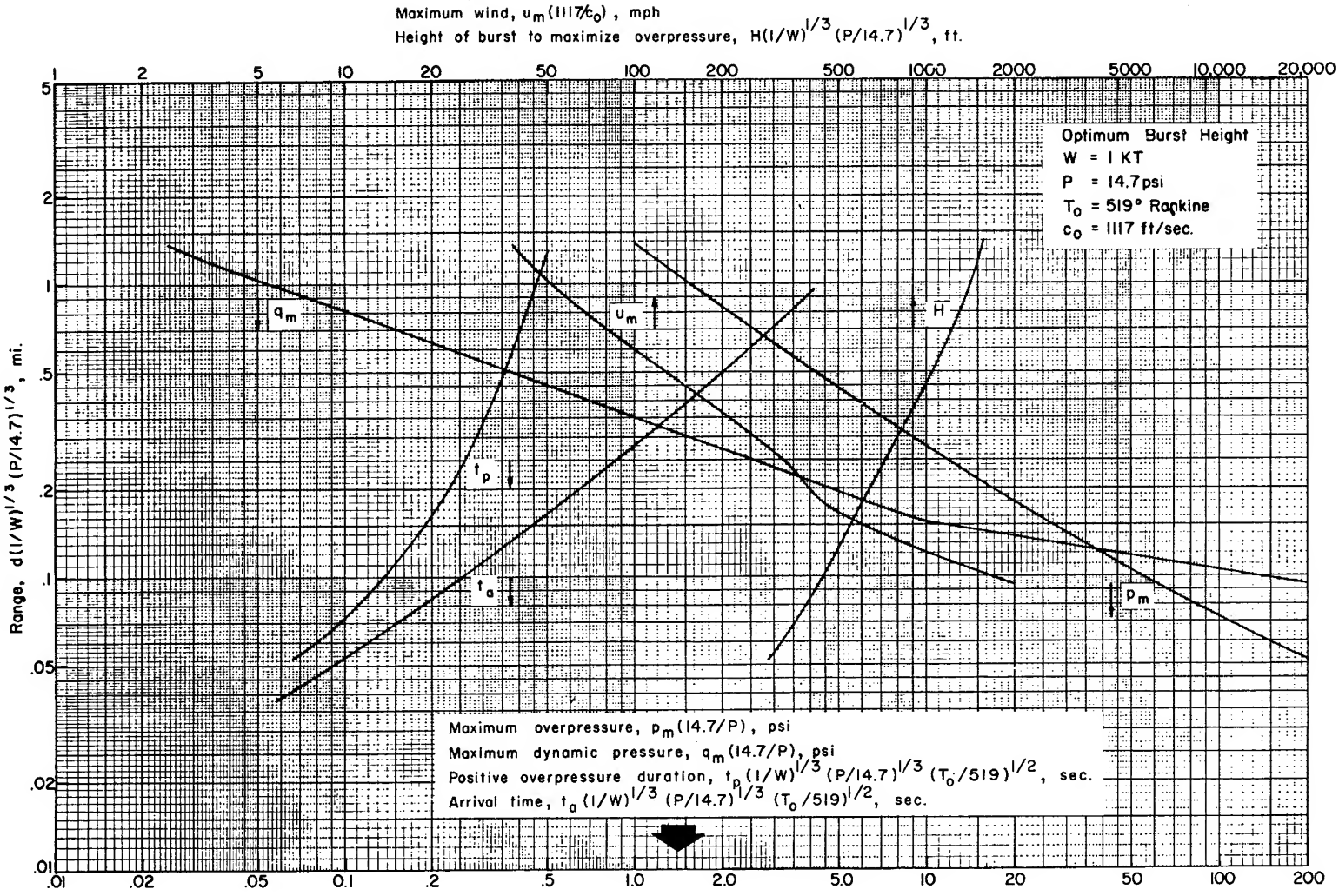

Fig. 2.9—Scaled blast parameters for optimum heights of burst as a function of scaled range. These are plots of Eqs. 2.60, 2.62, 2.64, 2.66, 2.70, 2.74, 2.76, and 2.79 given in Table 2.9.

approximate $(t_a)_{OPT}$ is based on the HOB giving $(p_m)_{OPT}$

ρ_0 and P_0 being the standard sea-level values of air density and pressure, respectively.

Equations presented in Tables 2.2 through 2.8 are similar to those in Table 2.1 for maximum overpressure, maximum dynamic pressure, and duration of the positive overpressure (all functions of range and yield), except that they apply to scaled heights of burst of 100, 200, 300, 400, 500, 600, and 700 ft, respectively. Some equations (listed in footnotes to the tables) are also presented in graphical form. These equations are plotted in figures whose numbers correspond to the table numbers.

Equations for the optimum heights of burst are listed in Table 2.9. The optimum-height-of-burst data were derived from the height-of-burst plots in Chap. 3 of Ref. 1. The optimum burst height is defined as that height of burst which causes a particular value of a parameter to extend to the maximum range. The last two equations in Table 2.9 specify the optimum burst heights for maximum overpressure as functions of maximum overpressure and yield and of range and yield, respectively. Optimum burst heights for dynamic pressure (not specified by equation) are, in general, different from those for maximum overpressure. The maximum winds were computed by Eqs. 2.2 and 2.3 using the appropriate maximum dynamic pressures and maximum overpressures evaluated at the optimum heights of burst for dynamic pressure. Equations noted in Table 2.9 by the symbol ‡ are plotted in Fig. 2.9.

2.3 REFLECTED OVERPRESSURE AT NORMAL INCIDENCE

When a blast wave with a well-defined shock strikes a flat surface placed at an angle of 90° to the direction of wave propagation, an immediate rise in pressure is noted near the flat surface which is defined[1] by

$$p_r = 2p_m \frac{7P + 4p_m}{7P + p_m} \tag{2.80}$$

where p_r = reflected overpressure
P = ambient or barometric pressure
p_m = maximum or shock overpressure before reflection

Equation 2.80 is plotted in Fig. 2.10 for the condition that P = 14.7 psi. Note, however, that the coordinates are labeled in scaled form so that values of reflected overpressure can be evaluated for conditions where other ambient pressures exist.

To facilitate computation of the scale for reflected overpressure vs. maximum overpressure on the slide rule, Eq. 2.80 was solved for p_m:

$$p_m = \frac{p_r - 14P + \sqrt{p_r^2 + 196\, p_r\, P + 196\, P^2}}{16} \tag{2.81}$$

2.4 TRANSLATIONAL VELOCITIES FOR MAN AND WINDOW GLASS AT 10-FT DISPLACEMENT

The assumptions and conditions applicable to the material in this section are discussed in Sec. 4.3. The discussion here will be confined to the numerical procedures and approximations used to determine the equations listed in Table 2.10.

Results reported in Refs. 2 and 3 were used to determine, for weapons burst at the optimum height and at the surface, the ranges at which man and window glass would attain given velocities in 10 ft of travel. The results of this effort are represented in Table 2.10 by 16 regression equations defining range as a function of yield for particular: (1) objects (man or

(Text continues on page 40.)

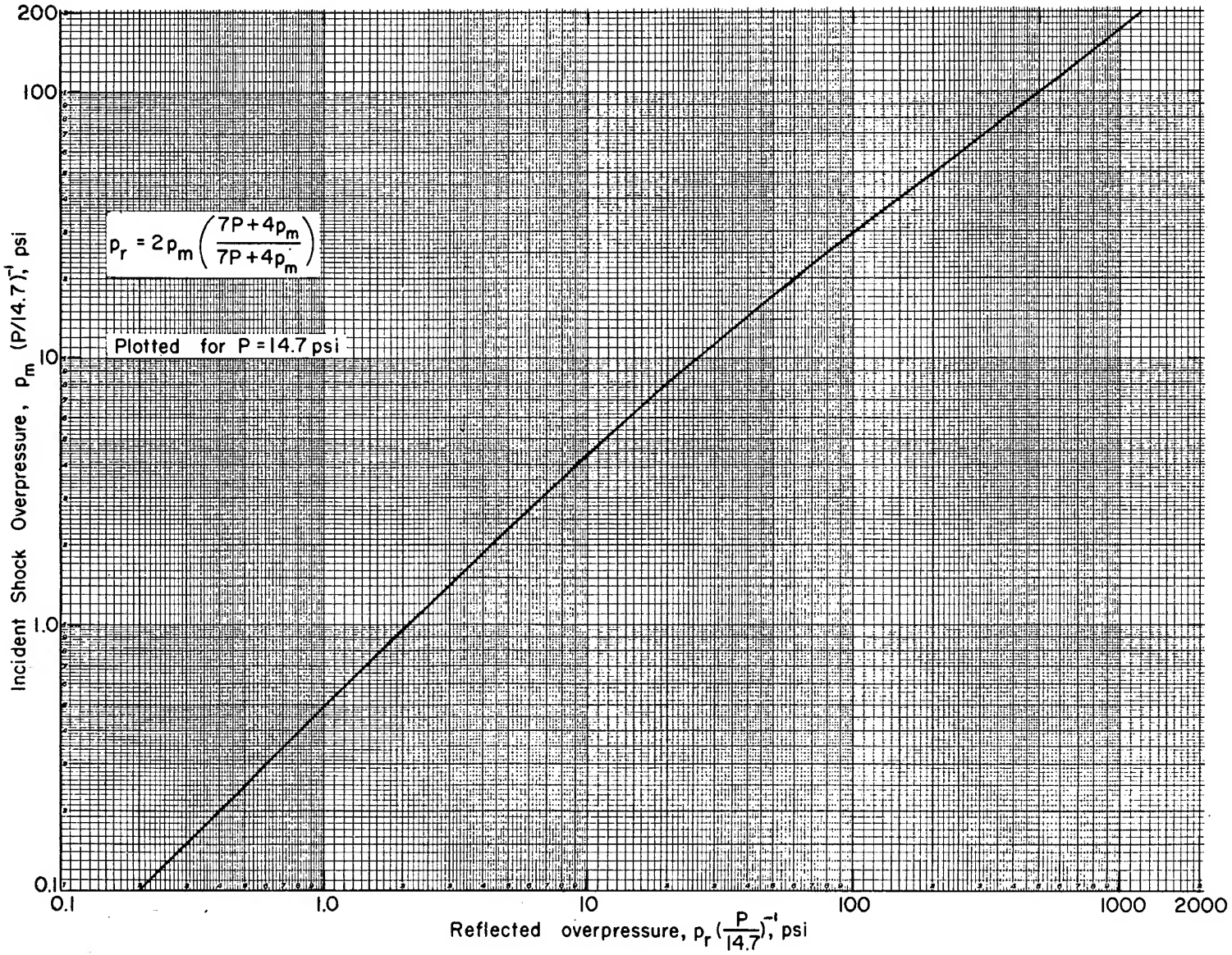

Fig. 2.10—Reflected overpressure at normal incidence as a function of incident overpressure.

TABLE 2.10—EQUATIONS* FOR VELOCITY OF MAN OR WINDOW GLASS AT A 10-FT DISPLACEMENT FOR SURFACE BURST OR OPTIMUM BURST HEIGHT

$$\log y = a + b (\log x) + c (\log x)^2$$

Eq.	Type burst	Object	$v_{10\ ft}$	y	x	Limits of x	a	b	c	$(E_{1y})\%$
2.82	Optimum	Man†	10	d	W	1 to 20,000	−0.4363424	+0.4781674	−0.0116938	1.8
2.83	Optimum	Man	20	d	W	1 to 20,000	−0.5549846	+0.4722507	−0.0146448	0.3
2.84	Optimum	Man	30	d	W	1 to 20,000	−0.6348220	+0.4701340	−0.0161922	0.9
2.85	Optimum	Man	40	d	W	1 to 20,000	−0.6926139	+0.4673666	−0.0171205	1.1
2.86‡	Optimum	Man		$v_{10\ ft(m)}$	$d/(W)^{0.4}$	0.2173 to 0.4484	+0.2110630	−2.4489933	−0.5292686	0.2
2.87§	Optimum	Man		$d/(W)^{0.4}$	$v_{10\ ft(m)}$	10 to 40	+0.0520158	−0.3242644	−0.0761458	0.1
2.88	Surface	Man	10	d	W	1 to 20,000	−0.6192752	+0.4515675	−0.0089664	1.7
2.89	Surface	Man	20	d	W	1 to 20,000	−0.7151170	+0.4461348	−0.0118821	0.3
2.90	Surface	Man	30	d	W	1 to 20,000	−0.7762995	+0.4412225	−0.0126691	0.5
2.91	Surface	Man	40	d	W	1 to 20,000	−0.8223441	+0.4391498	−0.0134394	0.9
2.92‡	Surface	Man		$v_{10\ ft(m)}$	$d/(W)^{0.4}$	0.1485 to 0.2692	−0.5011010	−2.8434981	−0.3676657	0.1
2.93	Surface	Man		$d/(W)^{0.4}$	$v_{10\ ft(m)}$	10 to 40	−0.1874271	−0.3532710	−0.0292066	0.05
2.94	Optimum	Glass¶	50	d	W	1 to 20,000	−0.0503093	+0.4188503	−0.0105591	1.7
2.95	Optimum	Glass	100	d	W	1 to 20,000	−0.2023333	+0.3901263	−0.0075365	0.4
2.96	Optimum	Glass	200	d	W	1 to 20,000	−0.3711231	+0.3682720	−0.0047432	0.7
2.97	Optimum	Glass	400	d	W	1 to 20,000	−0.5547838	+0.3536225	−0.0023343	0.7
2.98‡	Optimum	Glass		$v_{10\ ft(g)}$	$d/(W)^{0.35}$	0.2736 to 1.058	+1.7379493	−1.5783619	−0.0768745	0.2
2.99§	Optimum	Glass		$d/(W)^{0.35}$	$v_{10\ ft(g)}$	50 to 400	+1.0364069	−0.5595410	−0.0211707	0.1
2.100	Surface	Glass	50	d	W	1 to 20,000	−0.2948006	+0.4108761	−0.0097760	1.3
2.101	Surface	Glass	100	d	W	1 to 20,000	−0.4270421	+0.3810870	−0.0061578	0.7
2.102	Surface	Glass	200	d	W	1 to 20,000	−0.5672298	+0.3621193	−0.0039206	0.7
2.103	Surface	Glass	400	d	W	1 to 20,000	−0.7136894	+0.3499070	−0.0019774	0.5
2.104‡	Surface	Glass		$v_{10\ ft(g)}$	$d/(W)^{0.35}$	0.1875 to 0.5885	+1.3133856	−1.6302906	+0.1954137	0.1
2.105	Surface	Glass		$d/(W)^{0.35}$	$v_{10\ ft(g)}$	50 to 400	+0.8484278	−0.6901637	+0.0325463	0.05

* Definitions:
d, miles (range)
$(E_{1y})\%$, % (standard error of estimate of log y in percentage of y)
$v_{10\ ft}$, ft/sec (velocity of object at 10-ft displacement) (object: m, man; g, window glass)
W, kt (yield)

† Man mass = 165 lb (acceleration coefficient: 0.03 sq ft/lb).

‡ Plotted in Fig. 2.11 (with W = 1 kt, P = 14.7 psi, c_0 = 1117 ft/sec).

§ Used to determine circular-computer values.

¶ Window-glass mass = 0.1 to 10 g (0.125 in. thick; acceleration coefficient, 0.72 sq ft/lb).

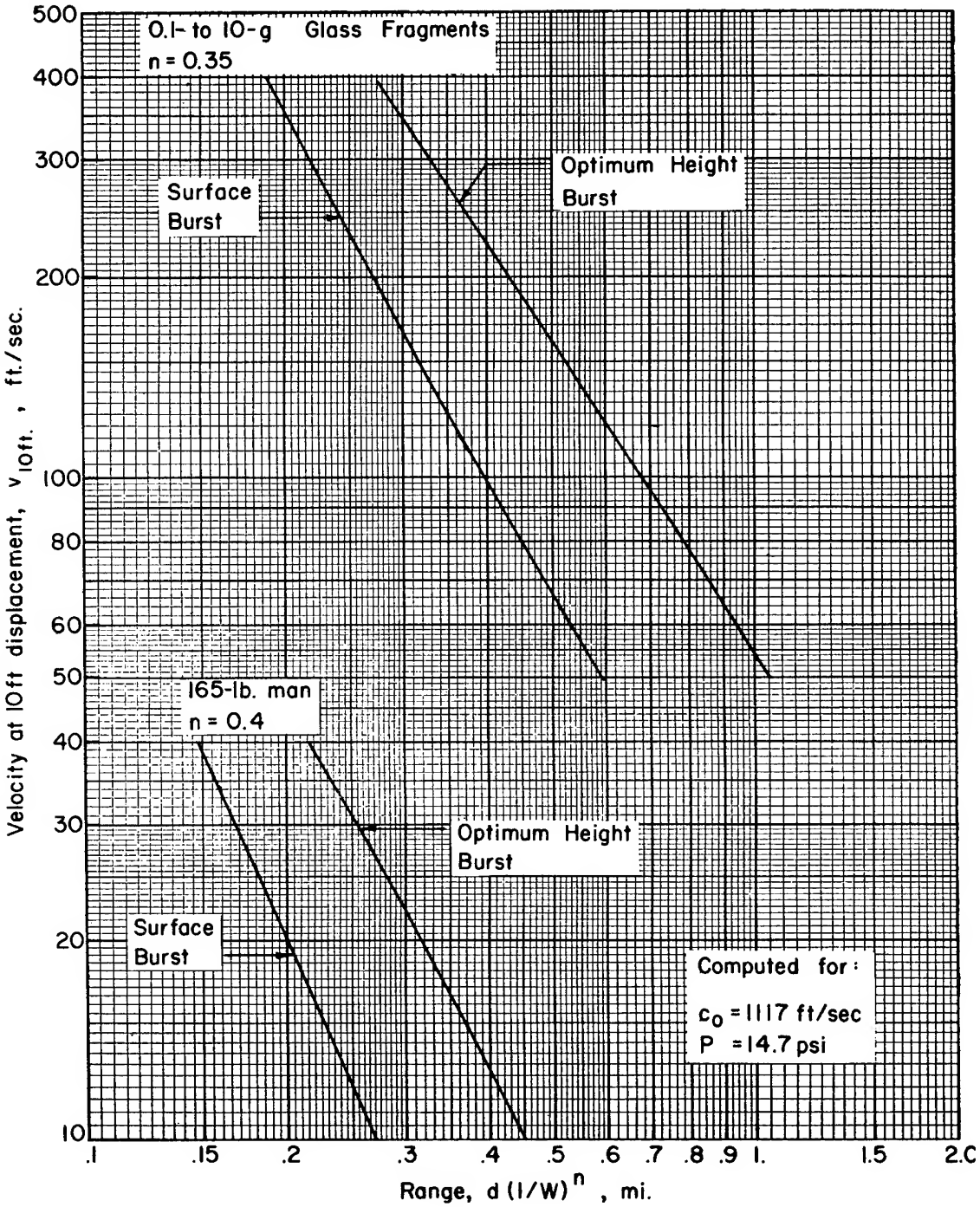

Fig. 2.11—Velocity of man or window glass at a 10-ft displacement for surface bursts or optimum heights of burst as a function of scaled range (see Eqs. 2.86, 2.92, 2.98, and 2.104 in Table 2.10).

TABLE 2.11 — EQUATIONS* FOR THERMAL RADIATION AND FIRST- OR SECOND-DEGREE BURNS FOR SURFACE AND AIR BURSTS

$$\log y = a + b \log x + c (\log x)^2 + d (\log x)^3 + e (\log x)^4 + f (\log x)^5$$

Eq.	Type burst	y	x	Limits of x	a	b	c	d	e	f	$(E_{1y})\%$
2.106	Air	$Q(1/W)$	d_s	0.05 to 50	−0.0401874	−2.0823477	−0.0511744	−0.0074958			0.4
2.107	Surface	$Q(1/0.7W)$	d	0.05 to 50	−0.0401874	−2.0823477	−0.0511744	−0.0074958			0.4
2.108†‡	Air	d_s	$Q(1/W)$	0.0001 to 100	−0.0193419	−0.4804553	−0.0055685	+0.0002013			0.2
2.109†§	Surface	d	$Q(1/0.7W)$	0.0001 to 100	−0.0193419	−0.4804553	−0.0055685	+0.0002013			0.2
2.110†¶	Air or surface	Q_{1st}	W	1 to 20,000	+0.3141555	+0.0599042	+0.0007636	−0.0002015			0.2
2.111†¶	Air or surface	Q_{2nd}	W	1 to 20,000	+0.6025982	+0.0201394	+0.0139640	+0.0008559			0.3
2.112**	Air or surface	Q%	$t/W^{1/3}$	0.012 to 0.285	+1.7457220	−1.9692127	−6.0520927	−7.4741163	−4.1282124	−0.7737418	4.1
2.113	Air or surface	$t/W^{1/3}$	Q%	1 to 80	−1.9905166	+0.7255752	−2.2779098	+4.1860716	−3.0182367	+0.7627880	3.0

* Definitions:

d, miles (range)

d_s, miles (slant range)

$(E_{1y})\%$, % (standard error of estimate of log y in percentage of y)

$Q(1/W)$, cal/cm^2 (thermal radiation)

Q_{1st}, cal/cm^2 (thermal radiation producing first-degree burns, bare white skin)

Q_{2nd}, cal/cm^2 (thermal radiation producing second-degree burns, bare white skin)

W, kt (yield)

Q%, % (percentage of total thermal radiation)

$t/W^{1/3}$, sec (time after detonation)

† Used to determine circular-computer values.

‡ Plotted in Fig. 2.12.

§ Plotted in Fig. 2.13.

¶ Plotted in Figs. 2.12 and 2.13.

** Plotted in Fig. 2.14.

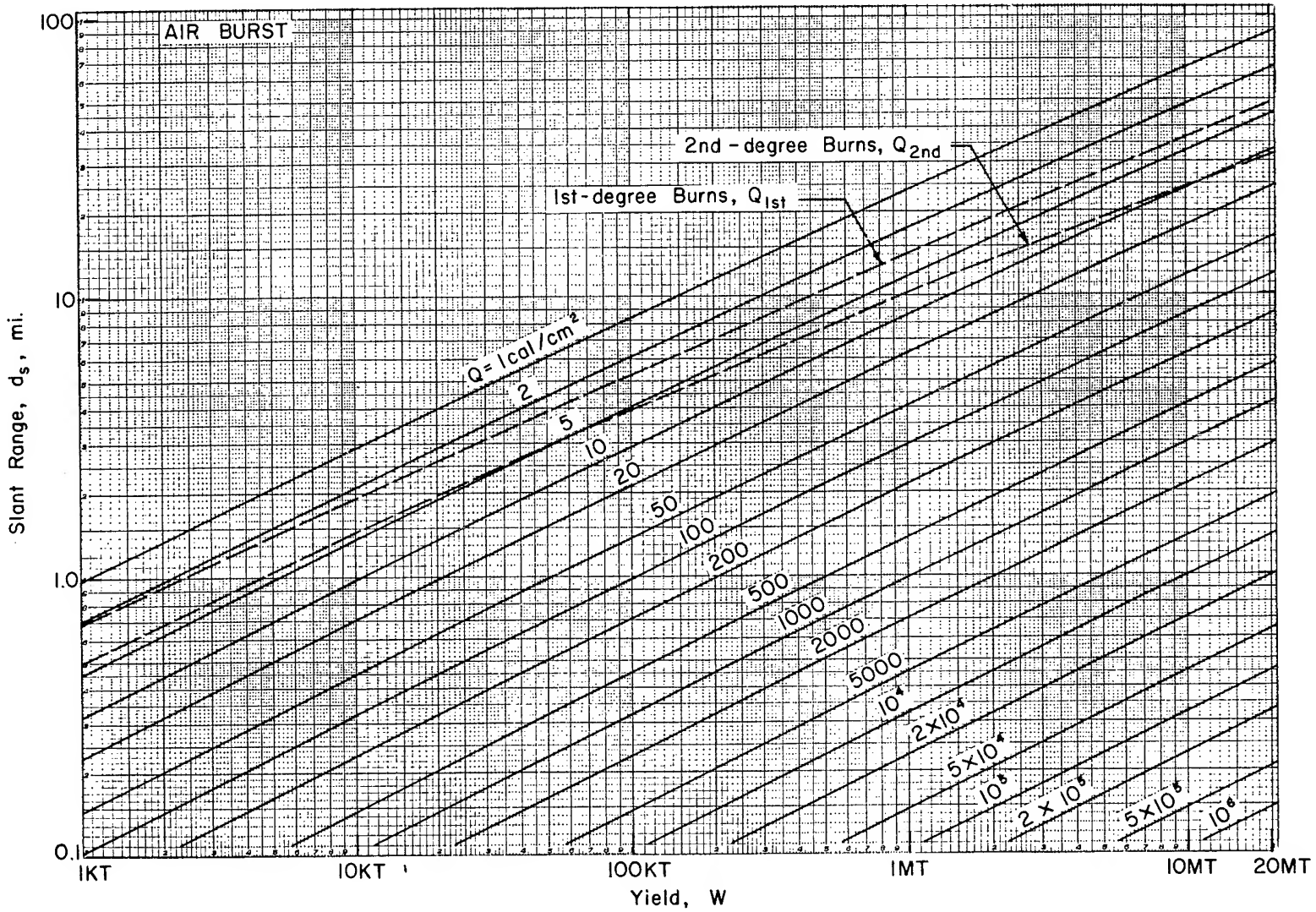

Fig. 2.12—Thermal radiation for air bursts as a function of yield and slant range (50-mile visibility). Also shown are first- and second-degree-burn lines applying to bare white skin as a function of yield (see Eqs. 2.108, 2.110, and 2.111 in Table 2.11).

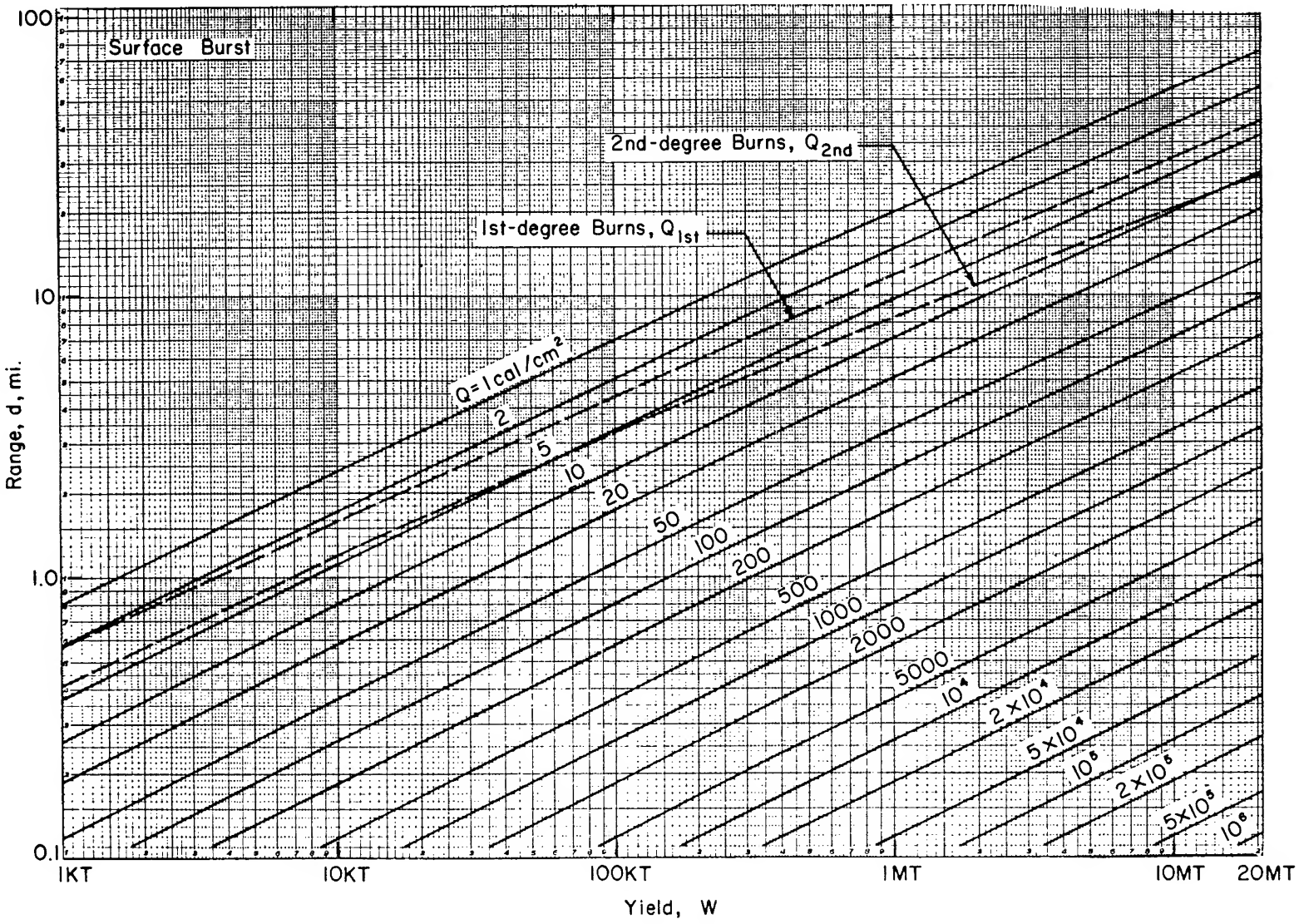

Fig. 2.13—Thermal radiation for surface bursts as a function of range and yield (50-mile visibility) and first- and second-degree burns for bare white skin vs. yield (see Eqs. 2.109 through 2.111 in Table 2.11).

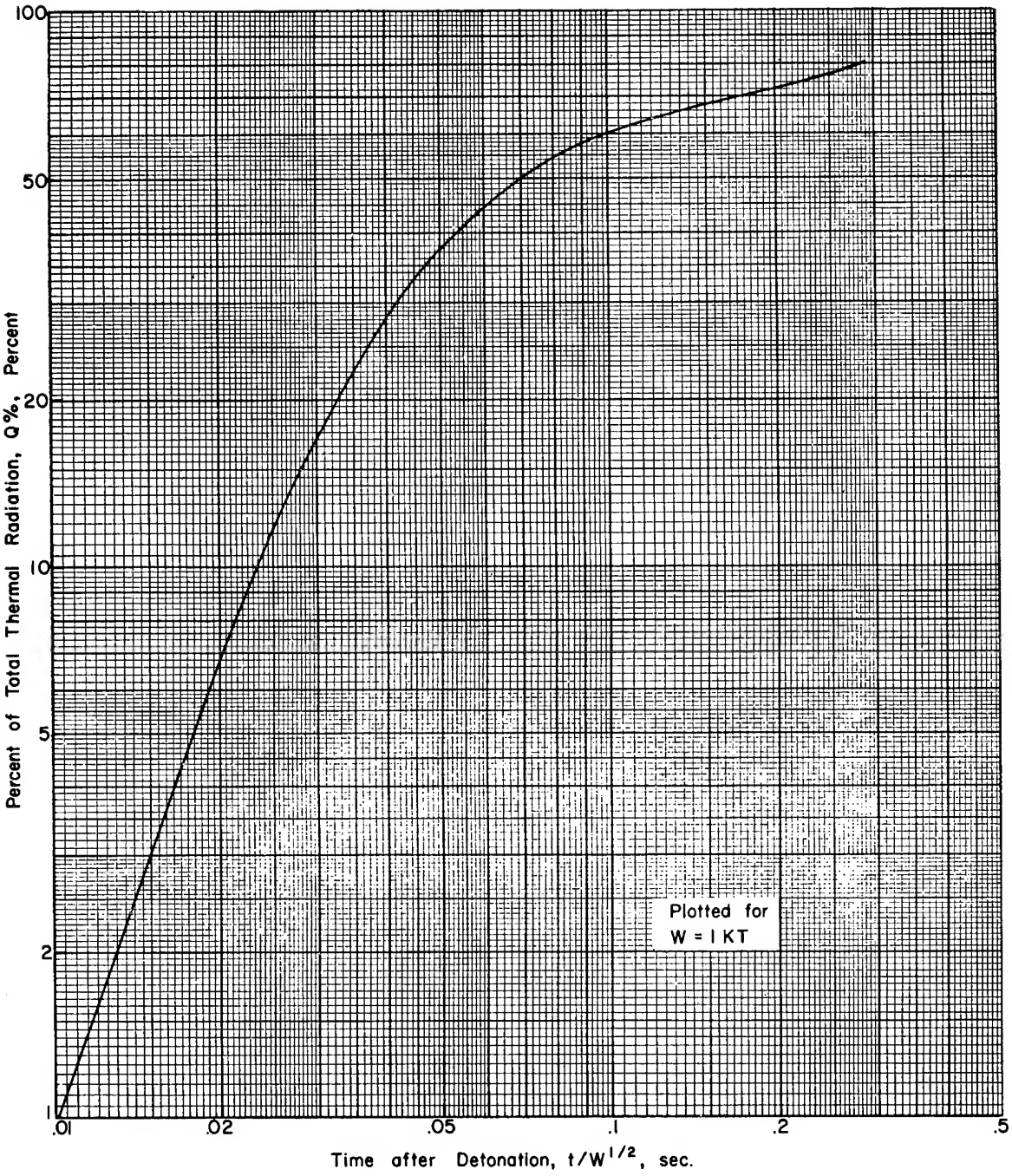

Fig. 2.14—Percentage of total thermal radiation emitted vs. scaled time after detonation for both surface and air bursts (see Eq. 2.112 in Table 2.11).

window glass), (2) velocities (10, 20, 30, or 40 ft/sec for man, and 50, 100, 200, or 400 ft/sec for window glass), and (3) types of bursts (optimum burst height or surface burst).

Range as a function of yield was plotted on logarithm paper for each set of four equations for particular types of burst and objects, e.g., Eqs. 2.94 through 2.97. The slopes of the curves for man were almost constant, having an average value of 0.40. Similarly, slopes of the curves for window glass had an average value of 0.35. Each set of curves was then fitted with a straight line whose slope was 0.40 (for man) or 0.35 (for window glass).

The importance of the constant-slope concept is that it allowed range and yield to be expressed as a single variable, i.e., $d/W^{0.4}$ for man and $d/W^{0.35}$ for window glass. Thus equations such as Eqs. 2.86 and 2.87 could be derived which would define the relation between velocity and scaled range. Figure 2.11 illustrates graphically this relation for window-glass fragments and man for the two burst conditions.

It is of interest to note that the range at which a particular maximum overpressure occurs varies as $W^{1/3}$, whereas the range at which a given velocity for glass or man occurs is proportional to $W^{0.35}$ or $W^{0.40}$, respectively. This signifies that the same translational velocities occur at lower overpressures as yield increases, the reason being that for a particular maximum overpressure, the duration of the blast wave increases with increased yield. Furthermore, it can be said that the velocity of a man is more sensitive to the duration of the blast wave than is the velocity of window glass (compare the exponents, 0.40 and 0.35).

2.5 THERMAL RADIATION

Incident thermal radiation was computed from information given in Chap. 7 of Ref. 1 for a visibility of 50 miles. Data for slant ranges less than 0.1 mile and greater than 25 miles were obtained by extrapolation. Equations 2.106 and 2.108 in Table 2.11 specify the relations between thermal radiation, slant range, and yield for air bursts.

For the same range and yield, the thermal radiation received from a surface burst is somewhat less than that from an air burst, mostly because of reduced visibility along the earth's surface. Thus the thermal radiation received at a particular distance from a surface burst is from 0.5 to 0.8 of that from an air burst of the same yield and at the same distance.[1] The exact amount of attenuation is undefined but depends on yield, range, nature of the terrain, etc. For simplicity of presentation on the slide rule, the surface-burst thermal was assumed to be always 0.7 of that for an air burst. This made it possible to use the equations for air-burst thermal to compute surface-burst thermal by the simple substitution of 0.7 W for W. In Table 2.11 compare Eqs. 2.107 and 2.109 with Eqs. 2.106 and 2.108.

Because of increased time of delivery, the thermal radiation necessary to produce a given biologic effect increases with yield. The defining equations for first- and second-degree burns as functions of yield for either surface or air bursts are listed in Table 2.11, Eqs. 2.110 and 2.111.

The duration of the thermal pulse, or any fraction thereof, varies as the square root of the yield. Equations 2.112 and 2.113 define this relation for fractions of the total thermal energy between 1 and 80 per cent.

For illustrative purposes the equations noted in Table 2.11 are presented graphically in Figs. 2.12 through 2.14. The chart in Fig. 2.12 shows, for an air burst, the range for various thermal doses as a function of yield. Also shown on this chart is the range (or thermal dose) at which first- or second-degree burns for bare white skin occur as a function of yield (dashed lines). Similar material is plotted in Fig. 2.13 for a surface burst.

The percentage of total thermal radiation emitted is plotted in Fig. 2.14 as a function of scaled time after the detonation, $t/W^{1/2}$. These data apply to both air and surface bursts.

2.6 INITIAL NUCLEAR RADIATION

The following equation defining total exposure dose from initial nuclear radiation (gamma

plus neutron) for air bursts was derived from information given in Chaps. 8 and 11 of Ref. 1:

$$I = \frac{W}{d_s^2}\left\{4997.41 \exp\left[-9.263158\left(\frac{\rho}{\rho_0}\right)d_s\right] + 1033\left(\frac{W'}{W}\right)\exp\left[-5.415385\left(\frac{\rho}{\rho_0}\right)d_s\right]\right\} \qquad (2.114)$$

where W = yield, kt
W' = scaling factor (see Fig. 2.15)
d_s = slant range, miles
ρ = density of air through which radiation passes
ρ_0 = standard sea-level air density

It should be noted that Eq. 2.114 becomes unreliable at short ranges, especially for those less than 0.28 mile.*

The ratio of scaling factor to yield, W'/W, for initial gamma radiation which is required to evaluate Eq. 2.114 is given by

$$\log (W'/W) = -2.1343121 + 5.6948378 \log W - 5.7707609 (\log W)^2 + 2.7712520 (\log W)^3 - 0.6206012 (\log W)^4 + 0.0526380 (\log W)^5 \qquad (2.115)$$

for $10 < W \leq 20{,}000$. $(E_{1\,W'/W})\% = 5.1\%$. For yields of 10 kt or less, the ratio W'/W is unity. Equation 2.115 is plotted in Fig. 2.15.

Although Eqs. 2.114 and 2.115 express the relation between total exposure dose, range, and yield, explicit solutions could not be obtained for either range or yield, and therefore the equations could not be used directly to compute the scales of the slide rule. For this reason an empirical relation was sought defining range as a function of dose and yield. This was done by fitting the following polynomial to sets of values of range, yield, and dose obtained from Eqs. 2.114 and 2.115:

$$\begin{aligned}\log d_s = {} & a + [b + a' \log I + d' (\log I)^2 + g'(\log I)^3] \log W \\ & + [c + b' (\log I) + e' (\log I)^2 + h' (\log I)^3] (\log W)^3 \\ & + [d + c' (\log I) + f' (\log I)^2 + i' (\log I)^3] (\log W)^5 \\ & + e (\log W)^7 + f (\log I) + g (\log I)^2 + h (\log I)^3 \\ & + i (\log I)^5 \end{aligned} \qquad (2.116)$$

$a = +0.1237561$	$a' = +0.0143624$	
$b = +0.0994027$	$b' = -0.0000816$	
$c = +0.0011878$	$c' = -0.0000014$	$\rho/\rho_0 = 0.9$
$d = -0.0002481$	$d' = +0.0054734$	$(E_{1d_s})\% = 2.1\%$
$e = +0.0000096$	$e' = -0.0003272$	d_s = slant range, miles
$f = -0.1308215$	$f' = +0.0000106$	W = explosive yield, kt
$g = +0.0009881$	$g' = -0.0001220$	I = initial nuclear radiation, rem
$h = +0.0032363$	$h' = +0.0000217$	
$i = +0.0000111$	$i' = -0.0000006$	

Limits for the equation fit $1 \leq W \leq 20{,}000$
$1 \leq I \leq 10^8$

*See paragraph 8.104 of Ref. 1.

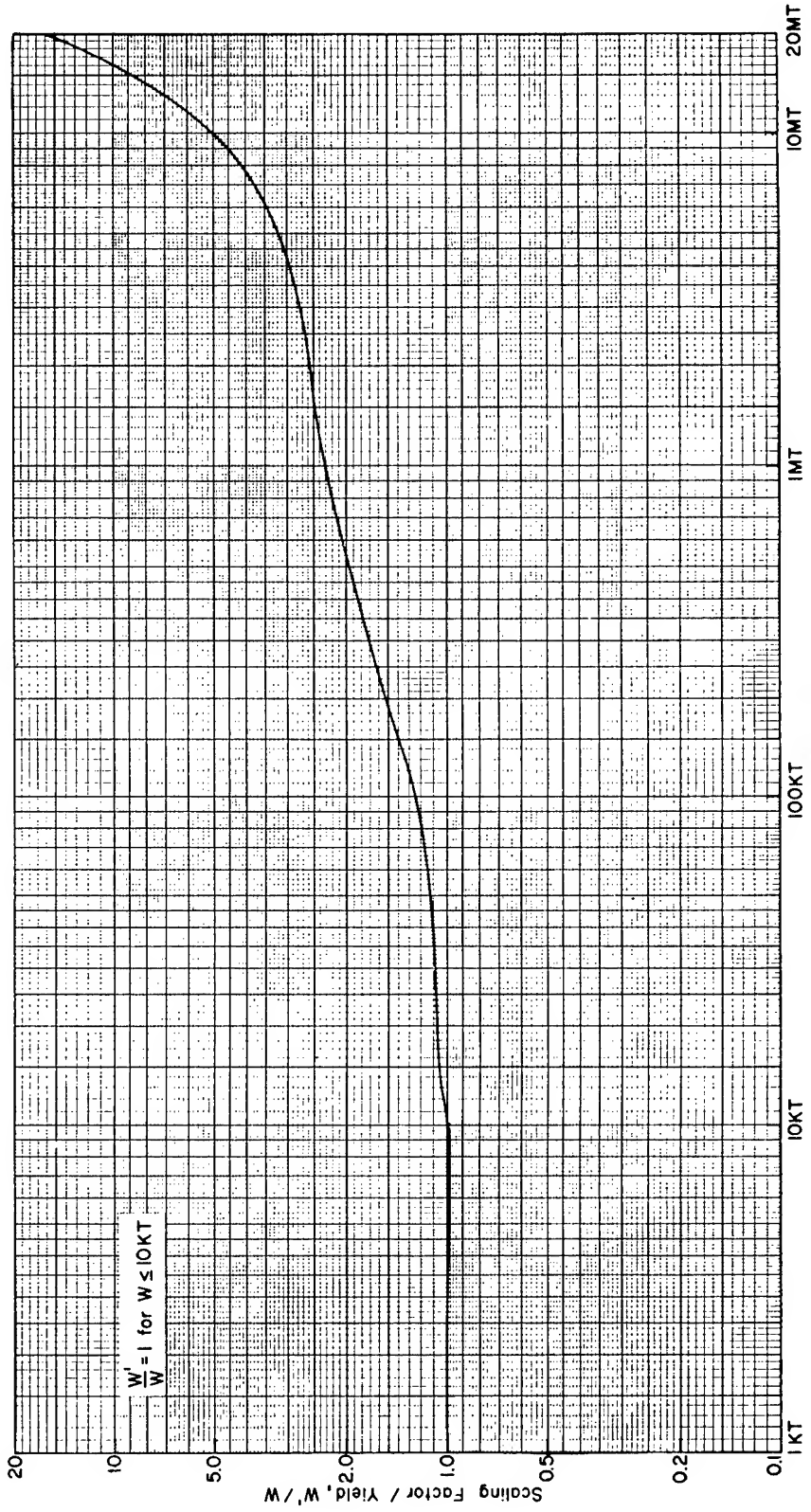

Fig. 2.15—Scaling factor for initial gamma radiation divided by yield as a function of yield (see Eq. 2.115).

Equation 2.116 was used to prepare Fig. 2.16, which is a plot of range vs. yield for nine values of initial nuclear radiation. This material (which also appears on the slide rule) is applicable to air bursts where the effective air density between the burst and the target is 0.9 that of the standard sea-level value.

Initial nuclear radiation for surface bursts is lower than that for air bursts of the same yield and at the same distance (slant range) from the burst. This is a result of the higher air density for the surface burst and the presence of dust and debris near the surface, both of which cause a reduction in the gamma-radiation dose. Equations 2.114 and 2.115 were used to compute initial nuclear radiation from surface bursts by assuming that $\rho/\rho_0 = 1.0$ and by replacing the constant "1033" in Eq. 2.114 with $\frac{2}{3}$ 1033 or 688.7. The latter procedure is equivalent to reducing the gamma-radiation dose to $\frac{2}{3}$ of the value for air bursts. The results of these computations are plotted in Fig. 2.17, which shows range vs. initial nuclear radiation for six values of yield.

The relation between slant range and ground range will be explored in more detail, but, first, it should be noted that a number of uncertainties are involved in estimating the initial ionizing radiation composed of very early, or prompt, pulses of gamma rays and neutrons plus delayed radiation (mostly gamma) up to 1 min. The latter emanates from the fission products in the rising cloud. The very early radiation, characterized by various neutron–gamma ratios that change with yield, range, and weapon design, is fairly sensitive to the relatively high air density associated with contact surface bursts at sea level. Two additional factors influencing the delayed-gamma-radiation dose should be considered: the radiation dose at a given location tends to decrease as the cloud rises, but the dose at that location tends to increase since the air through which the gamma rays pass becomes less dense because of (a) the increased height of the cloud and (b) the negative phase of the blast wave.

In the case of the transition from a contact surface to an air burst, the interplay between these factors, air density and distance, "fixes" a burst height which maximizes the ground range of a given radiation dose for each yield. This relation is such that for the air burst the ground range of a given dose is maximized for that burst height where the fireball at maximal brillance just touches the ground. However, the ground ranges for such bursts are significantly less than the slant ranges for the larger yields since the latter are associated with disproportionately larger fireballs. Thus on a ground-range basis, the contact surface burst maximizes the initial nuclear radiation for the higher yields at all ranges of interest, but the air burst, with the fireball just touching the ground, does so for the lower yields at the greater ranges.

A study of the range–yield–dose relations in Figs. 2.16 and 2.17 shows that, with reasonable error, the slant range for the air burst may be considered as ground range for the surface burst. This is illustrated by the following data derived from Figs. 2.16 and 2.17:

Dose, rem	Yield	Surface burst range, miles	Air burst slant range, miles
10^2	20 Mt	2.4	2.6
	100 kt	1.2	1.4
	1 kt	0.62	0.69
10^6	20 Mt	1.0	1.1
	100 kt	0.26	0.26
	1 kt	0.059	0.057

Thus the nuclear-radiation data shown on the slide rule, applying strictly to the slant range for the air burst, *can be regarded as a reasonable approximation of the dose–range relation for the surface burst.* Any errors involved in assuming that the slant range for the air burst applies to range for the surface burst are likely to be small compared with those due to many other factors, such as differences between conjectured and actual locations of Ground Zero.

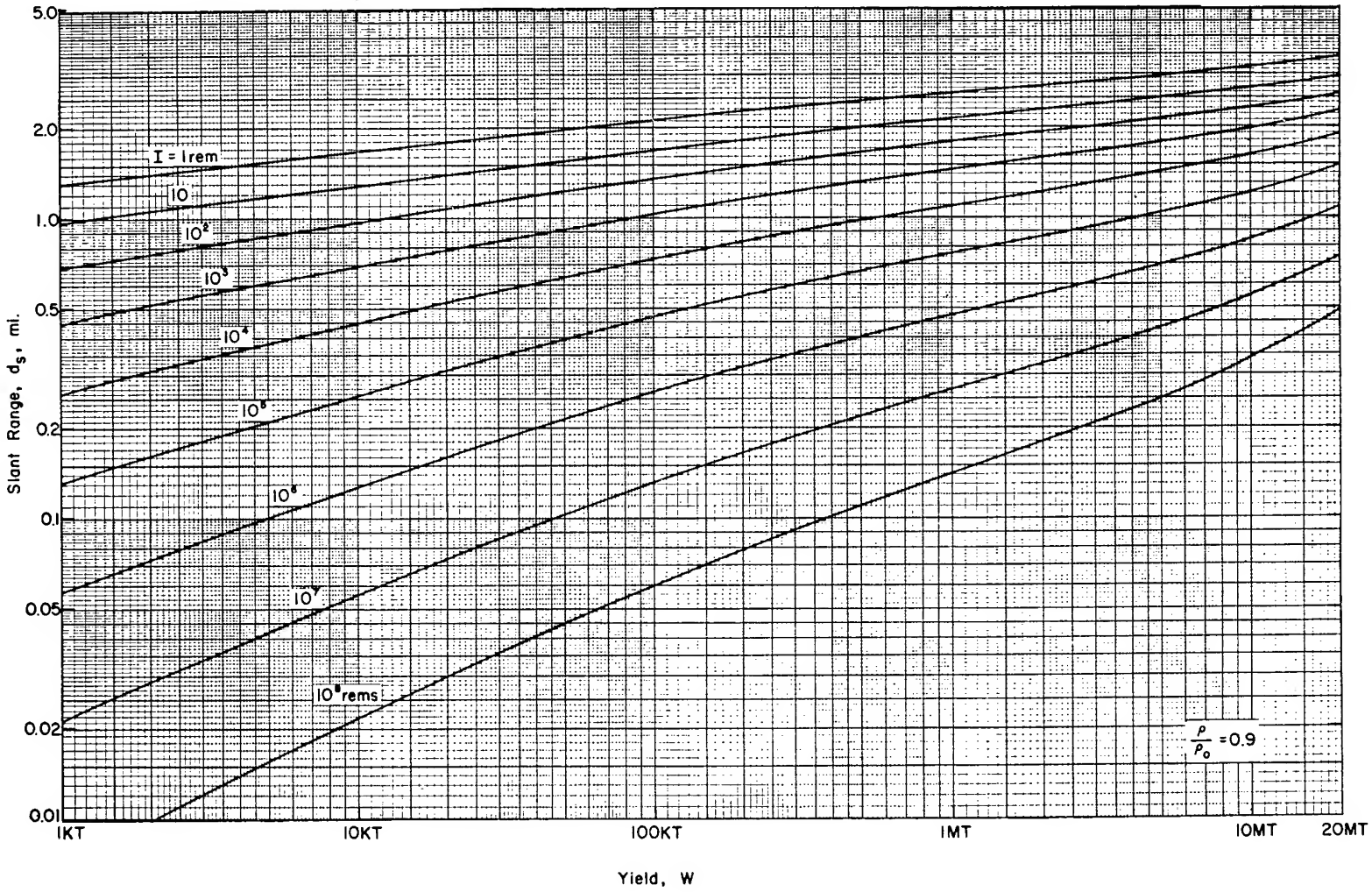

Fig. 2.16—Initial nuclear radiation as a function of slant range and yield for air bursts (see Eq. 2.116).

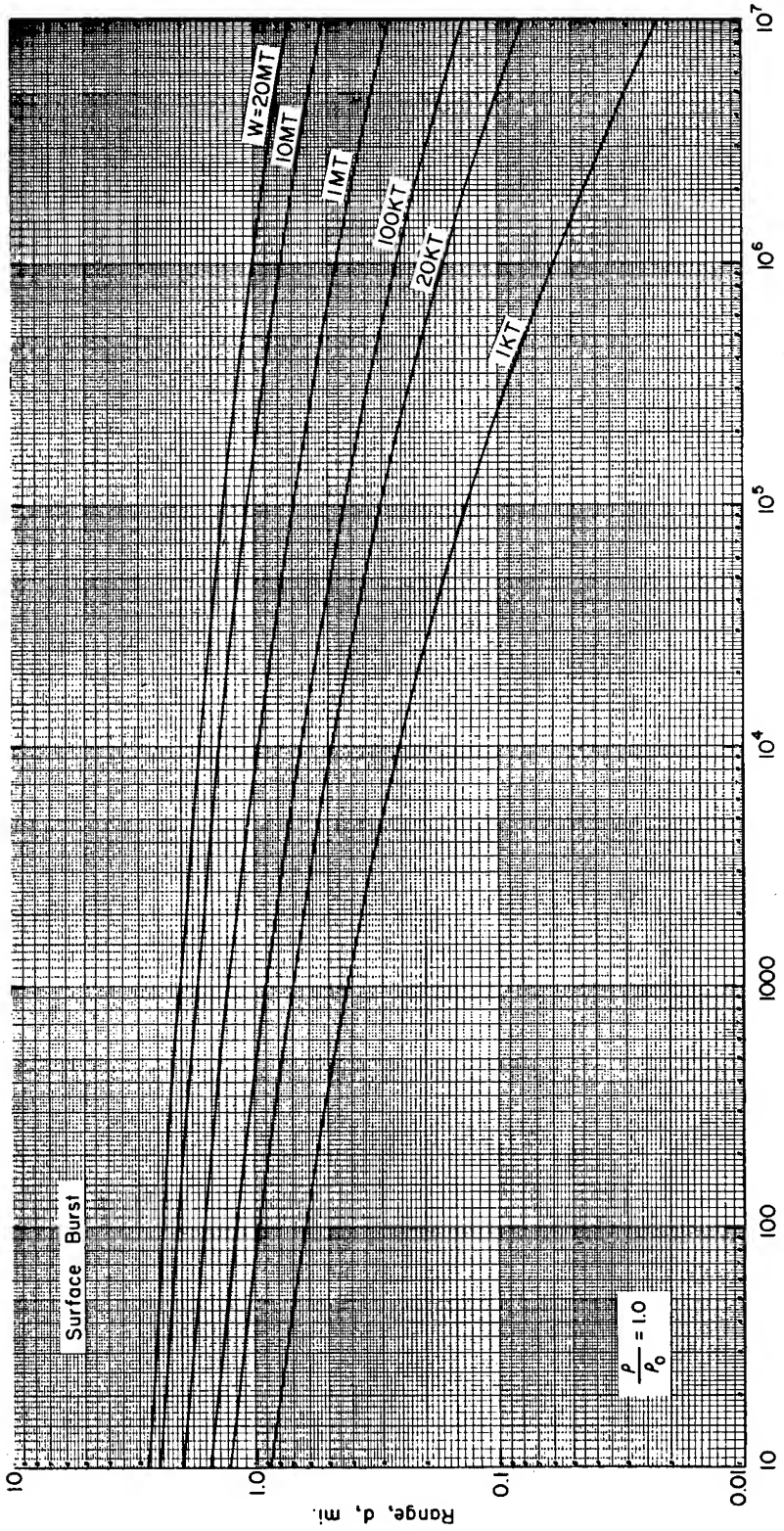

Fig. 2.17—Initial nuclear radiation as a function of range and yield for surface bursts (see Eq. 2.115).

Since ground range is a more useful concept for planning purposes (as are also the burst conditions which maximize the range of a given hazard), it is well to explore further the concepts of slant range and ground range for the maximizing air burst noted previously. One can, for example, use the fireball radius at maximal brilliance* for various yields as the maximizing burst height for air detonations and compute the ground ranges for given radiation doses. Results of these computations are tabulated below along with corresponding range values for the surface burst:

Dose, rem	Yield	Air burst		Surface burst ground range, miles
		Slant range, miles	Ground range, miles	
10^2	20 Mt	2.6	1.9	2.4
	100 kt	1.4	1.4	1.2
	1 kt	0.69	0.69	0.62
10^3	20 Mt	2.3	1.4	2.0
	100 kt	1.0	0.98	0.9
	1 kt	0.44	0.44	0.42
10^6	20 Mt	1.1	*	1.0
	100 kt	0.26	0.15	0.26
	1 kt	0.057	0.046	0.059

* The dose on the surface directly beneath the bomb (hypocenter) would be about 2×10^4 rem.

The data shown in the last two columns serve as numerical verification of the general statements made previously: (1) For high yields (20 Mt), the surface burst maximizes the range at which all radiation doses of interest occur. (2) For low and intermediate yields (1 kt and 100 kt), the surface burst maximizes the ranges at which high radiation doses (10^6 rem) occur, and the air burst maximizes the ranges at which lower doses (10^3 and 10^2 rem) occur. More important, however, each slant-range value for air bursts is approximately the same as the larger of the figures in the last two columns. *This means that for planning purposes the range–dose relation shown on the slide rule can be taken to mean ground range for maximizing burst conditions whether these conditions involve an air or surface burst.*

This assumption that the relation between slant range and dose shown on the slide rule for the air burst is a reasonable approximation of the ground-range–dose relation for maximizing burst conditions is not likely to involve a significant error considering all the other uncertainties involved, particularly the variations due to nuclear-bomb design and yield and to the difference in assumed and actual ranges.

2.7 EARLY FALLOUT DOSE RATE

Early fallout dose rate can be computed with the following expression from Chap. 9 of Ref. 1:

$$\frac{R}{R_0} = \left(\frac{t}{t_0}\right)^{-1.2} \tag{2.117}$$

where R_0 is known dose rate at time t_0 after detonation and R is dose rate at any time t after detonation.

*The value of this parameter is the same as that for minimum height of burst for negligible fallout, which can be evaluated on the slide rule.

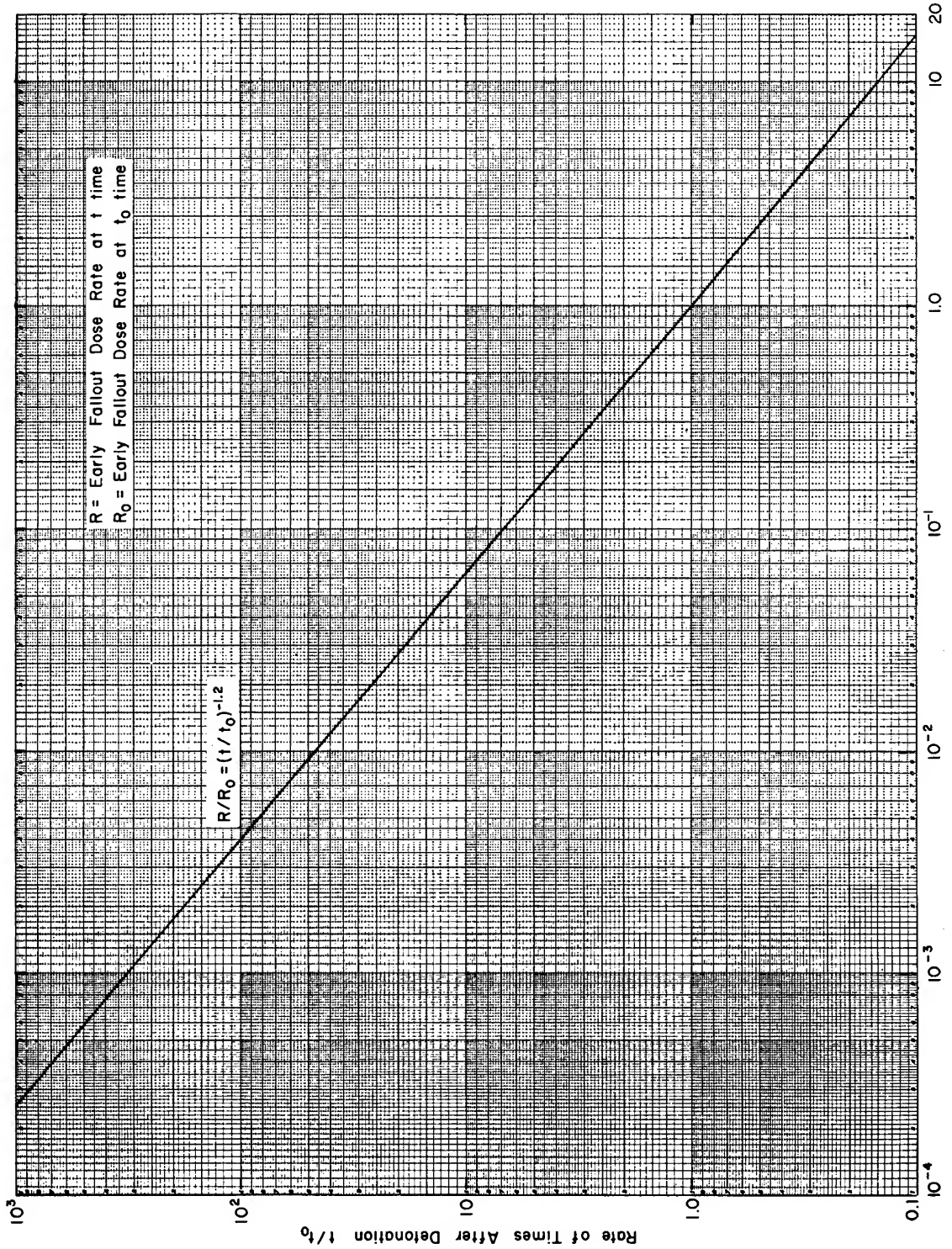

Fig. 2.18—Ratio of early fallout dose rates as a function of ratio of times after detonation.

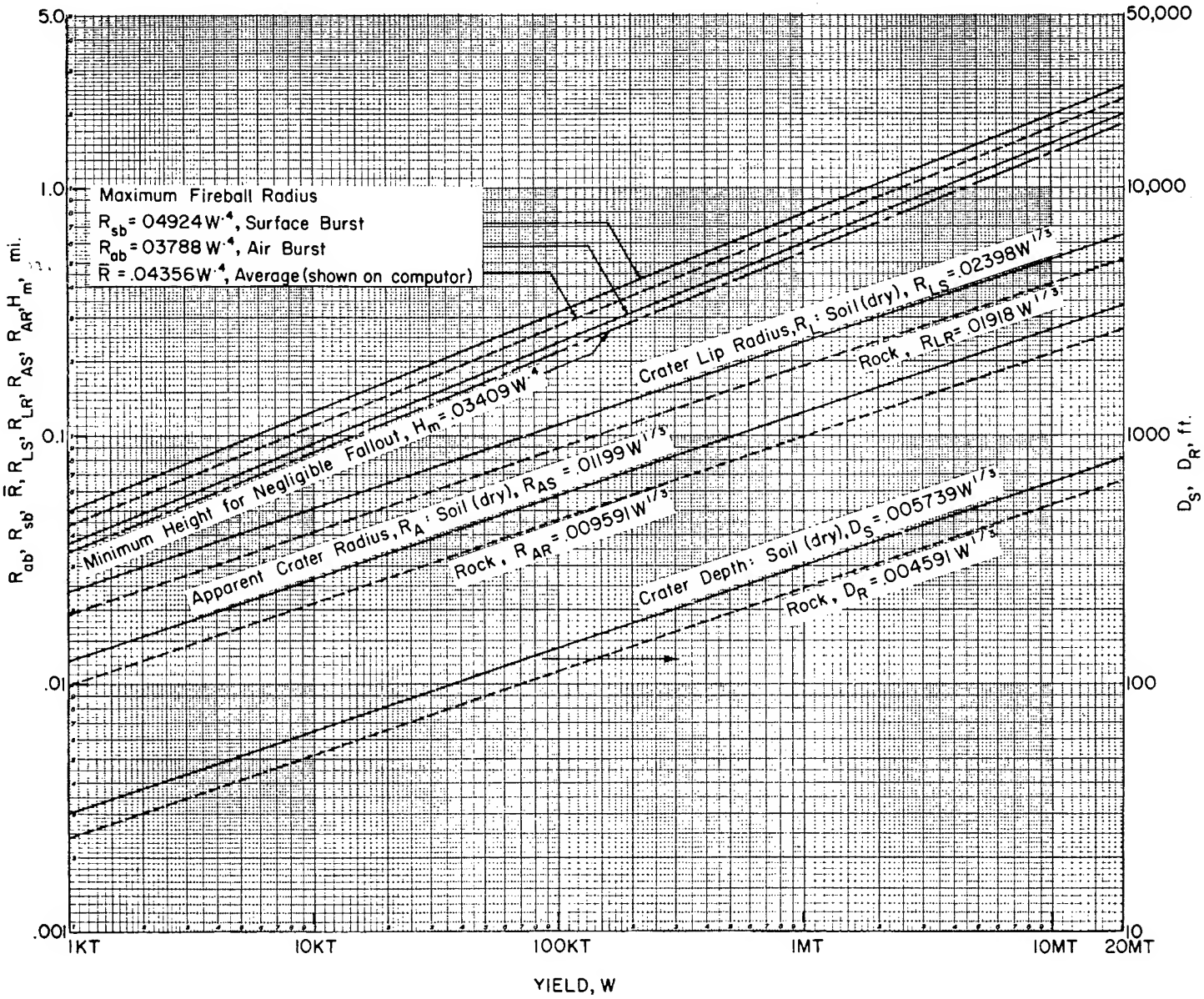

Fig. 2.19—Crater and fireball dimensions as a function of yield. Also shown are minimum heights of burst for negligible fallout vs. yield.

Equation 2.117 is applicable to a fixed quantity of radioactive particles; i.e., it is assumed that fallout is complete and that radioactive particles are not removed from the vicinity of measurement (or exposure) by decontamination procedures or by other processes, such as wind erosion.

A plotted form of Eq. 2.117 appears in Fig. 2.18 showing R/R_0 as a function of t/t_0. Note that, when time increases by a factor of 7, fallout dose rate decreases by a factor of 10.

2.8 CRATER AND FIREBALL DIMENSIONS AND MINIMUM HEIGHT OF BURST FOR NEGLIGIBLE FALLOUT

The material presented in this section from Chaps. 2 and 6 of Ref. 1 required no numerical treatment to facilitate computation of the appropriate slide-rule scales. For the sake of completeness, the various relations are presented in graphical and equation form in Fig. 2.19. (See Secs. 4.7 and 4.8 for a discussion of the parameters.) The average values of the maximum fireball radius (average between maximum fireball radius for a surface burst and that for an air burst, shown as a dashed line in Fig. 2.19) were placed on the slide rule.

REFERENCES

1. S. Glasstone (Ed.), *The Effects of Nuclear Weapons*, rev. ed., Superintendent of Documents, U. S. Government Printing Office, Washington, D. C., 1962.
2. I. G. Bowen, R. W. Albright, E. R. Fletcher, and C. S. White, *A Model Designed to Predict the Motion of Objects Translated by Classical Blast Waves*, USAEC Report CEX-58.9, June 1961.
3. E. R. Fletcher, R. W. Albright, V. C. Goldizen, and I. G. Bowen, *Determinations of Aerodynamic-drag Parameters of Small Irregular Objects by Means of Drop Tests*, USAEC Report CEX-59.14, October 1961.

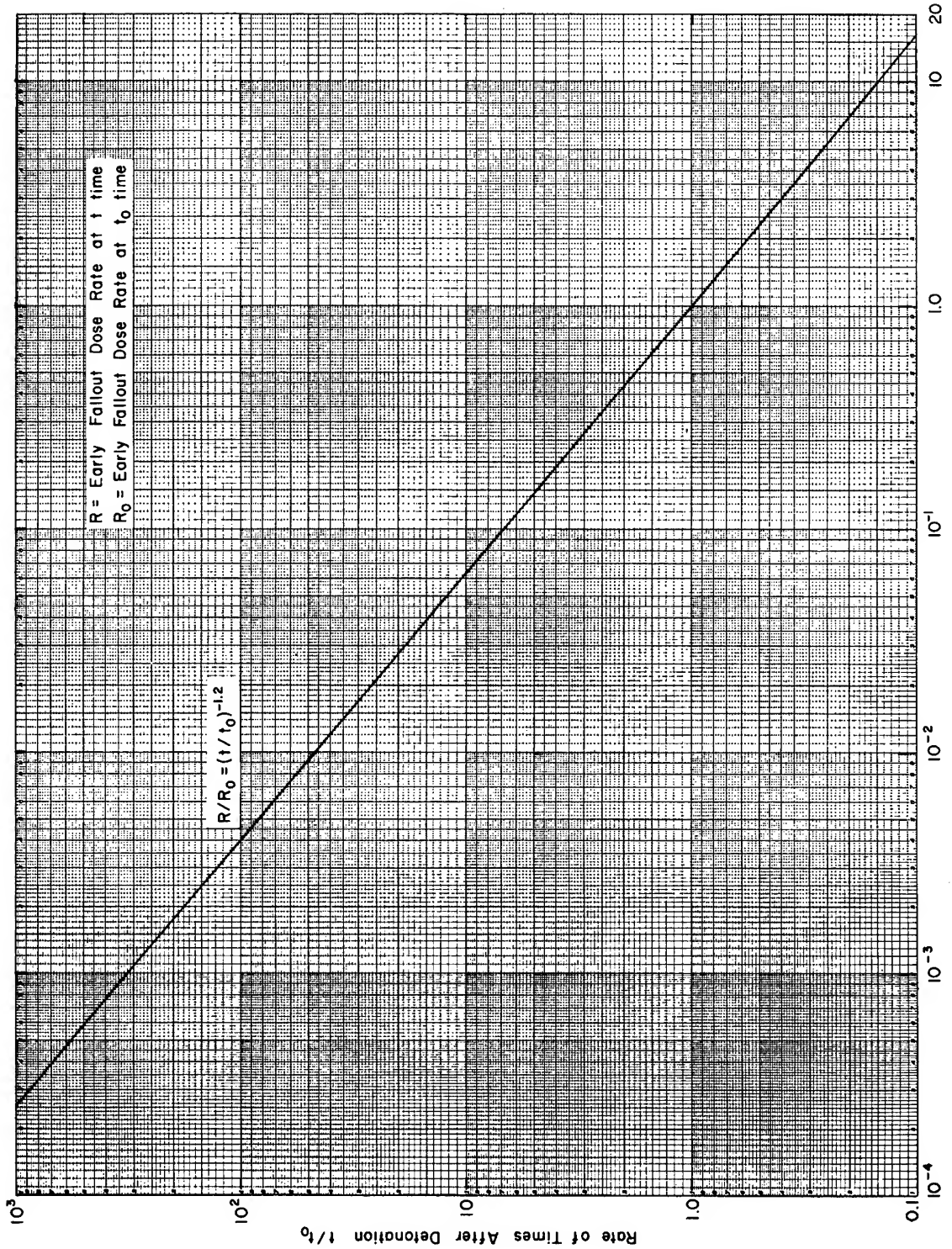

Fig. 2.18—Ratio of early fallout dose rates as a function of ratio of times after detonation.

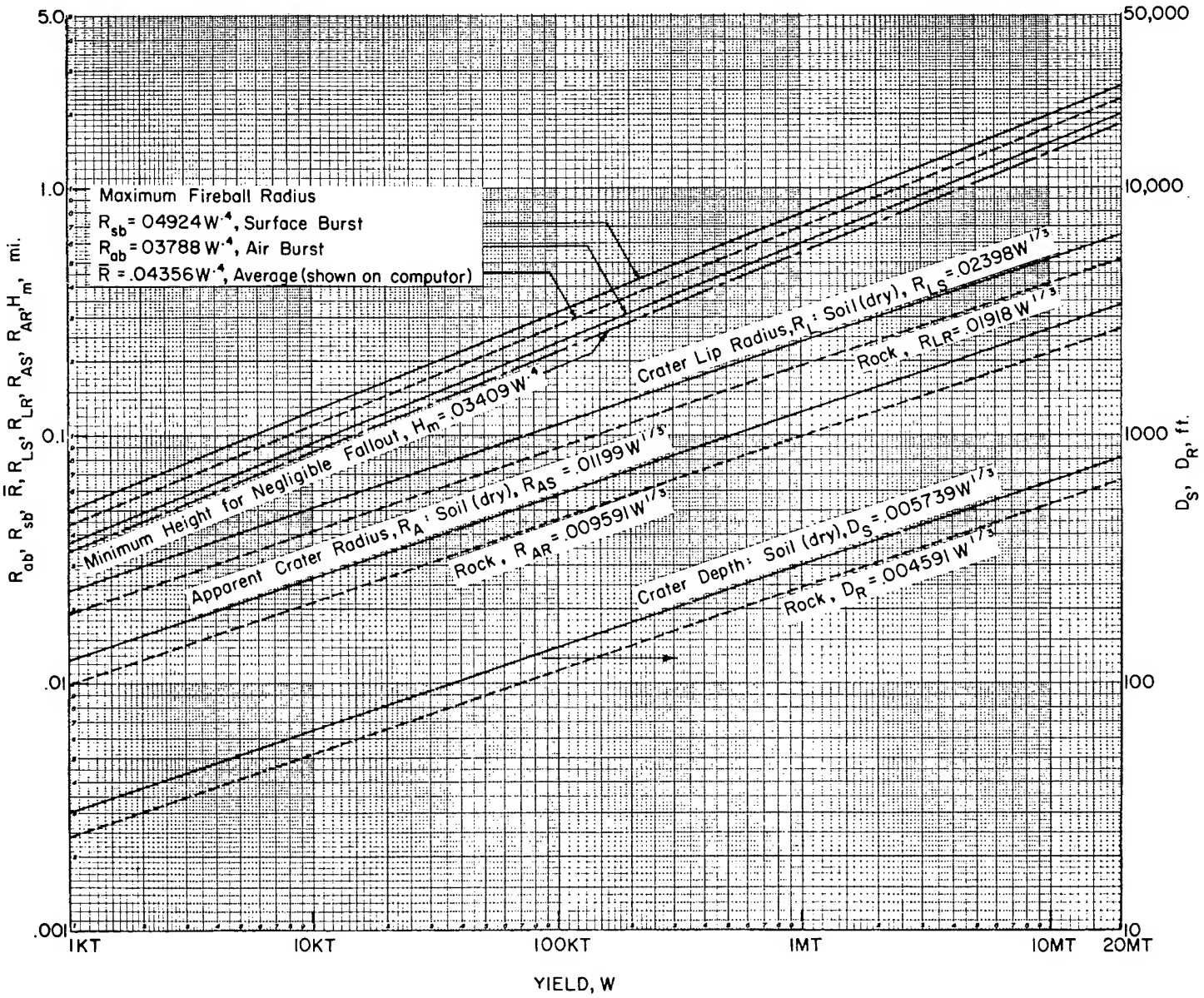

Fig. 2.19—Crater and fireball dimensions as a function of yield. Also shown are minimum heights of burst for negligible fallout vs. yield.

Equation 2.117 is applicable to a fixed quantity of radioactive particles; i.e., it is assumed that fallout is complete and that radioactive particles are not removed from the vicinity of measurement (or exposure) by decontamination procedures or by other processes, such as wind erosion.

A plotted form of Eq. 2.117 appears in Fig. 2.18 showing R/R_0 as a function of t/t_0. Note that, when time increases by a factor of 7, fallout dose rate decreases by a factor of 10.

2.8 CRATER AND FIREBALL DIMENSIONS AND MINIMUM HEIGHT OF BURST FOR NEGLIGIBLE FALLOUT

The material presented in this section from Chaps. 2 and 6 of Ref. 1 required no numerical treatment to facilitate computation of the appropriate slide-rule scales. For the sake of completeness, the various relations are presented in graphical and equation form in Fig. 2.19. (See Secs. 4.7 and 4.8 for a discussion of the parameters.) The average values of the maximum fireball radius (average between maximum fireball radius for a surface burst and that for an air burst, shown as a dashed line in Fig. 2.19) were placed on the slide rule.

REFERENCES

1. S. Glasstone (Ed.), *The Effects of Nuclear Weapons,* rev. ed., Superintendent of Documents, U. S. Government Printing Office, Washington, D. C., 1962.
2. I. G. Bowen, R. W. Albright, E. R. Fletcher, and C. S. White, *A Model Designed to Predict the Motion of Objects Translated by Classical Blast Waves,* USAEC Report CEX-58.9, June 1961.
3. E. R. Fletcher, R. W. Albright, V. C. Goldizen, and I. G. Bowen, *Determinations of Aerodynamic-drag Parameters of Small Irregular Objects by Means of Drop Tests,* USAEC Report CEX-59.14, October 1961.

Chapter 3

DESIGN OF THE CIRCULAR SLIDE RULE

3.1 GENERAL

The purpose of this chapter is to formalize the analytical procedures that were used in the design of the Nuclear Bomb Effects Computer. Most of the parameters placed on the computer are functions of weapon yield or of yield and range. Although this circumstance allowed condensing of information through sharing of scales, it necessitated careful analysis to properly synthesize the many components into a workable computer.

The basic design criteria and the mechanical structure of the computer will be considered before proceeding to the details of the design. Figure 3.1 shows the front of the computer, and Fig. 3.2, the back. On the front the central disk (F_1 in Figs. 3.1 and 3.3) contains a yield scale near its perimeter and, in the interior, various other scales that can be viewed only through windows in the two overlying disks (F_2 in Figs. 3.1 and 3.4 and F_3 in Figs. 3.1 and 3.5). The smaller of the disks (F_3) is oriented with respect to the central disk (F_1) by means of a yield setting made with the hairline tab. The next larger disk (F_2) contains a range scale near its perimeter, which is also set with respect to the yield scale on disk F_1. The two smaller disks can be adjusted independently with respect to the yield scale.

On the back the central disk (B_1) contains two families of curves, one for thermal radiation (red lines) and the other for initial nuclear radiation (black lines) (see Figs. 3.2 and 3.6). These curves are read at the intersection of the hairline on tab B_3 (connected mechanically to F_3) and the spiral on disk B_2 (connected mechanically to F_2), the hairline and the spiral having the same color as the curves being read (see Figs. 3.4 and 3.5). The required input setting for the back of the computer is made on the front by rotating the disks (using appropriate tabs) until both the yield and range of interest are under the tab hairline. Thus the hairline on the back (an extension of the one on the front) is orientated with respect to weapon yield, and the spiral disk is adjusted according to range for a given yield. These settings are not independent of each other in the sense that they are for the front disks but must be made simultaneously; i.e., both the yield and range of interest must be adjusted to the hairline tab for any particular setting.

3.2 TWO- AND THREE-VARIABLE PROBLEMS INVOLVING YIELD

3.2.1 Variables That Are Separable: $f(x) + g(y) = h(z)$

The general three-variable problem will be considered here for the condition that the functions of each variable can be stated separately. The results of the analysis can also be applied to two-variable problems as degenerate cases of the three-variable problem.

If the three variables are called x, y, and z and their respective functions are called f, g, and h, then

$$f(x) + g(y) = h(z) \tag{3.1}$$

is a general statement of the problem considered in this section. It will be shown that a problem of this type can be placed on a circular slide rule with two disks and that any one of the three variables can be determined if the other two are specified. It is not required that any of the functions be of the logarithmic form.

To facilitate illustration of the problem by means of Figs. 3.1, 3.3, and 3.4, let x = W (yield), y = d (range), and z = p_m (maximum overpressure) and let f, g, and h be their respective functions. Then Eq. 3.1 can be restated

$$f(W) + g(d) = h(p_m) \tag{3.2}$$

First, a radial line was chosen on disk F_1 to serve as a reference from which to measure angular distance. Then a yield (W) scale was assigned to F_1 such that the angle for a given value of W is defined by the equation

$$\theta_W = K\, f(W) + A \tag{3.3}$$

where K is a constant determining the angular extent of the scale and A is another constant specifying the angular placement of the scale with respect to the zero reference angle.

Similarly, a reference line was chosen on disk F_2 and a range scale (d) was designed (to be read against the W scale on F_1) such that the angle for a given value of d is defined by

$$\theta_d = -K\, g(d) + B \tag{3.4}$$

where K is the same quantity previously defined, and B is a constant similar to A also previously defined.

If, now, range d is set opposite yield W, the reference line on disk F_2 will be at angle $(\theta_W - \theta_d)$ with respect to the reference line on F_1. This angular separation can be evaluated using Eqs. 3.3, 3.4, and 3.2 as follows:

$$\begin{aligned} \theta_W - \theta_d &= K\,[f(W) + g(d)] + A - B \\ &= K\, h(p_m) + A - B \end{aligned} \tag{3.5}$$

The quantity $(\theta_W - \theta_d)$ is, according to Eq. 3.5, a function of maximum overpressure (p_m) alone. Thus, if a scale for p_m were constructed on disk F_1 (also containing the W scale) such that

$$\theta_{p_m} = K\, h(p_m) + A - B + C \tag{3.6}$$

with respect to the reference line, then a hairline placed at $\theta_h = C$ on disk F_2 would be at the value for p_m corresponding to the input values of W and d.

To recapitulate, the central disk (F_1) contains a yield scale specified by Eq. 3.3 and a maximum-overpressure scale defined by Eq. 3.6. The smaller disk (F_2) contains a range scale, Eq. 3.4, placed so that it can be read with respect to the yield scale, and a hairline placed at $\theta_h = C$ and at a radial distance consistent with the maximum-overpressure scale on F_1.

Note that the three-variable problem presented here was developed in terms of arbitrary functions f, g, and h. For a more specific example the mathematical expression for p_m which was set forth in Chap. 2 will now be considered. By this procedure other considerations influential in the overall design of the circular slide rule will be brought into focus.

Maximum-overpressure (p_m) data were fitted by least squares to an equation of the form

$$\log\left(\frac{d}{W^{1/3}}\right) = j\ (\log p_m) \tag{3.7}$$

where j is a polynominal in log p_m.*

*See Eqs. 2.5 in Table 2.1 and 2.61 in Table 2.9.

Rearranging, we have

$$\log W - 3 \log d = -3\, j\, (\log p_m) \tag{3.8}$$

Equation 3.8 is in the form of Eq. 3.2, where $f(W) = \log W$, $g(d) = -3 \log d$, and $h(p_m) = -3\, j\, (\log p_m)$. With Eqs. 3.3, 3.4, and 3.6, the scales for this problem were computed as follows:

Disk F_1

$$\theta_W = K \log W + A \tag{3.9}$$

$$\theta_{p_m} = -3\, K\, j\, (\log p_m) + A - B + C \tag{3.10}$$

Disk F_2

$$\theta_d = 3\, K \log d + B \tag{3.11}$$

$$\theta_h = C \tag{3.12}$$

The constant A in Eq. 3.9 determines the angular displacement of the yield scale from an arbitrarily chosen reference line on disk F_1. The constant B assumes a similar role on disk F_2. The constant C locates the hairline in the large window on F_2. The three constants A, B, and C determine the angular position of the maximum-overpressure scale on F_1. The constant K, as previously defined, determines the angular extent of the scales. These constants were so chosen that on disk F_1 the center of the yield scale would be opposite the center of the overpressure scale. This made it feasible to choose a bottom and a top for the circular computer; i.e., the scales were labeled so that the yield scale was at the bottom and the overpressure scale at the top. Other scales were arranged to be consistent with this scheme.

The constant K determines, along with the numerical limits, the angular distance or arc occupied by each of the scales. As noted in Sec. 3.1, the yield scale is also used by the thermal- and nuclear-radiation scales on the back of the computer. Thus it was necessary to limit the yield scale to 180°. However, to allow space for labeling of the scales on the back, an arc of approximately 139° was used. This resulted in a value for K of about 32.32°. (The numerical limits for the yield scale are 1 to 20,000 kt or 0 to 4.30103 log units.)

Other considerations in the choice of a value for K should be mentioned. First, the range scale, extending from 0.05 to 100 miles, was limited to 360° of arc less the space occupied by the large window in disk F_2 (see Figs. 3.1 and 3.4). Second, the value of K should be small enough that erroneous readings are not possible. For example, if 100 miles is set opposite 1 kt, the indicator (hairline) for maximum overpressure should show no reading since overpressure is not defined for these conditions. However, if the scales are expanded too much (K too large), the hairline indicator would traverse the blank space between the low and high ends of the overpressure scale and indicate a false value for pressure at the high end of the scale.

The analysis presented in the preceding paragraphs is applicable to the three-variable problem for the condition that the variables can be stated separately. Although maximum overpressure was used to illustrate the development, the results are equally applicable to maximum dynamic pressure (q_m) and to maximum wind velocity (u_m) by the simple substitution of q_m or u_m for p_m in Eq. 3.10.

The parameters appearing in windows on disk F_3 (Figs. 3.1 and 3.3) are functions of yield alone or yield and another variable. The analytical procedure for these parameters is similar to that described above. Since only one yield scale appears on the slide rule, the value of K and A must be the same for all problems involving yield (see Eq. 3.9). Also, for the material on disk F_3, a common hairline was used, i.e., the hairline that appears on the tab connected to F_3.

For three-variable problems utilizing disk F_3 [e.g., duration of positive overpressure (t_p)

as a function of overpressure and yield], the scale for one of the variables (overpressure in this instance) is placed along the window on F_3 and the other (duration) on F_1 so that it can be read through the window. The choice of positions for the two nonyield variables, although arbitrary in theory, was made such that the most information could be packed in the space available. For instance, the time scale in the example just cited is shared by four pressure scales: pressure for (1) duration of positive overpressure, optimum burst height; (2) duration, surface burst; (3) arrival time of the blast wave, optimum burst height; and (4) arrival time, surface burst (see also Eqs. 2.11 and 2.15 in Table 2.1 and Eqs. 2.69 and 2.73 in Table 2.9).

Data obtained from Ref. 1 for crater and fireball dimensions (including minimum height of burst for negligible fallout) are functions of yield alone.* In the analysis the variable that previously was represented on F_3 was replaced by the appropriate constant. The length scale was placed on disk F_1 to be read through windows on F_3. Because the third variable assumed a constant value, the scale along the windows was replaced by an indicator line drawn across the windows for each parameter.

The fact that all crater dimensions* for a contact surface burst vary as $W^{1/3}$ made it possible to indicate crater dimensions on a single length scale constructed so that one log cycle of length occupies the same angular distance as three log cycles of yield. Also, it is of interest to note that fireball dimensions,* minimum height of burst for neglibible fallout,* and range at which a man† would attain a given velocity through displacement of 10 ft, all vary as $W^{0.4}$ and therefore share a common length scale plotted on disk F_1 and viewed through two windows placed at the same radius.

3.2.2 Variables Not Separable: f(x,y,z) = 0

The techniques described in this section are applicable to the general three-variable problem. If the relation between variables can be represented by contour plots, the problem can be placed on a circular slide rule consisting of two disks and a hairline free to rotate about the center of the disks.

It was necessary to employ these techniques to place initial-nuclear-radiation data on the slide rule since the functional relation between the three variables involved could not be stated in individual terms each containing a single variable (see Eq. 2.114).

Thermal radiation can be expressed as separate functions of yield and range (see Table 2.11) and, therefore, could have been represented on the slide rule according to the procedures presented in Sec. 3.2.1. However, it was necessary to use the more generally applicable techniques of this section to show the burn criteria as functions of yield on the same scale used for the thermal data.

As noted in Sec. 3.1, the hairline on the back of the rule, which measures an angle from an arbitrary reference point, is set on the yield scale appearing on disk F_1 (see Figs. 3.1, 3.2, and 3.5). The spiral disk B_2 is set for a specified yield according to range using the yield and range scales on disk F_1 and F_2, respectively. Thus, for any hairline (yield) setting, the range is represented as a function of the radial distance of the hairline–spiral intersection from the center of the rule, the radial distance increasing monotonically with range.

The types of spirals used on B_2 (Fig. 3.4) are, of course, arbitrary. The following forms were chosen since their use resulted in a near-uniform separation of the contour lines plotted on disk B_1 (Fig. 3.6):

$$r_I = \frac{A'}{\theta_d + B'} \tag{3.13}$$

$$r_Q = C' \, (\theta_d + 180°) + D' \tag{3.14}$$

*See equations in Fig. 2.19.

†See Eq. 2.87 in Table 2.10.

where r_I = radius on disk B_1 for initial nuclear radiation
r_Q = radius on disk B_1 for thermal radiation
θ_d = the angle at which range d is plotted on the range scale on disk F_2, defined by Eq. 3.11
A′, B′, C′, and D′ = constants determined by the minimum and maximum ranges to be represented and the radial interval available on the slide rule

Note that the curves for thermal radiation (Fig. 3.6) are opposite those for initial nuclear radiation on disk B_1, thus 180° is added to θ_d in Eq. 3.14. Also, for convenience positive angles on the back of the rule were measured in a clockwise direction to be consistent with counterclockwise positive direction on the front.

Since the angle of the hairline on B_3 is controlled by the yield scale on F_1, the governing equations are similar to Eq. 3.9 for the yield scale:

$$(\theta_W)_I = K \log W + A \tag{3.15}$$

$$(\theta_W)_Q = 180° + K \log W + A \tag{3.16}$$

The subscripts I and Q refer to initial nuclear radiation and thermal radiation, respectively. The remaining notation was defined in Sec. 3.2.1.

The family of curves for initial nuclear radiation were prepared in the following manner. Equation 2.116 was used to find the slant range at which a dose of 1 rem would occur for a yield of 1 kt for an air burst. Then Eqs. 3.11 and 3.13 were employed to determine a radius and Eq. 3.15 was employed to determine an angle, which together determined a point on the 1-rem contour. Succeeding points were found by repeating this procedure for yields of increasing magnitude. In practice, log intervals of yield were used to determine successive points on the dose lines for 1 rem, 3 rem, 10 rem, etc.

The family of curves appearing on disk B_1 for thermal radiation were computed using Eq. 2.108 in Table 2.11, Eq. 3.14, and Eq. 3.16. The plotting techniques employed were similar to those described in the previous paragraph for initial nuclear radiation. The data presented apply to an air burst and slant range. However, through the use of a simple device, described below, the same plots were made applicable to a surface burst and ground range. Inspection of the thermal equations, Eqs. 2.106 to 2.109 appearing in Table 2.11, reveals that for a particular range and yield the thermal radiation for a surface burst is 0.7 that of an air burst*, i.e., the surface-burst thermal for yield W is indicated on the slide rule if the tab hairline and range are set at 0.7 W. For convenience a small mark was placed on the yield–range tab to the right of the hairline (see Fig. 3.1). The mark is located so that, when it is set to W, the hairline is positioned at 0.7 W.

The thermal radiation necessary to produce first- and second-degree burns (Q_{1st} and Q_{2nd}, respectively) is specified by Eqs. 2.110 and 2.111 in Table 2.11 as a function of yield. With values of Q_{1st} and Q_{2nd} for given yields, appropriate slant ranges were determined employing Eq. 2.108 in Table 2.11. Thus first- and second-degree-burn lines could be plotted on the slide rule by techniques similar to those already described for plotting families of curves on disk B_1.

3.3 PROBLEMS NOT INVOLVING YIELD

3.3.1 Early Fallout Dose Rate

Early fallout dose rate is usually described by Eq. 2.117:

$$\frac{R}{R_0} = \left(\frac{t}{t_0}\right)^{-1.2}$$

*See discussion in Sec. 2.5.

where R is dose rate at time t after the detonation and R_0 is dose rate at time t_0 after the detonation. The ratios make it possible to express both dose rate and time in arbitrary units.*

Equation 2.117 can also be expressed as

$$\log R + 1.2 \log t = \log R_0 + 1.2 \log t_0 = C'' \tag{3.17}$$

where C″ is a constant for any particular problem in which R_0 is a measured dose rate at time t_0. Equation 3.18 suggests that two scales be constructed to rotate with respect to each other, one in log R and the other in $-1.2 \log t$, so that for any particular setting the sum of any log R and the corresponding 1.2 log t will be a constant. This condition can only be satisfied if one of the scales increases clockwise and the other increases counterclockwise. Thus the equation used for the construction of the dose-rate scale is

$$\theta_R = K'' \log R + A''$$

and that for time scale is

$$\theta_t = -1.2\, K'' \log t + B''$$

where K″ is an arbitrary scale-expansion factor, A″ and B″ are constants determining the angular location of each of the scales, and θ_R and θ_t are the angles at which dose rate R and time t are indicated on their respective scales.

3.3.2 Reflected Overpressure vs. Incident Overpressure

Reflected overpressure is plotted on the slide rule as a function of maximum, or shock, overpressure for the conditions that (1) the shock wave approaches the reflecting surface at a 90° angle and (2) the ambient pressure is 14.7 psi. Thus the problem is reduced to two variables that can be represented by two adjacent scales (see also Fig. 2.10). An arc was drawn on disk F_2 (see Figs. 3.1 and 3.4) in the space that remained after other scales were constructed. An incident-overpressure scale was plotted in logarithmic form on one side of the arc, and the corresponding values of reflected pressure were computed using Eq. 2.4 from which a scale was constructed on the other side of the arc.

REFERENCE

1. Samuel Glasstone (Ed.), *The Effects of Nuclear Weapons* , rev. ed., 1962, Superintendent of Documents, U. S. Government Printing Office, Washington, D. C., 1962.

*On the slide rule R is expressed in arbitrary units, e.g., roentgens per hour or milliroentgens per hour; however, time units were labeled, for convenience, in hours or days.

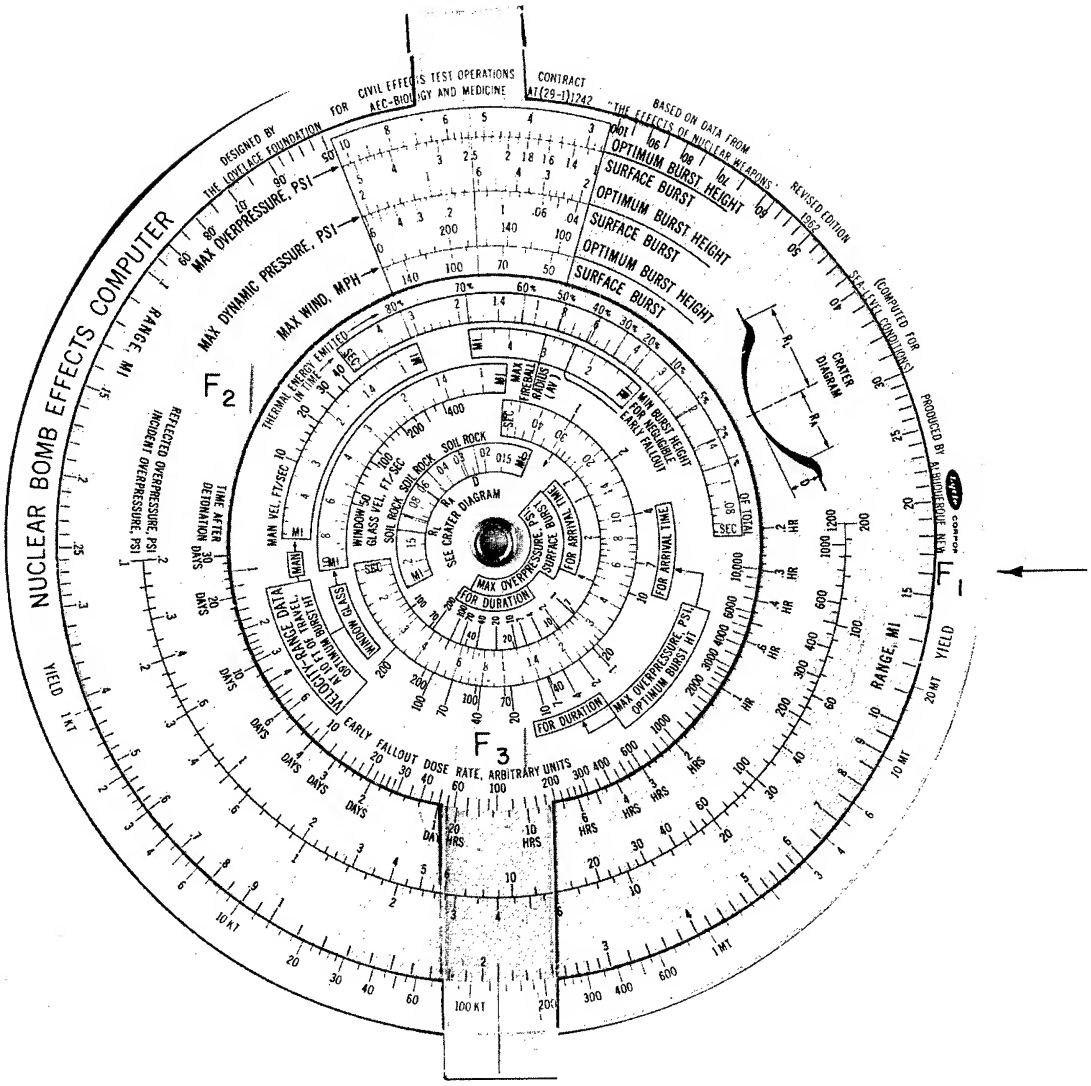

FRONT VIEW

Fig. 3.1—Front of the assembled computer.

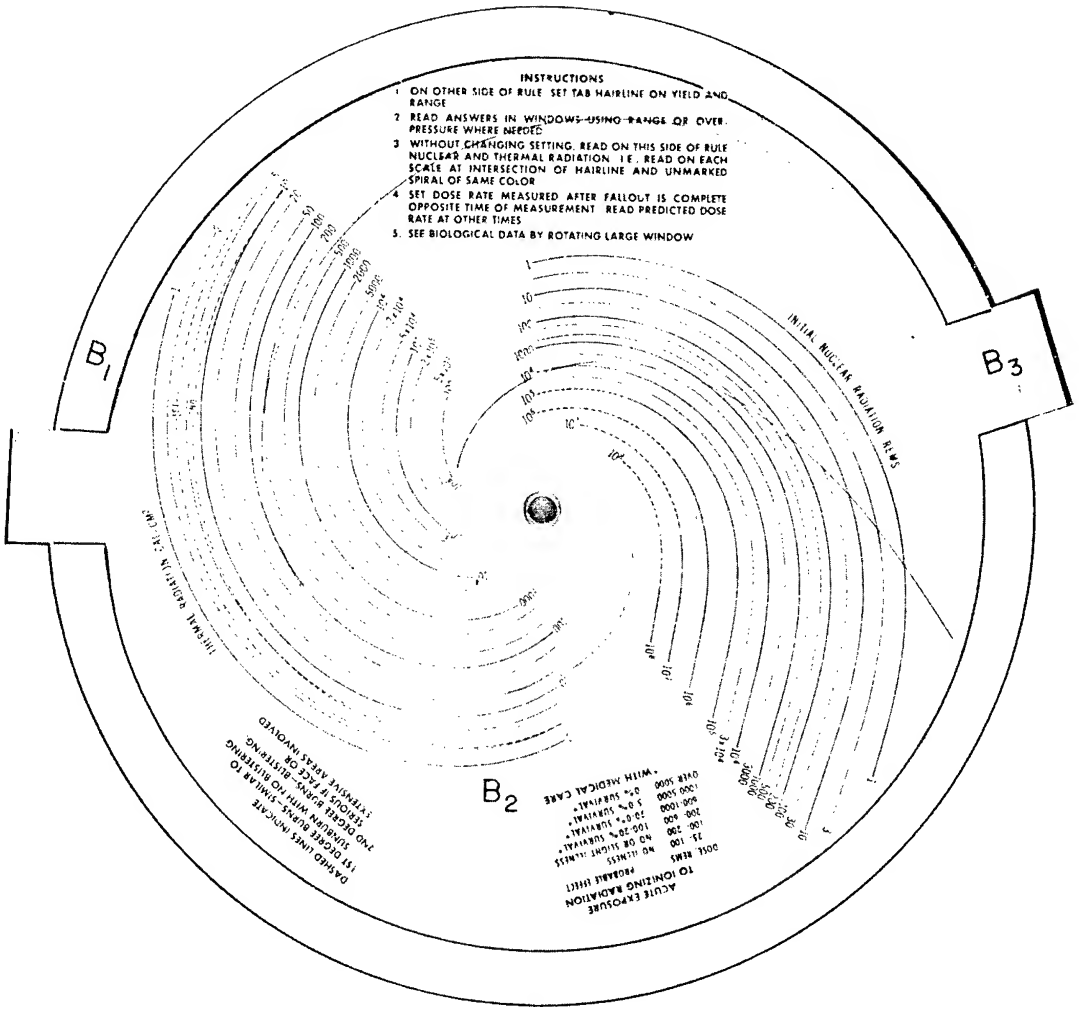

BACK VIEW

Fig. 3.2—Back of the assembled circular slide rule. The two families of curves for initial nuclear radiation (in black) and thermal radiation (in red) are on disk B_1. The red and black spirals are on disk B_2, and the red and black hairlines are on tab-extension B_3.

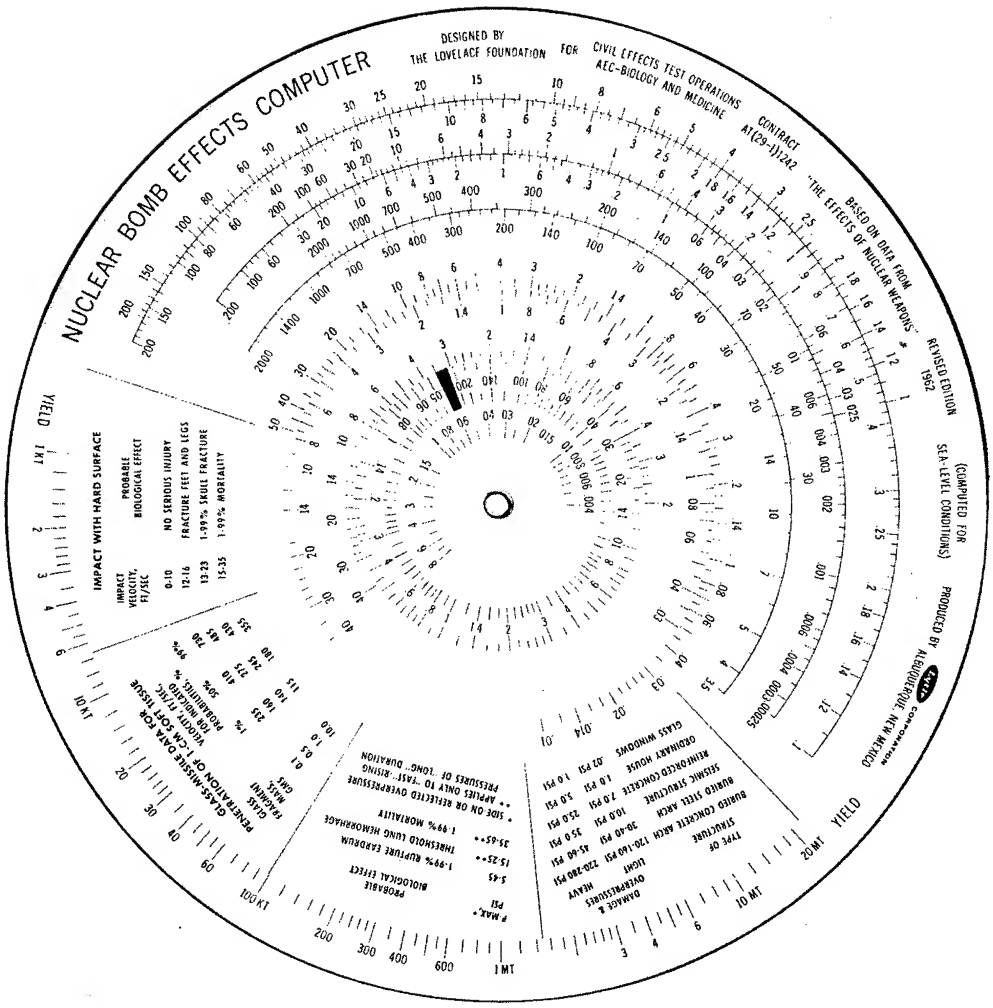

F_1

Fig. 3.3—Front of the largest, or central, disk of the computer (view before assembly).

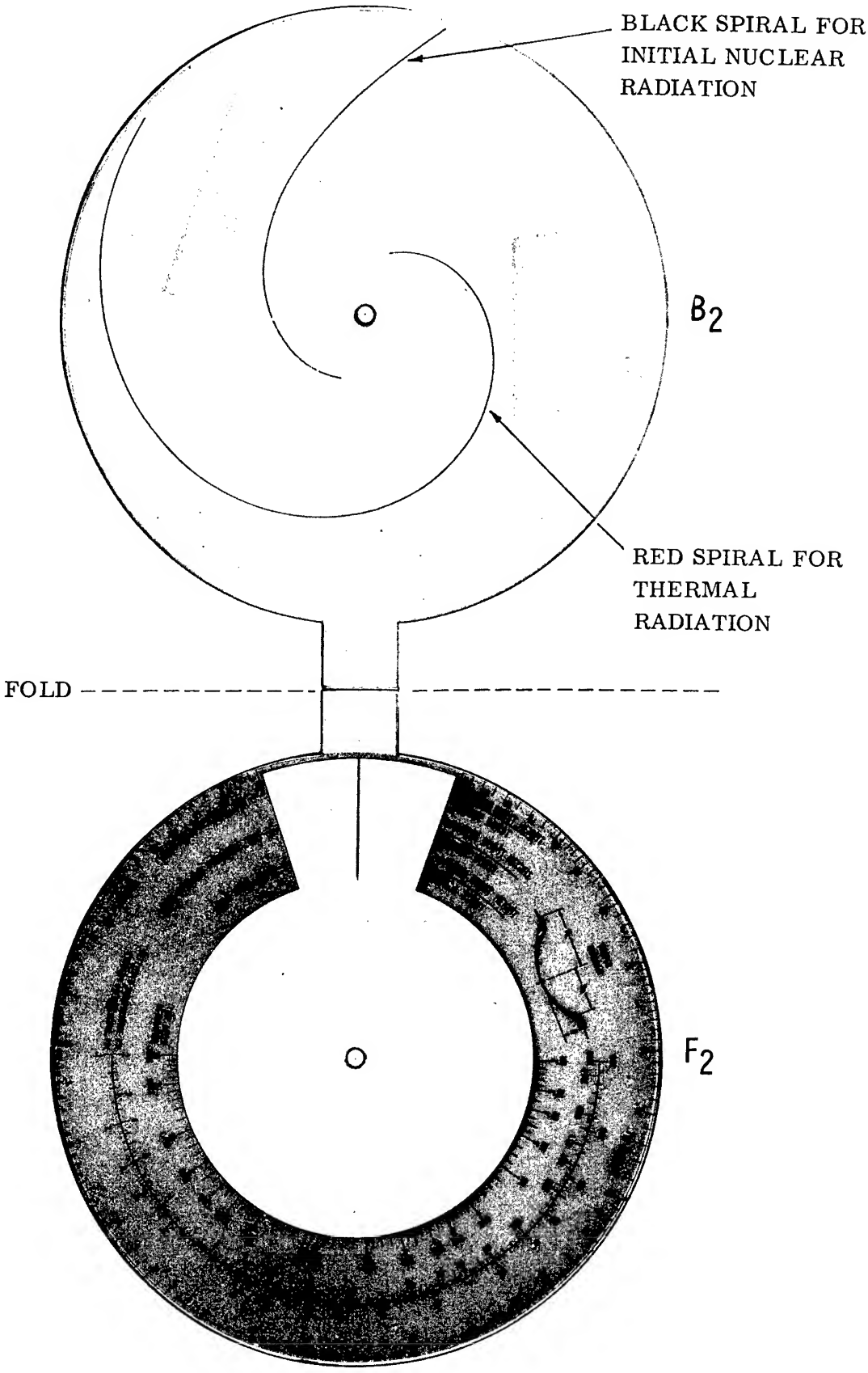

Fig. 3.4—Disks F_2 (front) and B_2 (back) of the unassembled circular computer. These disks are connected by means of the plastic tab which is folded at the black line.

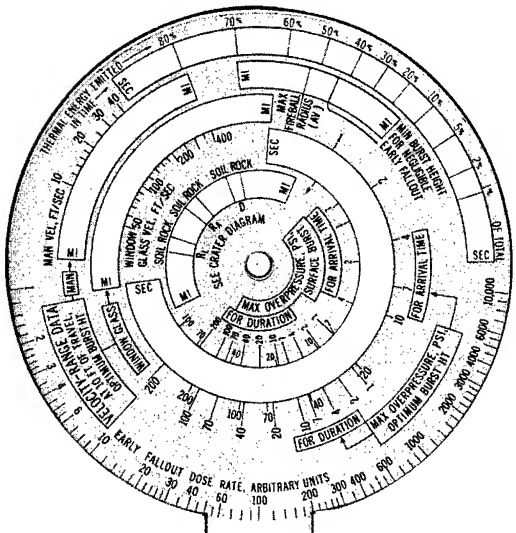

TAB HAIRLINE

MARK FOR USE WITH SURFACE BURST THERMAL

$\frac{F_3}{B_3}$

FOLD

BLACK HAIRLINE FOR INITIAL NUCLEAR RADIATION

RED HAIRLINE FOR THERMAL RADIATION

Fig. 3.5—Disk F_3 (front) and tab extension B_3 (back) of the unassembled computer.

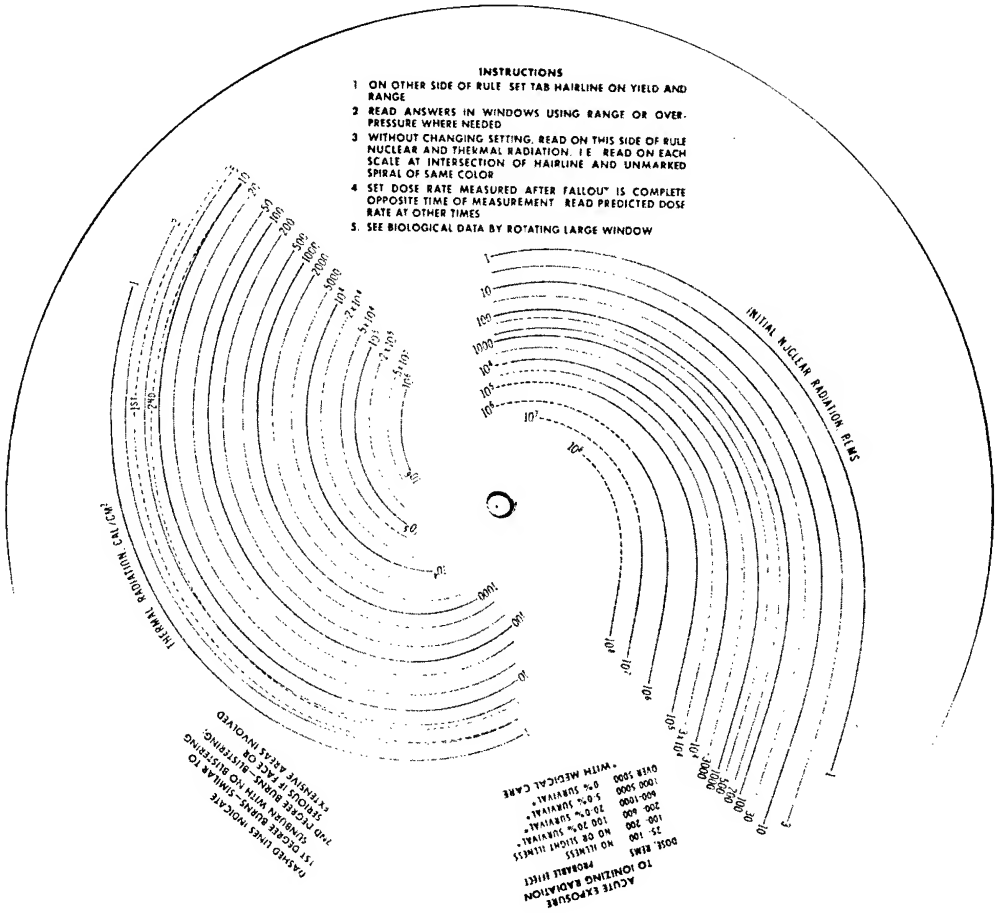

B_1

Fig. 3.6—Back of largest, or central, disk (B_1) of the computer (view before assembly).

Chapter 4
COMPUTER (SLIDE-RULE) EVALUATION OF FREE-FIELD WEAPONS-EFFECTS DATA

4.1 GENERAL

The preceding chapters have been concerned principally with the mathematical treatment of weapons-effects data and the design of a circular slide rule for easy evaluation of free-field effects parameters. The purposes of this chapter are: (1) to describe in detail the use of the slide rule in determining numerical values of effects parameters, (2) to discuss briefly various criteria for biological and structural damage which are presented on the computer in tabular or graphical form, and (3) to describe a few simple procedures that will make it possible to use the slide rule for estimates of most of the effects parameters for yields greater than 20 Mt or less than 1 kt. The material in Chaps. 2 and 3 is not essential to that presented here.

Table 4.1 lists 28 sets of variables, each set representing an effects problem that can be solved on the slide rule; i.e., any one of the variables can be evaluated if the others in the set are known. The second column of the table specifies the type of burst for which the data are applicable. The principal conditions of applicability are noted in the third column. In the last column are listed the sections of this chapter in which detailed instructions are given for the evaluation of the variables as well as a brief discussion of the biological and structural significance of some of the weapons effects.

4.2 BLAST-WAVE PARAMETERS

4.2.1 Incident Blast Wave*

The blast parameters presented are those which would describe a wave propagated along the ground in open, relatively flat areas, assuming nearly ideal surface conditions† and a standard sea-level atmosphere. Maximum overpressure (p_m), maximum dynamic pressure (q_m), maximum wind velocity (u_m), arrival time of the blast wave (t_a), and duration of the positive-overpressure phase of the blast wave (t_p) are detailed for two burst conditions, viz., surface burst (SB) and optimum burst height (OBH). The latter is defined as a burst at that height which maximizes an effect for a particular range and yield; e.g., for a yield of 1 Mt, a burst height of 5000 ft maximizes the overpressure at a 1.2-mile range, whereas a 10,000-ft height would be required for a range of 5 miles. Maximum winds for the OBH condition were computed by using the maximum dynamic pressures for OBH and the corresponding overpressures.

---

*See Chap. 3 of Ref. 1.

†A nearly ideal surface can be defined as one not conducive to the formation of precursor waves (see Ref. 1).

Use of the slide rule to determine the parameters of the incident blast wave can be illustrated by means of Fig. 4.1. The tab hairline is placed at 100-kt yield and 1.6-mile range. In the large window the following values are read for the indicated parameters:

	SB	OBH
p_m	3.4 psi	7.0 psi
q_m	0.25 psi	1.1 psi
u_m	110 mph	220 mph

These values are also applicable to any number of yield–range combinations that can be read directly from the two scales, e.g., 1 Mt at 3.4-mile range or 20 Mt at 9.4-mile range.

Duration of positive overpressure and arrival time of the blast wave can be read in the appropriate window on the small disk. The only rule setting necessary for these readings involves moving the hairline on the tab to the yield of interest.

Continuing the example cited above (Fig. 4.1), if the hairline is set on 100 kt, we find (reading in the second window from the center) that for a surface burst the blast wave of 3.4-psi maximum overpressure arrives 5.0 sec after the detonation and has a positive-overpressure duration of 1.7 sec. Similar evaluations can be obtained for bursts at optimum height by using the overpressure scales appearing on the outer scale in the window.

4.2.2 Reflected Blast Wave*

When an ideal or classical blast wave strikes a flat surface head on, i.e., at normal incidence, there is an instantaneous rise in overpressure to two or more times the incident value. The magnitude of the reflected overpressure can be read on the slide rule as a function of incident overpressure using the fixed scales plotted along an arc near the range scale on the middle disk (Fig. 4.1). Suppose, for example, that a blast wave of ideal-wave shape with a maximum overpressure of 30 psi strikes the side of a building head on. From the reflected overpressure scale, it can be determined that 100-psi overpressure results from this reflection. It should be noted that the reflected overpressures shown on the slide rule are applicable to locations where the ambient pressure is 14.7 psi.

4.2.3 Structural and Biological Damage Associated with Various Maximum Overpressures

Criteria for structural and biological damage are presented on the slide rule in the form of tables that can be viewed by rotating the large window on disk F_2 beyond the blast-parameter scales (see Figs. 3.1 and 3.3). The table describing structural damage is reproduced in Table 4.2. The large difference in overpressures tolerated by the buried concrete arch and the buried steel arch is to some extent a result of the differences in the method of burial of the structures. The concrete arch referred to is an underground structure with an earth mound at the surface; the steel arch is a surface structure with an earth cover mounded to a depth of 5 ft at the crown of the arch (see footnotes to Table 4.2). Thus the steel structure would encounter additional blast loads owing to dynamic pressure and reflected overpressure.

Damage criteria in Table 4.2 for seismic and reinforced-concrete structures were estimated from data reported† for destruction of buildings in Hiroshima and Nagasaki during World War II. The weapons detonated over these cities had yields of about 20 kt. Damaging overpressures for ordinary houses were estimated from data obtained from a 15-kt shot in 1953 and a 30-kt shot in 1955 at the Nevada Test Site.† Since the duration of the blast wave increases for greater yields, the expected structural damages for a given maximum overpressure would be somewhat greater than those tabulated.

*See Chap. 3 of Ref. 1.

†See Chap. 5 of Ref. 1.

The biological-damage criteria* listed in Table 4.3 are those resulting from overpressure *per se* (biological effects due to translation and missiles are discussed later). Rupture of the eardrum is mostly dependent on the maximum overpressure experienced. Lung hemorrhage and mortality, however, are greatly dependent on the shape and duration of the overpressure pulse as well as on the maximum value of overpressure. The data reported were derived from shock-tube studies[4] using animals as biological test subjects and for the following conditions: (1) the incident overpressure wave was accompanied by a shock and (2) the total duration of the overpressure was about 0.4 sec. Experience has indicated that overpressure waves of durations greater than 0.4 sec would produce about the same mortality.

As noted above, the basic data were obtained from experimental animals. The damage estimates for man reported in Table 4.3 (items 2 and 3) were made by extrapolating the animal data to a biological subject weighing 70 kg (approximate weight of man).

4.3 TRANSLATIONAL VELOCITIES FOR MAN AND WINDOW GLASS†

The translational velocities for man and window glass, which appear on the small disk (F_3 in Fig. 3.1), were computed for the following conditions: (1) The velocities are those which would be attained after 10 ft of travel from the original position. (2) The range–velocity relations shown apply to a burst at the optimum height to maximize overpressure. (Velocities that would apply to a surface burst can be estimated by a method illustrated below.) (3) The velocities for man apply to a 165-lb man standing in an open area at the time of arrival of the blast wave. (4) The velocities for window glass apply to fragments (0.1 to 10 g) of double-strength glass ($\frac{1}{8}$ in. thick) from windows facing Ground Zero. (5) The blast wave was assumed to be classical or near ideal (see Sec. 4.2.1).

Velocities of translation for man and window glass are found by setting the tab hairline on the yield of interest and reading, in the appropriate windows, velocities as a function of range. If the yield is 100 kt, as illustrated in Fig. 4.1, at a 1.6-mile range the velocity for man is 30 ft/sec and for window glass, 320 ft/sec. These velocities apply to a burst of optimum height which would produce a maximum overpressure of 7.0 psi at this range (Fig. 4.1). However, a surface burst of this yield would produce at 1.6 miles a maximum overpressure of only 3.4 psi. From the overpressure, yield, and range scales illustrated in Fig. 4.2, it is found that a 3.4-psi maximum overpressure occurs at 2.6 miles for an optimum height of burst. From the appropriate velocity scales at the 2.6-mile range, it is found that the velocity for man is 12 ft/sec and for window glass it is 150 ft/sec at the 1.6-mile range for a surface burst of 100 kt. It is assumed that the velocities at 1.6 miles for a surface burst are the same as those at 2.7 miles for an optimum burst height because the maximum overpressures are the same for the two situations although the durations of the two waves are slightly different.

The translational velocities placed on the slide rule for window-glass fragments may imply a uniformity in behavior of fragments for a given situation. This, in reality, is not true, as has been demonstrated by field work[5,6] at the Nevada Test Site where thousands of glass-fragment velocities were measured. The fragment velocities placed on the slide rule were derived from theoretical and laboratory studies,[7,8] and it should be noted that, in general, they are consistent with those measured in the field studies if, for a given sample, only the fragments with the higher velocities are considered. Thus the velocities determined from the slide rule may be considered to be maximal rather than average.

Table 4.4 contains data placed on the slide rule in tabular form to enhance the significance of glass fragments striking a biological target.[9] Because the penetration data are for 1 cm of soft tissue, it should not be assumed that penetrations of lesser depths might not be significant, particularly where multiple lacerations or the eyes are involved.

---

*Placed on the slide rule in the table to the right of the one previously discussed for structural damage.

†See Chap. 11 of Ref. 1.

The translational velocities placed on the slide rule for man were also derived from theoretical and laboratory studies.[7,8] The data have been validated by full-scale weapons tests in only one instance where use was made of an anthropomorphic dummy.[10] As previously noted, the data were computed for a 165-lb man. A smaller man could be expected to have higher velocities, and a larger man, lower velocities.

The biological damage associated with the translation of man is generally considered to be dependent on subsequent impact with a hard, stationary object. The criteria placed on the slide rule and listed in Table 4.5 are based on perpendicular impact with a rigid, flat surface (references noted in table). Surfaces with sharp edges would probably be more injurious than flat ones.

4.4 THERMAL RADIATION*

The thermal-radiation scales, which are in red on the back of the circular computer, apply to air bursts and slant ranges where the visibility is 50 miles. Thermal data for distances less than 0.1 mile and greater than 25 miles were obtained by extrapolation. To estimate the thermal dose of a given location, set the range opposite yield on the front of the computer and place the tab hairline over this setting. Without moving the scales, turn the computer over and read the thermal scale at the intersection of the red spiral and the red hairline, e.g., if 100 kt and 1.6 mile slant range are set under the tab hairline as illustrated in Fig. 4.1, 34 cal/cm^2 is determined by interpolation on the thermal scale, as shown in Fig. 4.3.

Thermal radiation for a surface burst can also be obtained from the slide rule. For this case set the short mark to the right of the tab hairline on the yield of interest (100 kt) and then set the range (1.6 miles) on the tab hairline, as shown in Fig. 4.4. With this setting a dose of 24 cal/cm^2 is determined in the same manner as before on the thermal scale (Fig. 4.5).

The dashed lines on the thermal scale indicate as a function of yield (either air or surface burst) the thermal dose necessary for first- and second-degree burns to bare white skin. Thus, if the tab hairline is set on 100 kt as in Figs. 4.1 and 4.2, the thermal doses necessary to produce first- and second-degree burns are determined to be about 3 and 5 cal/cm^2, respectively (see Fig. 4.3). The definitions of first- and second-degree burns appear on the slide rule near the thermal scales (see Figs. 4.3 and 4.5). First-degree burns are compared to sunburn with no blistering. Second-degree burns involve blistering with serious consequences, particularly if the face or extensive areas of the body are involved.

The rate of delivery of thermal radiation is indicated on the front of the slide rule in the outer window on the small disk. If the tab hairline is set on 100 kt as in Figs. 4.1 and 4.2, it can be determined, for example, that 1 per cent of the thermal radiation is emitted in 0.1 sec, 50 per cent in 0.7 sec, and 80 per cent in 2.8 sec.

The rate of delivery of thermal radiation is significant in that it gives some indication of the time available for evasive action after a detonation. This concept is particularly important at the greater ranges from the larger weapons. For example, a total thermal-radiation dose of 20 cal/cm^2 is delivered at about 23 miles (slant range) from a 20-Mt air burst for a visibility of 50 miles; however, only 20 per cent of this dose is delivered in the first 4.5 sec after the detonation. Thus, if evasive action could be taken in this time, the thermal dose received would be only $20 \times 0.2 = 4$ cal/cm^2.

4.5 INITIAL NUCLEAR RADIATION†

Initial nuclear radiation, gamma plus neutron, is indicated on the computer in a manner similar to that used for the thermal radiation. The nuclear-radiation data were computed for air bursts, slant ranges, air-density ratio of 0.9, and a relative biological effectiveness (RBE)

*See Chaps. 7 and 9 of Ref. 1.

†See Chaps. 8 and 11 of Ref. 1.

of 1.0 for both gamma and neutron radiation.* To illustrate an evaluation of initial nuclear radiation, set the tab hairline opposite the 1.6-mile range and 100-kt yield (see Fig. 4.1) and read about 20 rem on the initial-nuclear-radiation scale at the intersection of the black spiral and the black hairline (see Fig. 4.3).

A summary of the effects of acute exposure to ionizing radiation[1] are tabulated on the back of the central disk of the computer (see Fig. 4.3).

4.6 EARLY FALLOUT DOSE RATE†

The early-fallout-dose-rate scales appearing on the small and middle disks on the front of the computer are independent of all the other scales. If, after the fallout is complete, a dose rate is measured at a known time after detonation, then dose rates at later times can be estimated. Suppose that 80 r/hr were measured 2 hr after a detonation and that the early fallout was complete. For convenience in reading the dose-rate scale at long periods of time, let 100 scale units represent 1 r/hr. Thus 80 r/hr would correspond to $80 \times 100 = 8000$ scale units. Set 8000 opposite 2 hr, as illustrated in Fig. 4.6, and read $1200/100 = 12$ r/hr at 10 hr; $110/100 = 1.1$ r/hr at 3 days; and $6.8/100 = 0.068$ r/hr at 30 days. Note that this procedure is essentially the same as moving the decimal point of all dose-rate numbers on the slide rule two places to the left. (The biological effects of acute exposure to ionizing radiation were noted in Sec. 4.5.)

4.7 CRATER DIMENSIONS‡

The crater dimensions defined on the computer apply to contact surface bursts where the surface material is dry soil or rock. The three crater dimensions used are illustrated by a diagram on the computer (see Fig. 4.1). The dimension R_A is the radius of the apparent crater, i.e., not including the rupture zone. R_L is the radius of the crater lip, and D is the depth of the crater measured from the level of the undisturbed ground to the bottom of the crater.

Crater dimensions are evaluated by setting the tab hairline on the appropriate yield and reading the dimensions described above in the window nearest the center of the computer. Thus a 100-kt contact surface burst is found to produce a crater whose depth (D) is 0.027 mile in soil or 0.022 mile in rock (see Fig. 4.1). The radius of the crater lip (R_L) for a weapon of this yield is 0.11 mile in soil or 0.09 mile in rock, and the radius of the apparent crater (R_A) is 0.056 mile in soil or 0.045 mile in rock.

4.8 MAXIMUM FIREBALL RADIUS AND MINIMUM HEIGHT OF BURST FOR NEGLIGIBLE EARLY FALLOUT§

The maximum fireball radius presented on the computer is an average between those for air and surface bursts, i.e., the fireball radius for a surface burst is 13 per cent larger than that indicated, and for an air burst, 13 per cent smaller.

The production of early (or local) fallout is dependent on the relative size of the fireball radius and the height of burst, other conditions being the same. Thus the empirically deter-

---

*It is shown in Sec. 2.6 that the nuclear-radiation data placed on the slide rule can also be applied, with reasonable accuracy, to a surface burst or an optimum height burst. This simple method of approximation is particularly useful for planning purposes where uncertainties in range are significant.

†See Chap. 9 of Ref. 1.

‡See Chap. 6 of Ref. 1.

§See Chap. 2 of Ref. 1.

mined minimum height of burst required for negligible fallout is shown by an indicator on the same scale defining the fireball radius.

To evaluate the parameters described in the preceding paragraph, set the tab hairline on the yield of interest and refer to the scale in the appropriate window on the small disk. For example, a 100-kt explosion produces a fireball with a maximum radius of 0.28 mile (see Fig. 4.1). The minimum height of burst for negligible early fallout, read in the same window, is 0.22 mile.

4.9 ESTIMATION OF EFFECTS PARAMETERS FOR YIELDS GREATER THAN 20 MT OR LESS THAN 1 KT

Although weapons effects for yields greater than 20 Mt have not been determined experimentally, estimates of the magnitude of several of the effects can easily be made with the slide rule by application of the scaling laws. Similar procedures can be used to evaluate effects for yields less than 1 kt.

For fixed values of ambient pressure and temperature, blast-wave parameters are functions of $d/W^{1/3}$, where d is range and W is explosive yield (see equations in Table 2.1, for example). If the convenient factor 10 is chosen, then

$$\frac{d}{W^{1/3}} = \frac{10d}{10W^{1/3}} = \frac{10d}{(1000W)^{1/3}} \tag{4.1}$$

or, if $^1/_{10}$ is used,

$$\frac{d}{W^{1/3}} = \frac{d/10}{W^{1/3}/10} = \frac{(d/10)}{(W/1000)^{1/3}} \tag{4.2}$$

Suppose it were desired to estimate values of the blast parameters at a distance of 16 miles from a 100-Mt (100,000-kt) surface burst.* If the scaling expressed by Eq. 4.2 is used, certain of the blast parameters for this yield and range would have the same values as those at $^{16}/_{10}$ = 1.6-mile range from a 100,000 kt/1000 = 100-kt burst. Thus, when a 1.6-mile range is set opposite 100-kt yield, the following values of blast parameters are obtained which are applicable to a 100-Mt surface burst at a 16-mile range:

Maximum overpressure	3.4 psi
Maximum dynamic pressure	0.25 psi
Maximum wind velocity	110 mph

When the tab hairline is set at 100 kt, the duration of the positive overpressure for a maximum overpressure of 3.4 psi is read in the appropriate window to be 1.7 sec. To find the duration of the blast wave of the same maximum overpressure, but from a 100-Mt explosion, multiply the 1.7-sec duration by $(100{,}000 \text{ kt}/100 \text{ kt})^{1/3} = 10$ to obtain a duration of 17 sec. A similar procedure results in an arrival time for the blast wave of $5.0 \times 10 = 50$ sec.

Since crater dimensions (like range, duration, and arrival time) are proportional to the cube root of the yield,† a method similar to that previously described can be used to estimate the size of craters for explosions greater than 20 Mt. The crater depth for a 100-kt yield is found from the slide rule to be 0.027 mile; therefore the crater depth for a 100-Mt explosion would be $0.027 \times 10 = 0.27$ mile. Similarly, the apparent crater radius is $0.056 \times 10 = 0.56$ mile, and the crater-lip radius is $0.11 \times 10 = 1.1$ miles. (The crater dimensions described in

*Caution should be exercised in extrapolating blast effects for the optimum burst height to high yields since the heights of burst required for optimization may be excessive and would result in serious errors owing to the low ambient air pressure of the point of detonation (see Eqs. 2.78 and 2.79 in Table 2.9).

†See equations in Fig. 2.19.

this example are applicable to a *contact* surface burst of 100 Mt and to dry soil. The tentative nature of these estimates should again be emphasized.)

The procedures for estimating blast and crater parameters for yields less than 1 kt are the same as those described for yields greater than 20 Mt, except that Eq. 4.1 is used instead of Eq. 4.2. As an example, to find the range at which 5.0-psi maximum overpressure would occur if 0.1 kt were detonated at the height which maximizes overpressure (optimum burst height), first, multiply 0.1 kt by 1000 to obtain 100 kt. Then, set the hairline in the large window at 5 psi on the optimum-burst-height scale, and read the 2.0-mile range opposite 100-kt yield. The final step is to divide the range for 100-kt yield by 10 to obtain the 0.2-mile range applicable to 0.1 kt.

Fireball dimensions (including minimum height for negligible fallout) vary as $W^{0.4}$. The equation for the fireball radius (R) averaged for surface and air bursts is

$$\bar{R} = KW^{0.4} \tag{4.3}$$

where K = 0.04356 mile. If both sides of the equation are multiplied by 100, we obtain

$$100\,\bar{R} = K\,100\,W^{0.4} = K\,(100{,}000\,W)^{0.4} \tag{4.4}$$

or, if both sides are divided by 100,

$$\frac{\bar{R}}{100} = K\left(\frac{W}{100{,}000}\right)^{0.4} \tag{4.5}$$

Thus the average fireball radius for a 100-Mt (100,000-kt) burst is found by setting the slide rule on 100,000 kt/100,000 = 1 kt, reading 0.044 mile in the appropriate window, and multiplying this radius by 100 to get 4.4 miles. This simplified procedure is not workable for yields between 20 and 100 Mt or for yields between 0.2 and 1 kt since the factor of 100,000 makes the reference yield too small or too large, respectively, to be read on the slide rule.

The thermal-radiation dose received at a given distance from a burst is directly proportional to the yield (see equations in Table 2.11). Therefore the thermal dose received at the 49-mile slant range from an air burst of 100 Mt can be found by reading 2.0 cal/cm^2 at 49 miles from a 10-Mt burst and multiplying this dose by 100/10 = 10 to obtain 20 cal/cm^2.

The time required to deliver a given percentage of the total thermal radiation is proportional to the square root of the yield (see Fig. 2.14). For example, to find the time after detonation at which 50 per cent of the thermal radiation is emitted from a 100-Mt burst, read 2.3 sec for a 1-Mt explosion and multiply this time by $(100/1)^{1/2} = 10$ to get 23 sec for the 100-Mt burst.

There is no simple method for extrapolating initial-nuclear-radiation doses for yields greater than 20 Mt. However, doses for yields less than 1 kt can be estimated by a method similar to that for thermal radiation provided that reference doses obtained from the slide rule are limited to yields between 1 and 10 kt (see Eq. 2.114 and Fig. 2.15). To find the initial-nuclear-radiation dose at 0.32-mile slant range from a 0.2-kt burst, for example, read 10^4 rem at 0.32 mile from a 0.2 × 10 = 2-kt burst and divide this dose by 10 to obtain 10^3 rem for a burst of 0.2-kt yield.

REFERENCES

1. S. Glasstone (Ed.), *The Effects of Nuclear Weapons*, rev. ed., Superintendent of Documents, U. S. Government Printing Office, Washington, D. C., 1962.
2. L. J. Vortman, *Curves for Estimating Low Blast Overpressure*, USAEC Report SCTM 195-58(51), Sandia Corporation, April 1958.

3. T. Zalewski, Experimentelle Untersuchungen über die Resistenzfähigkeit des Trommelfells, *Arch. Ohrenheilk., 52:* 109-128 (1906).
4. D. R. Richmond, V. R. Clare, V. C. Goldizen, D. E. Pratt, R. T. Sanchez, and C. S. White, Biological Effects of Overpressure. II. A Shock Tube Utilized to Produce Sharp-rising Overpressures of 400 Milliseconds Duration and Its Employment in Biomedical Experiments, *Aerospace Med. 32:* 997-1008 (November 1961).
5. I. G. Bowen, A. F. Strehler, and M. B. Wetherbe, *Distribution and Density of Missiles from Nuclear Explosions*, Operation Teapot Report, WT-1168, December 1956.
6. I. G. Bowen, M. E. Franklin, E. R. Fletcher, and R. W. Albright, *Secondary Missiles Generated by Nuclear-produced Blast Waves*, Operation Plumbbob Report, WT-1468 (in press).
7. E. R. Fletcher, R. W. Albright, V. C. Goldizen, and I. G. Bowen, *Determinations of Aerodynamic-drag Parameters of Small Irregular Objects by Means of Drop Tests*, USAEC Report CEX-59.14, October 1961.
8. I. G. Bowen, R. W. Albright, E. R. Fletcher, and C. S. White, *A Model Designed to Predict the Motion of Objects Translated by Classical Blast Waves*, USAEC Report CEX-58.9, January 1961.
9. I. G. Bowen, D. R. Richmond, M. B. Wetherbe, and C. S. White, *Biological Effects of Blast from Bombs. Glass Fragments as Penetrating Missiles and Some of the Biological Implications of Glass Fragmented by Atomic Explosions*, USAEC Report AECU-3350, Lovelace Foundation for Medical Education and Research, June 1956.
10. E. S. Gurdjian, J. E. Webster, and H. L. Lissner, *Medical Physics*, Vol. II, Biomechanics: Fractures, Skull, pp.99-105, Year Book Publishers, Chicago, 1950.
11. A. N. Black, D. G. Christopherson, and S. Zuckerman, *Fractures of the Head and Feet*, Report RC-334, Ministry of Home Security, Oxford, England, August 1942.
12. R. V. Taborelli, I. G. Bowen, and E. R. Fletcher, *Tertiary Effects of Blast—Displacement*, Operation Plumbbob Report, WT-1469, February 1959.
13. D. R. Richmond, I. G. Bowen, and C. S. White, Tertiary Blast Effects, Effects of Impact on Mice, Rats, Guinea Pigs and Rabbits, *Aerospace Med. 32:* 789-805 (September 1961).

TABLE 4.1—FUNCTIONS ON THE NUCLEAR BOMB EFFECTS COMPUTER*

Variables	Type of burst	Conditions	Described in section
p_m, d, W	SB	P = 14.7 psi	4.2
p_m, d, W	OBH	P = 14.7 psi	4.2
q_m, d, W	SB	P = 14.7 psi	4.2
q_m, d, W	OBH	P = 14.7 psi	4.2
u_m, d, W	SB	P = 14.7 psi; c_0 = 1117 ft/sec	4.2
u_m, d, W	OBH	P = 14.7 psi; c_0 = 1117 ft/sec	4.2
t_a, p_m, W	SB	P = 14.7 psi; T_0 = 519°Rankine	4.2
t_a, p_m, W	OBH	P = 14.7 psi; T_0 = 519°Rankine	4.2
t_p, p_m, W	SB	P = 14.7 psi; T_0 = 519°Rankine	4.2
t_p, p_m, W	OBH	P = 14.7 psi; T_0 = 519°Rankine	4.2
p_r, p_m		P = 14.7 psi	
$v_{10\ ft(m)}$, d, W	OBH	P = 14.7 psi; c_0 = 1117 ft/sec	4.3
$v_{10\ ft\ (g)}$, d, W	OBH	P = 14.7 psi; c_0 = 1117 ft/sec	4.3
Q, d_s, W	AB	Visibility = 50 miles	4.4
Q, d, W	SB	Visibility = 50 miles	4.4
Q_{1st}, W	SB, AB	Bare skin (white)	4.4
Q_{2nd}, W	SB, AB	Bare skin (white)	4.4
Q%, t, W	SB, AB		4.4
I, d_s, W	AB(SB, OBH)	ρ/ρ_0 = 0.9	4.5
R, t, R_0, t_0	SB		4.6
R_L, W	CSB	Dry soil	4.7
R_L, W	CSB	Rock	4.7
R_L, W	CSB	Dry soil	4.7
R_A, W	CSB	Rock	4.7
D, W	CSB	Dry soil	4.7
D, W	CSB	Rock	4.7
$\overline{R}$, W	SB, AB	Average for SB and AB	4.8
H_m, W	AB		4.8

*See List of Symbols for definition of terms.

TABLE 4.2—CRITERIA FOR STRUCTURAL DAMAGE

Types of structure	Overpressure, psi		Reference
	Light damage	Heavy damage	
Buried concrete arch*	120 to 160	220 to 280	Chap. 4 of Ref. 1
Buried steel arch†	30 to 40	45 to 60	Chap. 4 of Ref. 1
Seismic structure	10	35	Chap. 5 of Ref. 1
Reinforced concrete	7	25	Chap. 5 of Ref. 1
Ordinary house	1	5	Chap. 5 of Ref. 1
Glass windows	0.02	1	2

*Buried concrete arch with a 16-ft span and central angle of 180°; 8 in. thick with 4 ft of earth cover at the crown.

†Light corrugated-steel arch, surface structure (10-gauge corrugated steel with a span of 20 to 25 ft) central angle of 180° with 5 ft of earth cover at the crown.

TABLE 4.3 — CRITERIA FOR BIOLOGICAL DAMAGE DUE TO OVERPRESSURE

Overpressure,* psi	Probable biological effect	Reference
5 to 45	1 to 99% rupture of eardrum	3
15 to 25†	Threshold lung hemorrhage	4
35 to 65†	1 to 99% mortality	4

*Side-on or reflected overpressure.
†Applies only to fast-rising pressure of long duration.

TABLE 4.4 — GLASS-MISSILE DATA FOR PENETRATION OF 1-CM SOFT TISSUE

Glass fragment mass, g	Velocity for indicated probabilities, ft/sec			Reference
	1%	5%	99%	
0.1	235	410	730	9
0.5	160	275	485	9
1.0	140	245	430	9
10.0	115	180	300*	9

*This is a revised figure that does not appear on the slide rule.

TABLE 4.5 — BIOLOGICAL EFFECTS OF IMPACT AT 90° WITH A HARD SURFACE

Impact velocity, ft/sec	Probable biological effect	Reference
0 to 10	No serious injury	
12 to 16	Fracture of feet and legs	11
13 to 23	1 to 99% skull fracture	12
15 to 35	1 to 99% mortality	13

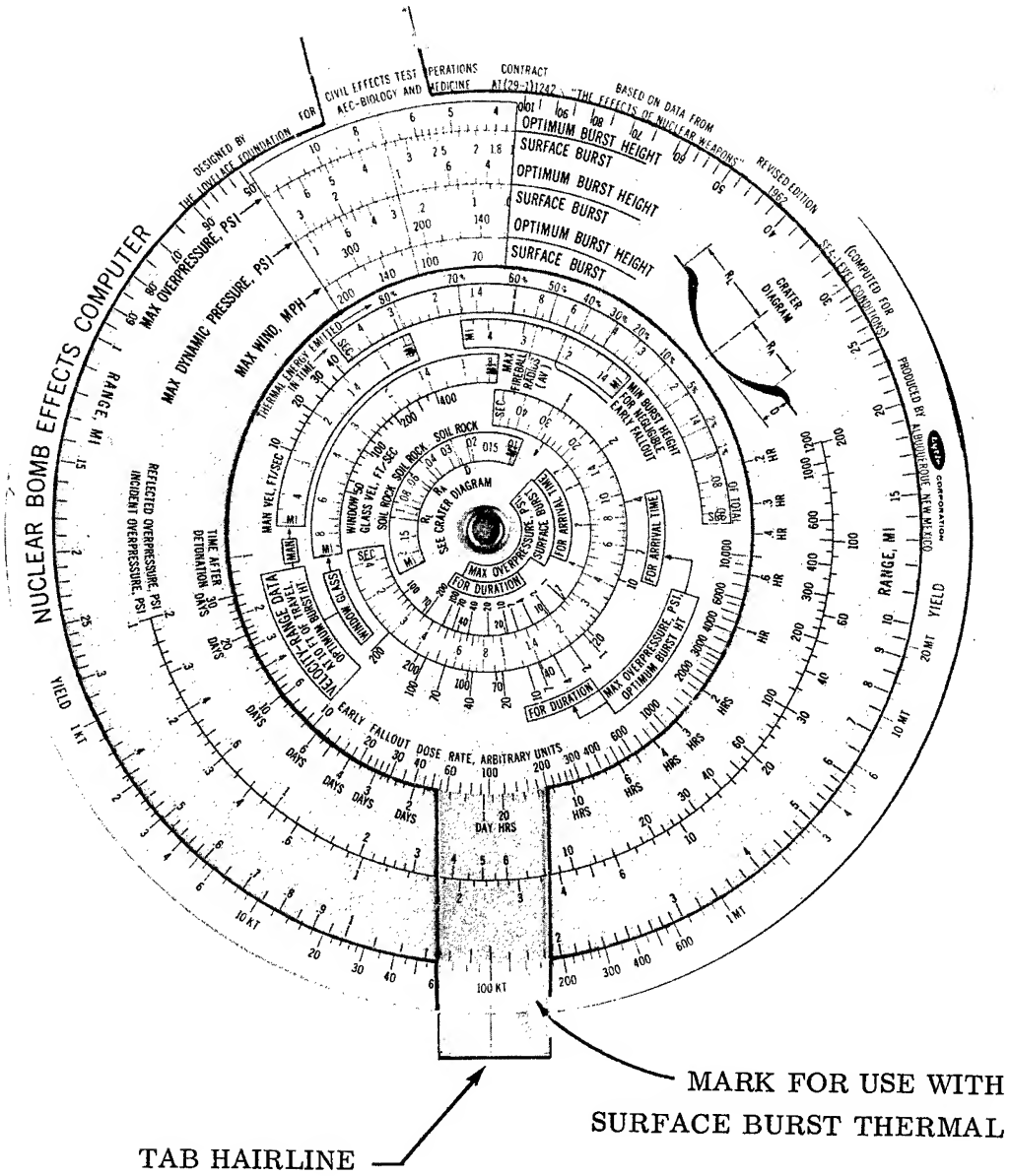

Fig. 4.1—Circular slide rule with yield set at 100 kt and range set at 1.6 miles (both by the tab hairline, as indicated by the arrow).

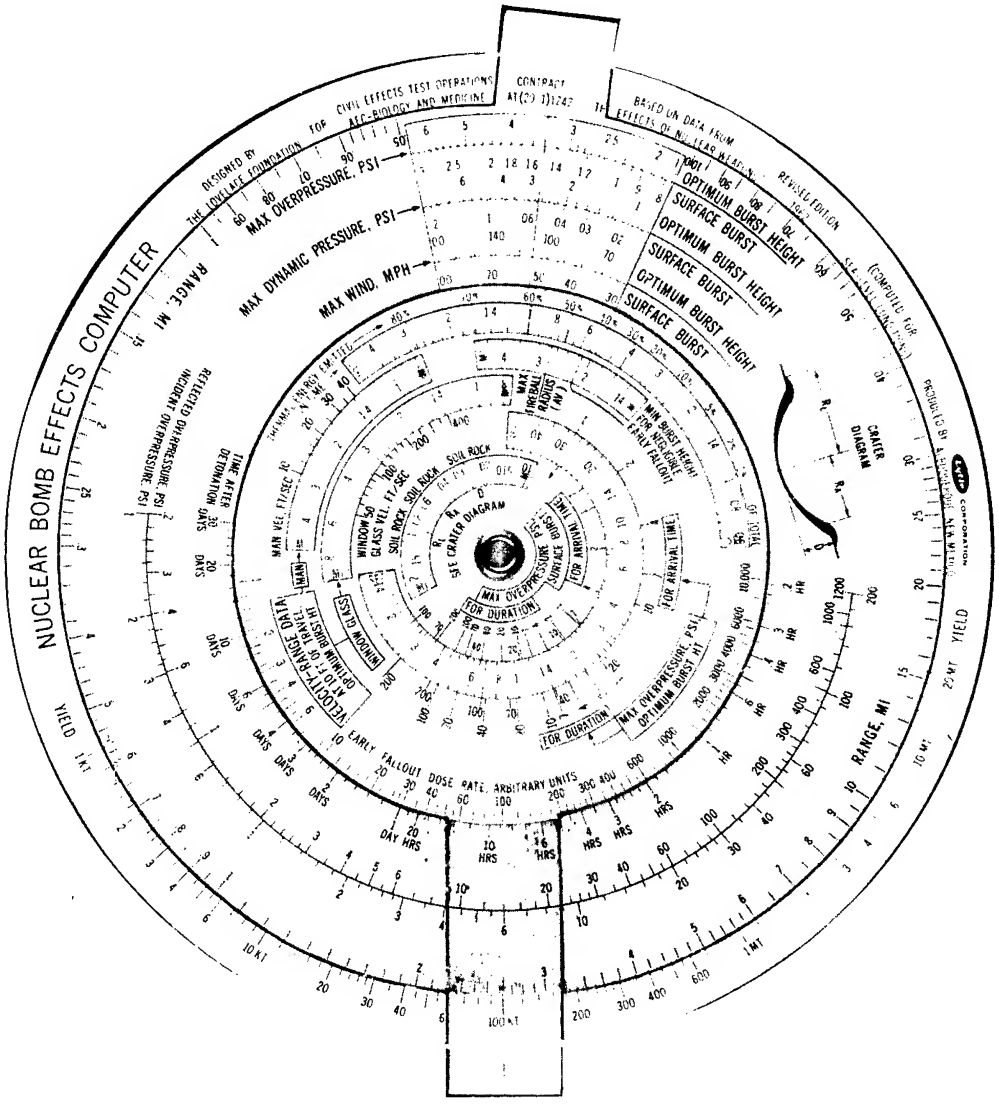

Fig. 4.2—Circular slide rule with yield (tab hairline) set at 100 kt and maximum overpressure for optimum burst height (hairline in large window) set at 3.4 psi.

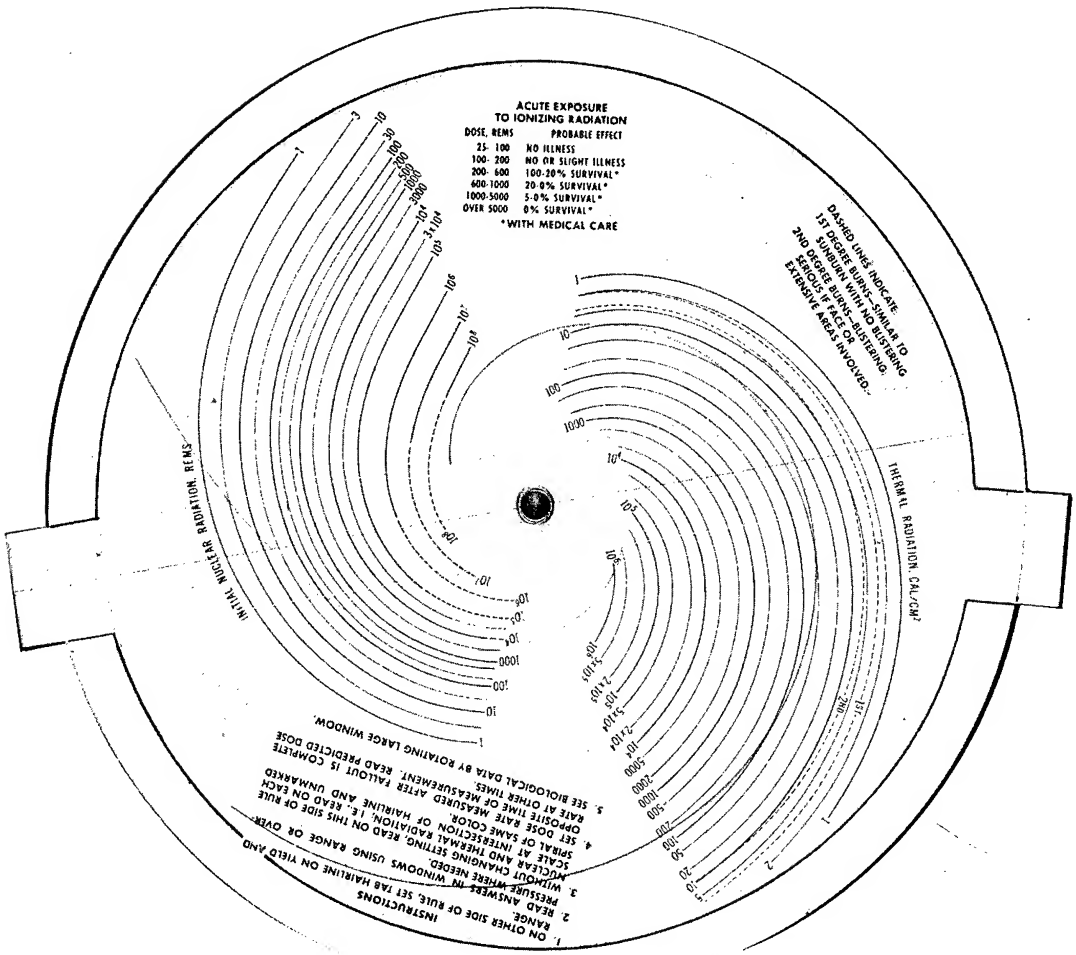

Fig. 4.3—Back of the circular slide rule with settings on the front of 100 kt for yield and 1.6 miles for range (both with the tab hairline). A thermal-radiation dose of 34 cal/cm^2 for air bursts is read at the intersection of the red spiral and red hairline on the thermal-radiation curves. The initial nuclear radiation for air bursts is read at intersection of black spiral and black hairline to be 20 rems.

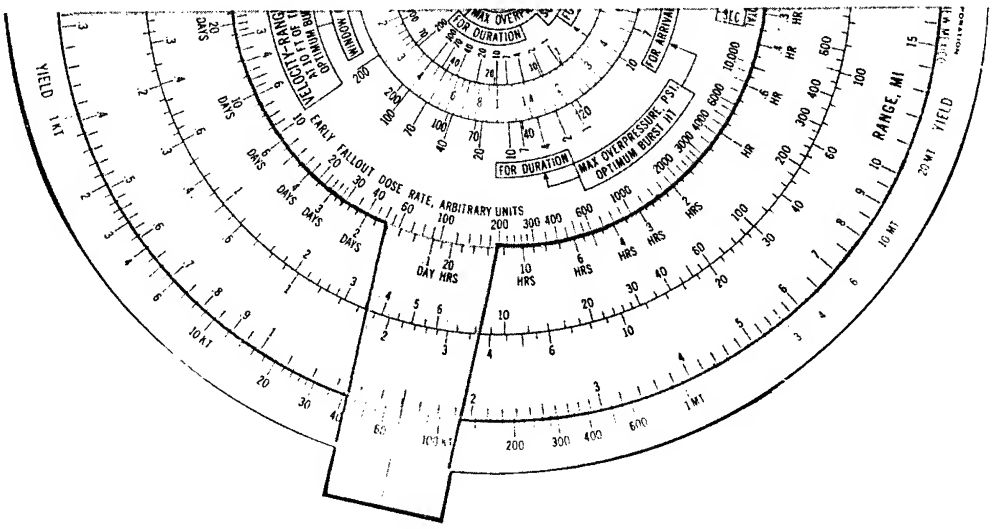

Fig. 4.4—Front of the computer with yield set at 100 kt using small mark to right of hairline and range set at 1.6 miles using tab hairline. This is the setting to read surface-burst thermal radiation in Fig. 4.5.

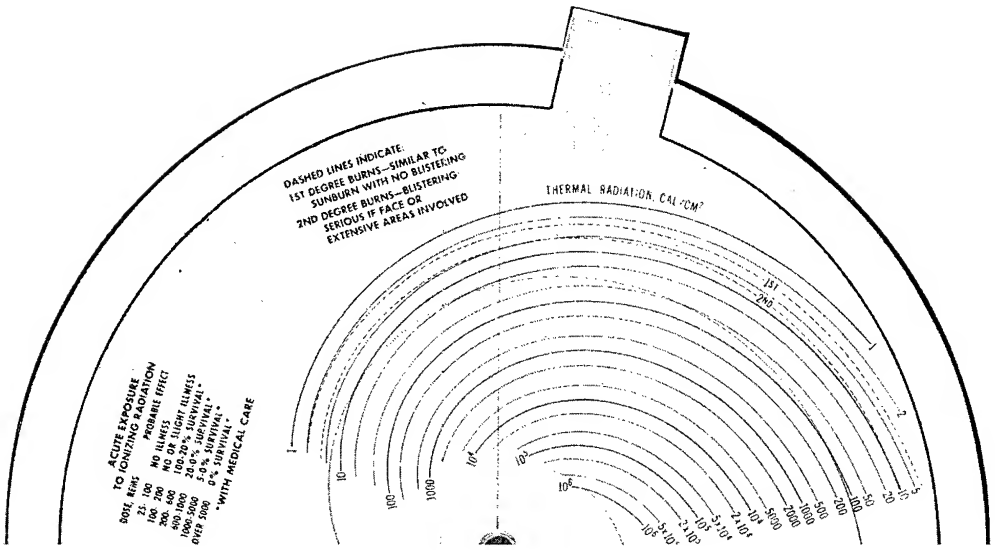

Fig. 4.5—Back of the computer showing reading of 24 cal/cm^2 for thermal radiation using yield and range settings indicated in Fig. 4.4.

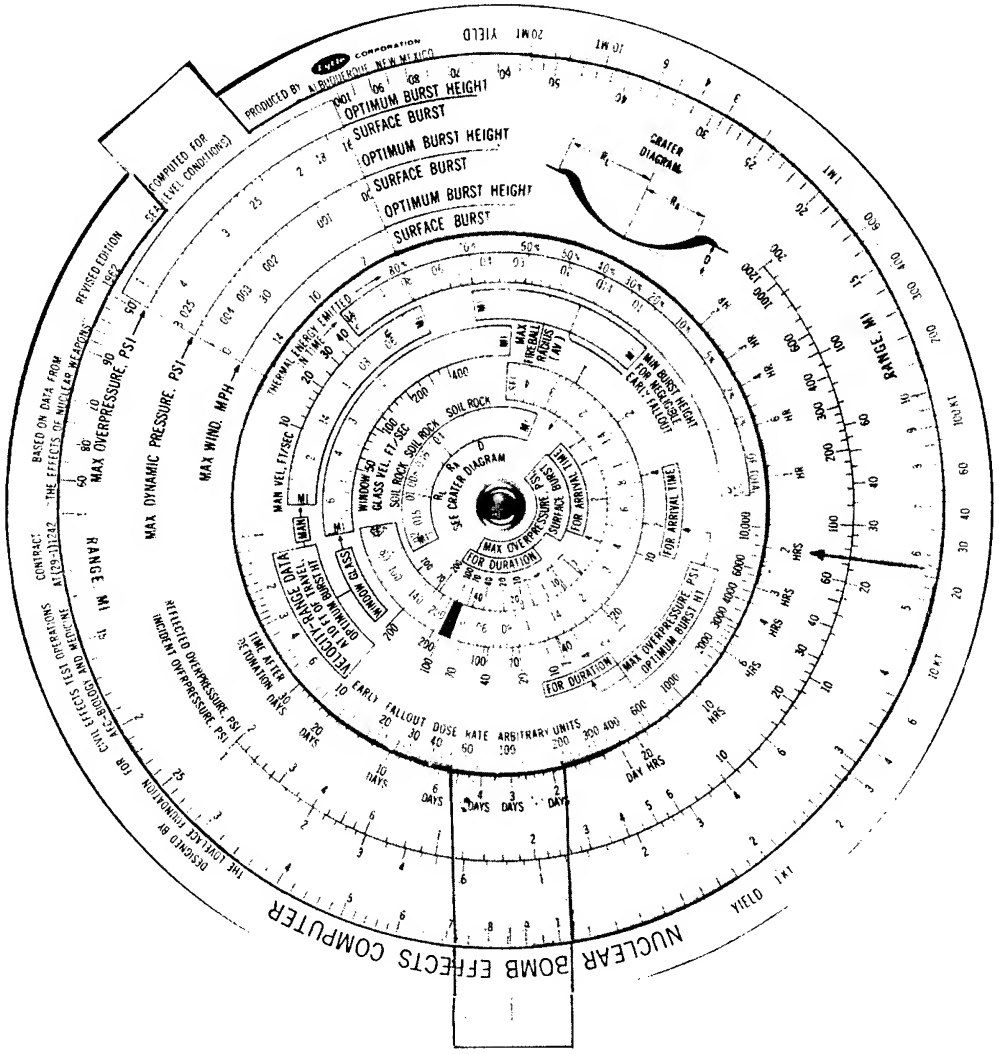

Fig. 4.6—Front of computer with arrow indicating early fallout dose rate of 8000 set at a time of 2 hr.

Appendix

OUTLINE OF THE PROCEDURE USED TO CONSTRUCT THE ORIGINAL PLOTS OF THE SLIDE-RULE DISKS

Construction of drawings from which each of the slide-rule disks was produced was greatly facilitated by use of machine techniques. The equipment employed* included a digital computer (Bendix G-15D), a magnetic tape for auxiliary storage of information (Bendix MTA-2), and a discrete-interval plotter with a plotting interval of 0.01 in. (Bendix PA-3).

The first step of the plotting procedure was to generate by computation the detailed data necessary for the plotting equipment. The data were computed, accumulated on magnetic tape, and then transmitted by the computer to the plotter as electrical pulses.

Each disk was drawn in detail (including windows and hairlines) to a scale that would make the largest disk 20 in. in diameter.† The plotter used roll paper with a plotting space of 11 in. in the short axis. Thus it was necessary to prepare each disk in two parts which could then be fitted together for drafting purposes by means of alignment marks appearing on each part. After the data had been computed and stored on magnetic tape, a complete set of plots could be prepared in about 4 hr.

*The Intercard programing system used in this work also requires an IBM 523 unit for card reading, an IBM 514 for punching cards, and an IBM 402 for tabulation (the IBM and Bendix equipment being made compatible by the Bendix CA-2 coupling unit).

†The largest disk of the manufactured slide rule is $5\frac{1}{8}$ in. in diameter.

CIVIL EFFECTS TEST OPERATIONS REPORT SERIES (CEX)

Through its Division of Biology and Medicine and Civil Effects Test Operations Office, the Atomic Energy Commission conducts certain technical tests, exercises, surveys, and research directed primarily toward practical applications of nuclear effects information and toward encouraging better technical, professional, and public understanding and utilization of the vast body of facts useful in the design of countermeasures against weapons effects. The activities carried out in these studies do not require nuclear detonations.

A complete listing of all the studies now underway is impossible in the space available here. However, the following is a list of all reports available from studies that have been completed. All reports listed are available from the Office of Technical Services, Department of Commerce, Washington 25, D. C., at the prices indicated.

CEX-57.1 ($0.75) The Radiological Assessment and Recovery of Contaminated Areas, Carl F. Miller, September 1960.

CEX-58.1 ($2.75) Experimental Evaluation of the Radiation Protection Afforded by Residential Structures Against Distributed Sources, J. A. Auxier, J. O. Buchanan, C. Eisenhauer, and H. E. Menker, January 1959.

CEX-58.2 ($0.75) The Scattering of Thermal Radiation into Open Underground Shelters, T. P. Davis, N. D. Miller, T. S. Ely, J. A. Basso, and H. E. Pearse, October 1959.

CEX-58.7 ($0.50) AEC Group Shelter, AEC Facilities Division, Holmes & Narver, Inc., June 1960.

CEX-58.8 ($1.00) Comparative Nuclear Effects of Biomedical Interest, Clayton S. White, I. Gerald Bowen, Donald R. Richmond, and Robert L. Corsbie, January 1961.

CEX-58.9 ($1.25) A Model Designed to Predict the Motion of Objects Translated by Classical Blast Waves, I. Gerald Bowen, Ray W. Albright, E. Royce Fletcher, and Clayton S. White, June 1961.

CEX-59.1 ($0.60) An Experimental Evaluation of the Radiation Protection Afforded by a Large Modern Concrete Office Building, J. F. Batter, Jr., A. L. Kaplan, and E. T. Clarke, January 1960.

CEX-59.4 ($1.25) Aerial Radiological Monitoring System. I. Theoretical Analysis, Design, and Operation of a Revised System, R. F. Merian, J. G. Lackey, and J. E. Hand, February 1961.

CEX-59.4 (Pt.II) ($1.50) Aerial Radiological Monitoring System. Part II. Performance, Calibration, and Operational Check-out of the EG&G Arms-II Revised System, J. E. Hand, R. B. Guillou, and H. M. Borella, Oct. 1, 1962.

CEX-59.7C ($0.50) Methods and Techniques of Fallout Studies Using a Particulate Simulant, William Lee and Henry Borella, February 1962.

CEX-59.13 ($0.50) Experimental Evaluation of the Radiation Protection Afforded by Typical Oak Ridge Homes Against Distributed Sources, T. D. Strickler and J. A. Auxier, April 1960.

CEX-59.14 ($1.75) Determinations of Aerodynamic-drag Parameters of Small Irregular Objects by Means of Drop Tests, E. P. Fletcher, R. W. Albright, V. C. Goldizen, and I. G. Bowen, October 1961.

CEX-60.1 ($1.75) Evaluation of the Fallout Protection Afforded by Brookhaven National Laboratory Medical Research Center, H. Borella, Z. Burson, and J. Jacovitch. February 1961.

CEX-60.3 ($1.50) Extended- and Point-source Radiometric Program, F. J. Davis and P. W. Reinhardt, August 1962.

CEX-60.6 ($1.00) Experimental Evaluation of the Radiation Protection Provided by an Earth-covered Shelter, Z. Burson and H. Borella, February 1962.

CEX-62.01 ($0.50) Technical Concept—Operation Bren, J. A. Auxier, F. W. Sanders, F. F. Haywood, J. H. Thorngate, and J. S. Cheka, January 1962.

CEX-62.02 ($2.25) Operation Plan and Hazards Report—Operation Bren, F. W. Sanders, F. F. Haywood, M. I. Lundin, L. W. Gilley, J. S. Cheka, and D. R. Ward, April 1962.